Developing novel remote sensing techniques to quantity glacier change in the Pan-Arctic

By

Asim Ali

Supervisors:

Professor Paul Dunlop

Professor Sonya Coleman

Dr Dermot Kerr

Dr Robert McNabb

Dr Riko Noormets

Faculty of Life and Health Science

School of Geography and Environmental Science Ulster University

This dissertation is submitted for the degree of Doctor of Philosophy

March 2023

Contents

Contents ii

Abstract vi

Acknowledgments vii

Common abbreviations viii

List of Figures x

List of Tables xiv

Chapter 1 1

1.1. Introduction 2

1.2. Aims and Objectives 5

1.3. References 7

Chapter 2 11

2.1. Introduction of remote sensing 12

2.2. Optical remote sensing satellites 14

2.3. Methods for glacier mapping 19

2.3.1. Manual Delineation 19

2.3.2. Index-based methods 19

2.3.3. Indices with morphometric parameters 21

2.3.4. Machine learning techniques 22

2.4. Glacier Inventory/outlines 24

2.5. Conclusions....26

2.6. References....28

Chapter 3....36

3.1. Abstract....37

3.2. Introduction....38

3.3. Study Area....41

3.4. Data and method....44

3.4.1. Data....44

3.4.2. Method: Object Based Image Analysis....46

3.4.2.1. Accuracy and Uncertainty....51

3.4.2.2. Uncertainty by random sampling....52

3.4.2.3. Uncertainty using buffer analysis....53

3.5. Results....53

3.5.1. Glacier area changes....55

3.6. Discussion....59

3.6.1. Glacier retreat....59

3.6.2. Comparison of glacier area loss with mass balance loss....62

3.6.3. Methodology framework in Google Earth Engine....64

3.7. Conclusion....66

3.8. References....69

Chapter 4 77

4.1. Abstract 78

4.2. Introduction 79

4.3. Study Area 81

4.4. Data and Methods 83

4.4.1. Data 83

4.4.2. Method: Object based image analysis in Google Earth Engine 85

4.4.2.1. Accuracy and Uncertainty 87

4.4.2.2. Uncertainty by random sampling 87

4.4.2.3. Uncertainty using buffer analysis. 89

4.5. Results 89

4.5.1. Glacier Area change 90

4.6. Discussion 92

4.6.1. Glacier area changes 92

4.6.2. Evaluating temperature with glacier area changes 94

4.6.3. Comparison of glacier area loss with mass balance 97

4.7. Conclusion 97

4.8. References 99

Chapter 5 104

5.1. Abstract 105

5.2. Introduction....106
5.3. Study Area....108
5.4. Method....109
5.4.1. Data sources....109
5.4.2. Glacier mapping: Object-based image analysis....111
5.4.3. Map description....112
5.5. Results....113
5.6. Conclusion....116
5.7. Software....117
5.8. References....118
Chapter 6....121
6. Discussion and summary....122
6.1. Discussion....122
6.2. Summary....124
6.3. Recommendations for future work....126
6.3. References....128
Appendix....130

Abstract

Since the last century, glaciers have been retreating due to climate change, especially in the Arctic, which is causing the sea level to rise, has the potential to change global weather and climate patterns. Therefore, it is important to understand climate change impacts on glaciers and to develop new automated approaches that can accurately quantify glacier area changes. In this study, we developed a new Object-based image analysis approach in Google Earth Engine, utilizing Landsat satellite imagery and mapped a total of 2,203 (≈32,894 km^2) glaciers in four regions in the Arctic and high latitudes: Novaya Zemlya, Russia, Baffin Island, Canada, Disko Island, Greenland and Kenai, Alaska at three different time periods; 1985-89, 2000-02, and 2019-21.

The results showed a clear reduction in the total glacier area in each region. 480 glaciers in Novaya Zemlya that cover an area of 22,990±301 km^2 experienced a 1,319±419 km^2 (5.7%) decline in total glacier area. 523 glaciers on Baffin Island covering 7,211±158 km^2 lost a total area of 452±227 Km^2 (6.6%). 748 glaciers on Disko Island covering 1,929±127 km^2 lost 457±168 km^2 (23.6%), and 452 glaciers in Kenai covering 764±60 km^2 lost 196±84 km^2 (25.7%). Seventy-three glaciers have completely retreated including sixty-nine on Disko Island, three on Novaya Zemlya, and one in Kenai. The results also show that glaciers area loss was greater in 2000-02 to 2019-21, compared to 1985-89 to 2000-02 in all four regions.

The accuracy of this method was evaluated by comparing manually corrected outlines, resulting in an overall accuracy estimate between 93% and 98% with the reference data based on random sampling approach. This demonstrates that our methodology in GEE is a powerful and robust tool for glacier mapping that reduces time required for manual correction and has the potential to be applied to other glacierised regions.

Acknowledgments

I would like to express my gratitude to my supervisors, Professor Paul Dunlop, Professor Sonya Coleman, Dr Dermot Kerr, and Dr Robert McNabb, and Riko Noormets for their invaluable guidance, encouragement and support throughout my doctoral studies. During my PhD studies, they passed onto me a number of good scientific ideas on which this thesis is based. I am grateful for their willingness to provide me with the necessary resources and tools to successfully complete my doctoral research.

I would like to thank my parents for their constant prayers and support, as well as my brothers Amjad Ali and Qaim Ali, for their frequent calls and motivation. I would also like to thank my friends and colleagues for their unwavering support throughout this journey.

Furthermore, I would like to thank the Ulster University for the financial support of my research through the Vice-Chancellor's Research Scholarships. Without this financial support, this research would not have been possible. I am grateful to the people who share such valuable scholarship opportunities with students on Facebook pages such as Pakistan Scholarship League and Scholarship Network.

Finally, I would like to thank all the anonymous reviewers of my published paper for their constructive comments and suggestions that helped improve this research.

Thank you all for your help and support.

Common abbreviations

OBIA – Object Based Image Analysis

GEE – Google Earth Engine

SNIC – Simple Non-Linear Iterative Clustering

DEM – Digital Elevation Model

GrIS – Greenland Ice sheet

NDSI – Normalized Difference Snow Index

RGI – Randolph Glacier Inventory

WGMS – World Glacier Monitoring Services

WGI – World Glacier Inventory

GLIMS – Global Land Ice Measurement from Space

ECMWF - European Centre for Medium-Range Weather Forecasts

MSS – Multispectral Scanner System

TM – Thematic Mapper

ETM+ – Enhanced Thematic Mapper plus.

OLI – Operational Land Imager

MSI – Multispectral Instrument

ASTER – Advanced Spaceborne Thermal Emission and Reflection Radiometer

SPOT - Satellite Pour l'Observation de la Terre

IPCC – Intergovernmental Panel on Climate Change

AMAP – Arctic Monitoring and Assessment Programme

SVM – Support Vector Machine

ANN – Artificial Neural Networks

CNN – Convolutional Neural Network

List of Figures

Figure 1 illustrates two main types of remote sensing, (A) Active and (B) passive remote sensing. Red arrows are the representation of reflected rays while yellow shows the emitted rays towards the target (CAP 2016.; Tammemagi 2012).....12

Figure 2 A) a debris-free glacier; B) the white arrow shows the debris-covered part of the glacier; C) representing the difference between supraglacial and periglacial debris-covered (Shukla et al. 2010). 14

Figure 3: The spectral curve of snow/debris-free glacier with the band positions of Landsat (5,7,8), from visible to short wave infrared region (Shao et al. 2020). 20

Figure 4: The study area of Novaya Zemlya, with glaciers outlines from RGI 6.0 shown. The ESRI World Ocean and World Terrain base maps are used in the background.....44

Figure 5: Workflow of the method for creating glacier outlines in Google Earth Engine. The green box shows the automated steps in Google Earth Engine, while orange shows the post-processing steps in ArcMap 10.5.1. 49

Figure 6: The process of generating outlines using an object-based image analysis approach in Google Earth Engine: (a) a false color composite of a Landsat 8 image (OLI Bands SWIR1, NIR, and Red); (b) the result of simple non-iterative clustering segmentation; (c) the final glacier outline, overlain on the original image.....51

Figure 7: The total area changes for lake, marine, and land-terminating glaciers in both km^2 (a) and percent area (b).....56

Figure 8: Area changes of Novaya Zemlya glaciers, (a) from 1986-89 to 2000-01 and (b) 2000-01 to 2019-21 in km^2, and (c) from 1986-89 to 2000-01 and (d) 2000-01 to

2019-21 as a percent. Stars in a and c show glaciers that surged during the 1986-89 and 2000-01 period. 57

Figure 9: Percent area change vs glacier area for each glacier from 1986-89 to 2019-21, for (a) lake-terminating, (b) marine-terminating, and (c) land-terminating glaciers. 58

Figure 10 Area change for glaciers on the Barents Sea vs Kara Sea (a) in km2 and (b) as a percentage. 60

Figure 11: Area change of marine (a, d), land (b, e) and lake-terminating (c, f) glaciers on the Barents Sea vs Kara Sea, in km2 (a-c) and percent area (d-f). 61

Figure 12: Time series of Landsat images showing Pavlov Glacier (RGI60-09.00070) in (a) 1986-07-26, (b) 2000-07-31, and (c) 2019-08-20, showing a clear advance associated with a surge between 1986 and 2000. 62

Figure 13: (a) Percent area change (2000-01 to 2019-21) and (b) area-averaged mass change (2000-2020) from Hugonnet et al. (2021) for each glacier type. 63

Figure 14: Area-averaged mass change (2000-2020) from Hugonnet et al. (2021) vs percent area change (2000-01 to 2019-21) for each glacier. 64

Figure 15: Comparison between object-based image analysis, Band Ratio, and Corrected outlines for two different sites in Novaya Zemlya. 65

Figure 16 The three study areas: A. Kenai, Alaska; B. Baffin, Canada; and C. Disko, Greenland. Red polygons show the RGI 6.0 outlines of the glaciers selected for the study. 82

Figure 17 The total area loss of Baffin, Disko, and Kenai glaciers from 1985-86 to 2000-02 and 2000-02 to 2019-21, in both area and percent area. A and C shows the area loss of glacier in km^2 while B and D show the area loss in percentage. 91

Figure 18 Represent the glacier area changes from 1985-86 to 2000-02 (A, B, and C) and between 2000-02-2019-21 (D, E, and F). (A-D) shows Baffin, (B-E) Disko, and (C-F) Kenai Alaska. The stars in B and E represent the surged glaciers. 92
Figure 19 Area loss of four regions in km^2 per year between two time periods. Data for Novaya Zemlya from Ali et al. (2023). 93
Figure 20 Representing the glaciers that have been retreated more than 80% of their areas during 1985-86 and 2019-21, x-axis shows the area of glacier from 1985-86 94
Figure 21 Annually average temperature of Baffin, Disko, and Kenai. The dashed line represents the average temperature of the study time periods. 95
Figure 22 Summer months (May-September) average temperature of Baffin, Disko, and Kenai. The dashed line represents the average temperature of the study time periods. 96
Figure 23 (A) shows total glacier area change (2000-02 to 2019-21) and (B) represent area-averaged mass change (2000-2020) from (Hugonnet et al. 2021). 97
Figure 24:The four study areas are, A) Novaya Zemlya; B) Baffin Island; C) Disko Island; and D) Kenai, Alaska. The red polygons in the insert images are the selected glaciers from RGI. 109
Figure 25. A close-up example of the area changes of glaciers mapped in Disko Island in 1985, 2001, and 2019. The Landsat images used for mapping are labelled in A-C. Black polygons were derived from Landsat 5 in 1985, Yellow from Landsat 7 in 2001 and Red from Landsat 8 in 2019. D shows a composite of the mapping done in three time periods, each colour represents a separate year and clearly illustrates the level of glacial change at this location. 114

Figure 26. A) the area loss of glacier in Novaya Zemlya, B) Baffin Island, C) Disko Island, and D) Kenai from 1985-89 to 2000-02 and between 2000-02 to 2019-21. 115

List of Tables

Table 1 The table shows the launch date, swath width, the spatial and temporal resolution of the main optical open-source satellites. 16

Table 2 List of spectral bands of Landsat 5, 7, and 8 (TM, ETM+, and OLI/TIRS).....18

Table 3: Details of images that are used in this study. 45

Table 4 Confusion matrices of each layer generated based on random sampling..52

Table 5 Computed areas (in km^2) of each layer based on the ±30 m buffer. 53

Table 6: The total area (in km^2) of glaciers computed manually corrected outlines (± 1 pixel buffer), both including and excluding glaciers that surged, and the automatically generated outlines (± 95% confidence interval) 55

Table 7: Details of images that are used in this study. 84

Table 8 Confusion matrices of each layer in Baffin, Disko, and Kenai generated based on random sampling. 88

Table 9 Computed areas (in km2) of each layer based on the ±30 m buffer. 89

Table 10 Overall accuracy and kappa coefficient of each layer of Baffin, Disko, and Kenai based on random sampling. 90

Table 11: Details of images that are used in this study for each location. 110

Table 12 Shows the UTM projection information used for each study area. 112

Chapter 1

Introduction

1.1. Introduction

The cryosphere is an important part of the earth's climate system that interacts with humans and natural environments (Marshall 2011; Rees 2006). Glaciers are one of the key elements of the cryosphere that store 75% of fresh water on the Earth, with the majority of that water being stored in the Antarctic and Greenland ice sheets (IPCC 2014). Glaciers play an important role in providing economic benefits to societies, as they are major tourist destinations, attracting millions of tourists each year for activities such as hiking, skiing, and ice climbing (Wang and Zhou 2019). Glaciers also support diverse ecosystems, which provide habitat for a variety of plant and animal species (Cauvy-Fraunié and Dangles 2019). Their meltwater is vital for many locations, particularly arid countries like Pakistan and Peru, where glacier meltwater is necessary for agriculture and many regions rely on this water for hydroelectric power generation (e.g, Biemans et al. 2019; Nie et al. 2021).

As a result of climate change, these large freshwater reservoirs are now melting at a fast rate, increasing global sea level (Hugonnet et al. 2021; Zemp et al. 2019) and there is growing concern about their instability in a warming world (e.g., Catania et al. 2020). Therefore, it is important to conduct research that can accurately monitor their trajectory that can inform mitigation strategies (Wrathall et al. 2019).

Another important element of the cryosphere that serves a vital purpose in regulating the Global Climate system is that snow and ice reflect the sun’s energy back into space due to having a higher albedo than darker land and sea surfaces. This reflection helps control the Earth's temperature by reducing surface temperatures that heat the atmosphere by radiating longwave infrared radiation

(Zarnetske et al. 2021). As global temperatures continue to rise, the loss of ice from the cryosphere has the potential to be part of a negative feedback loop that leads to the loss of further land and sea ice and increased surface and ocean warming. As surfaces with a lower albedo appear there is greater potential for increase absorption of incoming solar radiation and heating of the Earth's climate. Since 1880, the average global annual temperature has increased by 0.07°C per decade and started to increase at twice that rate after 1980 (NOAA 2019), a negative feedback loop as a result of ice loss has the potential to play an important role in future warming.

Climate change has led to the shrinking of the cryosphere, increased permafrost temperature, reduced glacier and ice volume, and reduced snow cover extent in the Arctic region (IPCC 2019). As a result of climate change, the Arctic is warming more rapidly than in any other region in the world (Dai et al. 2019). According to studies by Schädel et al. (2018) and You et al. (2021), the Arctic temperature over the last few decades increased more than twice as much as anywhere else in the world. A more recent study by Rantanen et al. (2022) suggests that Arctic warming has accelerated even further since 1979, with estimates indicating to be as much as four times higher than other parts of the world.

The Arctic plays an important role in the Earth's Climate System and changes in the Arctic can have impacts worldwide, including influencing ocean circulation and weather patterns, and Global sea level rise (AMAP 2017). Global sea-level rise is a major impact of climate change, that threatens millions of people living in or near the coastal areas and has the potential to displace populations all over the world

(Kulp and Strauss 2019). The main sources of global sea-level rise are ocean warming (thermal expansion) and melting ice sheets (IPCC 2021), especially Greenland which is the largest contributor of the 21st century (King et al. 2020).

Researchers have confirmed that most of the glaciers in the Arctic are thinning/retreating and contributing to sea level. For example, excluding the Greenland and Antarctic ice sheets, glaciers contributed 27±22mm of fresh water to global sea level from 1961 to 2016 (Zemp et al. 2019). Shepherd et al. (2020) found that between 1992 and 2018, Greenland Ice Sheet lost 3,902 ± 342 billion tonnes of ice, causing the mean sea level to rise by 10.8 ± 0.9 millimetres. Ciracì et al. (2020) observed the mass changes of glaciers and ice caps across the world and found that seven regions such as Alaska, Canadian Arctic Archipelago, Southern Andes, High Mountain Asia, Russian Arctic, Iceland, and Svalbard lost the most mass, with the largest share from Arctic between 2002 and 2019. Gardner et al. (2011) determined that the Canadian Arctic has lost 61±7 gigatons of ice per year from 2003 to 2009 contributing 0.17±0.02mm/year to sea-level rise. Howat and Eddy (2012) observed rapid retreat in all parts of the Greenland ice sheet and found that 90% of the Greenland glaciers retreated between 2000 and 2010. Carr et al. (2017) evaluated glaciers in Greenland, Svalbard, and the Russian Arctic and found that 97% of the selected glaciers across these three Arctic regions have retreated.

In addition to the threat of Global sea-level rise to coastal communities, changes in glaciers can interrupt the supply of water resources for drinking, agriculture and energy production (Zhang et al. 2022), as well as have a negative impact on industries such tourism and agriculture. Rapid changes can be hazardous for

mountain communities resulting in a higher frequency of events such as glacier avalanches (Jacquemart and Cicoira 2022) and Glacial Lake outburst floods (GLOFs) which can rapidly devastate a community, causing catastrophic landslides, flash floods, widespread destruction and death (Vilca et al. 2021).

Given the importance of glaciers in the Arctic and their potential to impact large parts of the whole world, it is necessary to develop more automated methods that can easily monitor regional glacial changes and provide a clear understanding of the climate change impacts on the glaciers in the Arctic. To monitor glacier changes over a vast region like the Arctic, remote sensing is an ideal tool as it can be used to map large glacierized areas relatively quickly (e.g., Winsvold et al 2014).

1.2. Aims and Objectives

The aim of this dissertation is to develop a new methodology for automated glacier mapping, that can be easily applicable in different regions, as well as to provide a clearer understanding of the impacts that climate change is having on Arctic glaciers.

The main objectives are to:

- Develop an automated remote sensing methodology for mapping glaciers that can be applied across the Arctic region.
- Create outlines of glaciers across the Arctic region for three different time periods: 1985-89, 2000-02, and 2019-21.
- Quantify glacier area changes in the Arctic region.
- Evaluate the changes in temperature against changes in glacier areas.

- Compare the derived area changes of glaciers with mass loss (Hugonnet et al. 2021).

1.3. References

AMAP. 2017. Snow, Water, Ice and Permafrost in the Arctic (SWIPA) 2017. Arctic Monitoring and Assessment Programme (AMAP), Oslo, Norway. Xiv + 269 Pp. ISBN 978-82-7971-101-8.

Biemans, H., C. Siderius, A. F. Lutz, S. Nepal, B. Ahmad, T. Hassan, W. von Bloh, R. R. Wijngaard, P. Wester, A. B. Shrestha, and W. W. Immerzeel. 2019. 'Importance of Snow and Glacier Meltwater for Agriculture on the Indo-Gangetic Plain'. Nature Sustainability 2(7):594–601. doi: 10.1038/s41893-019-0305-3.

Carr, J. Rachel, Chris R. Stokes, and Andreas Vieli. 2017. 'Threefold Increase in Marine-Terminating Outlet Glacier Retreat Rates across the Atlantic Arctic: 1992–2010'. Annals of Glaciology 58(74):72–91. doi: 10.1017/aog.2017.3.

Catania, G. A., L. A. Stearns, T. A. Moon, E. M. Enderlin, and R. H. Jackson. 2020. 'Future Evolution of Greenland's Marine-Terminating Outlet Glaciers'. Journal of Geophysical Research: Earth Surface 125(2):e2018JF004873. doi: 10.1029/2018JF004873.

Cauvy-Fraunié, Sophie, and Olivier Dangles. 2019. 'A Global Synthesis of Biodiversity Responses to Glacier Retreat'. Nature Ecology & Evolution 3(12):1675–85. doi: 10.1038/s41559-019-1042-8.

Ciracì, E., I. Velicogna, and S. Swenson. 2020. 'Continuity of the Mass Loss of the World's Glaciers and Ice Caps From the GRACE and GRACE Follow-On Missions'. Geophysical Research Letters 47(9):e2019GL086926. doi: 10.1029/2019GL086926.

Dai, Aiguo, Dehai Luo, Mirong Song, and Jiping Liu. 2019. 'Arctic Amplification Is Caused by Sea-Ice Loss under Increasing CO 2'. Nature Communications 10(1):1–13. doi: 10.1038/s41467-018-07954-9.

Gardner, Alex S., Geir Moholdt, Bert Wouters, Gabriel J. Wolken, David O. Burgess, Martin J. Sharp, J. Graham Cogley, Carsten Braun, and Claude Labine. 2011. 'Sharply Increased Mass Loss from Glaciers and Ice Caps in the Canadian Arctic Archipelago'. Nature 473(7347):357–60. doi: 10.1038/nature10089.

Howat, Ian M., and Alex Eddy. 2012. 'Multi-Decadal Retreat of Greenland ' s Marine-Terminating Glaciers'. 57(203):389–96.

Hugonnet, Romain, Robert McNabb, Etienne Berthier, Brian Menounos, Christopher Nuth, Luc Girod, Daniel Farinotti, Matthias Huss, Ines Dussaillant, Fanny Brun, and Andreas Kääb. 2021. 'Accelerated Global Glacier Mass Loss in the Early Twenty-First Century'. Nature 592(7856):726–31. doi: 10.1038/s41586-021-03436-z.

IPCC. 2021. 'Climate Change 2021: The Physical Science Basis. Contribution of Working Group I to the Sixth Assessment Report of the Intergovernmental Panel on Climate Change [Masson-Delmotte, V., P. Zhai, A. Pirani, S.L. Connors, C. Péan, S. Berger, N. Caud, Y. Chen, L. Goldfarb, M.I. Gomis, M. Huang, K. Leitzell, E. Lonnoy, J.B.R. Matthews, T.K. Maycock, T. Waterfield, O. Yelekçi, R. Yu, and B. Zhou (Eds.)]. Cambridge University Press. In Press.' (September):43.

IPCC, 2014. n.d. ‘IPCC, 2014: Annex II: Glossary [Mach, K.J., S. Planton and C. von Stechow (Eds.)]. In: Climate Change 2014: Synthesis Report. Contribution of Working Groups I, II and III to the Fifth Assessment Report of the Intergovernmental Panel on Climate Change [Core Writing Team, R.K. Pachauri and L.A. Meyer (Eds.)]. IPCC, Geneva, Switzerland, Pp. 117-130.’ Retrieved 8 November 2021 (https://www.ipcc.ch/report/ar5/syr/).

IPCC, 2019. n.d. ‘Climate Change and Land: An IPCC Special Report on Climate Change, Desertification, Land Degradation, Sustainable Land Management, Food Security, and Greenhouse Gas Fluxes in Terrestrial Ecosystems [P.R. Shukla, J. Skea, E. Calvo Buendia, V. Masson-Delmotte, H.-O. Pörtner, D. C. Roberts, P. Zhai, R. Slade, S. Connors, R. van Diemen, M. Ferrat, E. Haughey, S. Luz, S. Neogi, M. Pathak, J. Petzold, J. Portugal Pereira, P. Vyas, E. Huntley, K. Kissick, M. Belkacemi, J. Malley, (Eds.)].’ Retrieved 9 November 2021 (https://www.ipcc.ch/srccl/cite-report/).

Jacquemart, Mylène, and Alessandro Cicoira. 2022. ‘4.18 - Hazardous Glacier Instabilities: Ice Avalanches, Sudden Large-Volume Detachments of Low-Angle Mountain Glaciers, and Glacier Surges’. Pp. 330–45 in Treatise on Geomorphology (Second Edition), edited by J. (Jack) F. Shroder. Oxford: Academic Press.

King, Michalea D., Ian M. Howat, Salvatore G. Candela, Myoung J. Noh, Seongsu Jeong, Brice P. Y. Noël, Michiel R. van den Broeke, Bert Wouters, and Adelaide Negrete. 2020. ‘Dynamic Ice Loss from the Greenland Ice Sheet Driven by Sustained Glacier Retreat’. Communications Earth & Environment 1(1):1–7. doi: 10.1038/s43247-020-0001-2.

Kulp, Scott A., and Benjamin H. Strauss. 2019. ‘New Elevation Data Triple Estimates of Global Vulnerability to Sea-Level Rise and Coastal Flooding’. Nature Communications 10(1):4844. doi: 10.1038/s41467-019-12808-z.

Lehmann-Konera, Sara, Marek Ruman, Krystyna Kozioł, Grzegorz Gajek, and Żaneta Polkowska. 2017. ‘Glaciers as an Important Element of the World Glacier Monitoring Implemented in Svalbard’. Glaciers Evolution in a Changing World 3–36. doi: 10.5772/intechopen.69237.

Marshall, Shawn J. 2011. The Cryosphere. Princeton University Press.

Nie, Yong, Hamish D. Pritchard, Qiao Liu, Thomas Hennig, Wenling Wang, Xiaoming Wang, Shiyin Liu, Santosh Nepal, Denis Samyn, Kenneth Hewitt, and Xiaoqing Chen. 2021. ‘Glacial Change and Hydrological Implications in the Himalaya and Karakoram’. Nature Reviews Earth & Environment 2(2):91–106. doi: 10.1038/s43017-020-00124-w.

NOAA. n.d. NOAA National Centers for Environmental Information, State of the Climate: Global Climate Report for Annual 2019.

Rantanen, Mika, Alexey Yu Karpechko, Antti Lipponen, Kalle Nordling, Otto Hyvärinen, Kimmo Ruosteenoja, Timo Vihma, and Ari Laaksonen. 2022. ‘The Arctic Has Warmed Nearly Four Times Faster than the Globe since 1979’. Communications Earth & Environment 3(1):1–10. doi: 10.1038/s43247-022-00498-3.

Rees, Gareth. 2006. Remote Sensing of Snow and Ice.

Schädel, Christina, Charles D. Koven, David M. Lawrence, Gerardo Celis, Anthony J. Garnello, Jack Hutchings, Marguerite Mauritz, Susan M. Natali, Elaine Pegoraro, Heidi Rodenhizer, Verity G. Salmon, Meghan A. Taylor, Elizabeth E. Webb, William R. Wieder, and Edward AG Schuur. 2018. 'Divergent Patterns of Experimental and Model-Derived Permafrost Ecosystem Carbon Dynamics in Response to Arctic Warming'. 13(10):105002. doi: 10.1088/1748-9326/aae0ff.

Shepherd, A., E. Ivins, E. Rignot, B. Smith, M. van den Broeke, I. Velicogna, P. Whitehouse, K. Briggs, I. Joughin, G. Krinner, S. Nowicki, T. Payne, T. Scambos, N. Schlegel, G. A, C. Agosta, A. Ahlstrøm, G. Babonis, V. R. Barletta, A. A. Bjørk, A. Blazquez, J. Bonin, W. Colgan, B. Csatho, R. Cullather, M. E. Engdahl, D. Felikson, X. Fettweis, R. Forsberg, A. E. Hogg, H. Gallee, A. Gardner, L. Gilbert, N. Gourmelen, A. Groh, B. Gunter, E. Hanna, C. Harig, V. Helm, A. Horvath, M. Horwath, S. Khan, K. K. Kjeldsen, H. Konrad, P. L. Langen, B. Lecavalier, B. Loomis, S. Luthcke, M. McMillan, D. Melini, S. Mernild, Y. Mohajerani, P. Moore, R. Mottram, J. Mouginot, G. Moyano, A. Muir, T. Nagler, G. Nield, J. Nilsson, B. Noël, I. Otosaka, M. E. Pattle, W. R. Peltier, N. Pie, R. Rietbroek, H. Rott, L. Sandberg Sørensen, I. Sasgen, H. Save, B. Scheuchl, E. Schrama, L. Schröder, K. W. Seo, S. B. Simonsen, T. Slater, G. Spada, T. Sutterley, M. Talpe, L. Tarasov, W. J. van de Berg, W. van der Wal, M. van Wessem, B. D. Vishwakarma, D. Wiese, D. Wilton, T. Wagner, B. Wouters, and J. Wuite. 2020. 'Mass Balance of the Greenland Ice Sheet from 1992 to 2018'. Nature 579(7798):233–39.

Vilca, Oscar, Martin Mergili, Adam Emmer, Holger Frey, and Christian Huggel. 2021. 'The 2020 Glacial Lake Outburst Flood Process Chain at Lake Salkantaycocha (Cordillera Vilcabamba, Peru)'. Landslides 18(6):2211–23. doi: 10.1007/s10346-021-01670-0.

Wang, Shi-Jin, and Lan-Yue Zhou. 2019. 'Integrated Impacts of Climate Change on Glacier Tourism'. Advances in Climate Change Research 10(2):71–79. doi: 10.1016/j.accre.2019.06.006.

Winsvold, S. H., L. M. Andreassen, and C. Kienholz. 2014. 'Glacier Area and Length Changes in Norway from Repeat Inventories'. Cryosphere 8(5):1885–1903. doi: 10.5194/tc-8-1885-2014.

Wrathall, D. J., V. Mueller, P. U. Clark, A. Bell, M. Oppenheimer, M. Hauer, S. Kulp, E. Gilmore, H. Adams, R. Kopp, K. Abel, M. Call, J. Chen, A. deSherbinin, E. Fussell, C. Hay, B. Jones, N. Magliocca, E. Marino, A. Slangen, and K. Warner. 2019. 'Meeting the Looming Policy Challenge of Sea-Level Change and Human Migration'. Nature Climate Change 9(12):898–901. doi: 10.1038/s41558-019-0640-4.

You, Qinglong, Ziyi Cai, Nick Pepin, Deliang Chen, Bodo Ahrens, Zhihong Jiang, Fangying Wu, Shichang Kang, Ruonan Zhang, Tonghua Wu, Pengling Wang, Mingcai Li, Zhiyan Zuo, Yanhong Gao, Panmao Zhai, and Yuqing Zhang. 2021. 'Warming Amplification over the Arctic Pole and Third Pole: Trends, Mechanisms and Consequences'. Earth-Science Reviews 217:103625. doi: 10.1016/j.earscirev.2021.103625.

Zarnetske, Phoebe L., Jessica Gurevitch, Janet Franklin, Peter M. Groffman, Cheryl S. Harrison, Jessica J. Hellmann, Forrest M. Hoffman, Shan Kothari, Alan Robock,

Simone Tilmes, Daniele Visioni, Jin Wu, Lili Xia, and Cheng-En Yang. 2021. 'Potential Ecological Impacts of Climate Intervention by Reflecting Sunlight to Cool Earth'. Proceedings of the National Academy of Sciences 118(15):e1921854118. doi: 10.1073/pnas.1921854118.

Zemp, M., M. Huss, E. Thibert, N. Eckert, R. McNabb, J. Huber, M. Barandun, H. Machguth, S. U. Nussbaumer, I. Gärtner-Roer, L. Thomson, F. Paul, F. Maussion, S. Kutuzov, and J. G. Cogley. 2019. 'Global Glacier Mass Changes and Their Contributions to Sea-Level Rise from 1961 to 2016'. Nature 568(7752):382–86. doi: 10.1038/s41586-019-1071-0.

Zhang, Ting, Dongfeng Li, Amy E. East, Desmond E. Walling, Stuart Lane, Irina Overeem, Achim A. Beylich, Michèle Koppes, and Xixi Lu. 2022. 'Warming-Driven Erosion and Sediment Transport in Cold Regions'. Nature Reviews Earth & Environment 3(12):832–51. doi: 10.1038/s43017-022-00362-0.

Chapter 2

Background – review

2.1. Introduction of remote sensing

The process of obtaining information about an object without any physical contact with to it is called remote sensing (Campbell and Wynne 2011). Satellite remote sensing refers to acquiring information in a particular range of electromagnetic (EM) spectrum through mounted sensors on satellites (Pettorelli et al. 2018). There are two main types of remote sensing, active and passive (Figure 1). In active remote sensing, the sensor emits energy toward the target and measures the amount of energy reflected back again to the sensor, while passive remote sensing does not involve the sensor emitting energy; rather, the sensor measures the natural radiation emitted or reflected by the Earth's surface (Aggarwal 2004).

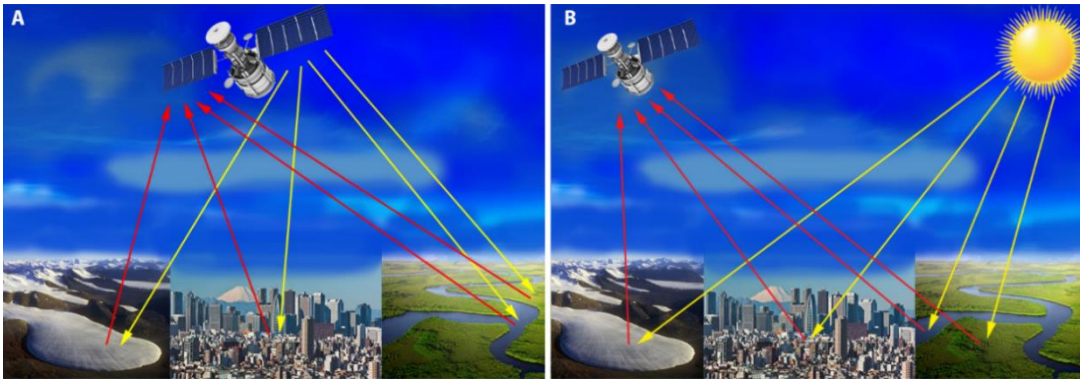

Figure 1 illustrates two main types of remote sensing, (A) Active and (B) passive remote sensing. Red arrows are the representation of reflected rays while yellow shows the emitted rays towards the target (CAP 2016.; Tammemagi 2012).

Remote sensing enables mapping of glaciers at both a regional and global scale in rough terrain and highly remote areas that are not feasible to monitor in the field (Racoviteanu, Arnaud, et al. 2008). Glacier surfaces are not only snow/ice, they can also be covered by rock debris and surface moraines. When covered in moraines or

has a layer of rock debris or other material covering its surface they are known as debris-covered glaciers whilst glaciers whose surfaces are free of debris are known as clean glaciers (Benn and Evans 2014) (Figure 2).

Mapping glaciers using remote sensing data depends on the spectral response of the glaciers. Spectral response refers to how an object reflects, absorbs, or emits electromagnetic radiation at different wavelengths. Methods for mapping debris-free glaciers (Figure 2A) are well established, as snow and ice have distinct spectral signatures to the surrounding terrain (e.g., Albert 2002; Paul et al. 2016). Debris-covered glaciers (Figure 2B) are more difficult to map because of the similar spectral response of the surrounding terrain (Ghosh et al. 2014). As demonstrated in Figure 2C, the periglacial debris is sediment, rock and other materials that accumulates at the base of glacier while supraglacial debris is debris that is deposited on glacier surface from rockfalls, landslides, other forms of erosion, and thus both has a similar spectral response (Paul et al. 2004).

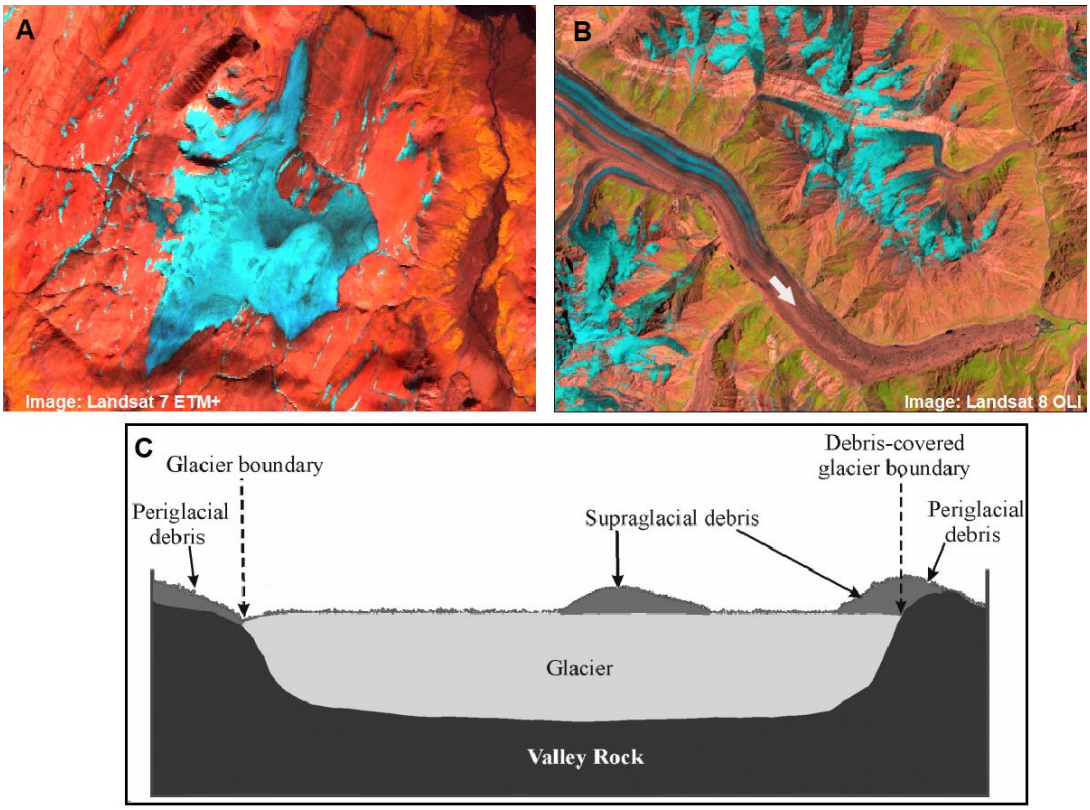

Figure 2 A) a debris-free glacier; B) the white arrow shows the debris-covered part of the glacier; C) representing the difference between supraglacial and periglacial debris-covered (Shukla et al. 2010).

2.2. Optical remote sensing satellites

Satellites with optical sensors are designed to measure reflected and radiated energy from the earth's surface in a well-defined range of the electromagnetic spectrum (Young et al. 2017). Every sensor records the reflected energy differently in terms of the spatial, spectral, radiometric, and temporal resolution. Spatial resolution relates to the smallest object that can be detected by the sensor; for example, a 30-metre spatial resolution represents an area of 30m x 30m on the ground. Temporal resolution is the revisit time of the same location by the satellite

(Théau 2008). Spectral resolution refers to the ability of the sensor to distinguish between spectral features/details, while the radiometric resolution is the sensor's ability to detect the variation of reflected energy from an area (Ose et al. 2016).

In the early 1970s, aerial photographs were the primary source of remote sensing for extracting glacier parameters (Racoviteanu et al. 2008). In most of the world, aerial photographs are not available due to the high survey costs or for political reasons where reconnaissance flights are not permitted (Racoviteanu al. 2008). Prior to the 1970s, there were spy satellites (e.g., Corona and Hexagon) that are now available to use for research purposes such as archaeological and historical research. The initial large-scale monitoring of glaciers using remote sensing started in the 1970s with the launch of the Landsat 1 satellite mission which had multispectral scanning capabilities in the visible and infrared part of the spectrum. Many other important optical satellites have since been launched following the successes of the early missions such as Landsat 5, 7, 8, and 9 that were launched in 1984, 1999, 2013 and 2021 respectively. The Advanced Spaceborne Thermal Emission and Reflection Radiometer (ASTER) sensor onboard the Terra satellite was launched in 1999 with a Moderate Resolution Imaging Spectroradiometer (MODIS) sensor, and Sentinel 2 Multi-Spectral Instrument (MSI) was launched in 2015 (Table 1).

Table 1 The table shows the launch date, swath width, the spatial and temporal resolution of the main optical open-source satellites.

Optical sensors	**Landsat TM, EMT+, OLI**	**ASTER**	**MODIS**	**Sentinel-2 MSI**
Launch date	1984, 1999, 2013,	1999	1999	2015
Revisit time	16 Days	16 Days	1-2 Days	10
Spatial resolution	30m to 120m	15m to 60m	250m to 1000m	10m to 60m
Swath width	185km	60km	2330km	290km

Landsat Thematic Mapper (TM), Enhanced Thematic Mapper Plus (ETM+), and Operational Land Imager (OLI) have become the primary source for glacier mapping due to the longer temporal record of images compared to other systems and have been widely used by many researchers. Zhang et al. (2019) used Landsat satellite sensors to map glacier changes in Central Asia from 1975 to 2016, and showed that warming temperature was one of the main reasons for glaciers melting in the Aksu River Basin (Central Asia). Morris et al. (2006) used Landsat and ASTER sensors to map glaciers in Colombian and Venezuela from 1984 to 2004, Earl and Gardner (2016) created outlines of glaciers in North Asia using Landsat sensors (TM, ETM+, and OLI). There are other optical sensors as well that provide data for glacier

mappings such as Satellite Pour l'Observation de la Terre (SPOT), IKONOS, ALOS, WorldView, GeoEye-1, RapidEye, and QuickBird but data from some of these sensors are expensive are not always freely available.

The swath width of the satellite is another important aspect to consider while selecting the sensor for glacier mapping for large regions like the Arctic. Swath width refers to the width of the image that the sensor can capture on the ground. MODIS acquires data between 250m and 1000m pixel size, with a 2330 km swath width and can used for wide-area analysis (Hall et al. 2006), but the resolution is too low for accurately delineating glaciers. Sentinel 2 MSI captures data at 10m to 20m spatial resolution from visible to shortwave infrared bands with a 290 km swath (Drusch et al. 2012). Sentinel-2 can be used to map glaciers on a regional basis, but it has a smaller archive of images (launched in 2015) which makes it a less suitable option for mapping glaciers over longer time spans. ASTER captures images with spatial resolution of 15-90m, and has the potential for debris-covered glacier mapping due to the availability of thermal bands (Sahu and Gupta 2020; Taschner and Ranzi 2002). However, ASTER has a smaller swath width (60km) than Landsat (185km), which limits the use of ASTER for regional glacier mapping. On the other hand, Landsat sensors such as TM, ETM+, and OLI/TIRS capture images at a medium resolution of 15m to 120m and the Landsat program's long image archive (1972-present) makes it an asset for glacier mapping. Details of Landsat TM, ETM+, and OLI/TIRS are shown in Table 2.

Table 2 represents, Landsat 5 TM consists of seven bands with a spatial resolution of 30m except band 6 which is 120m but resampled to 30m. Landsat 7 ETM+ has six bands (bands 1 to 5 and 7) with a spatial resolution of 30 metres, one thermal band which was collected at 60m but resampled to 30m, and one panchromatic band with 15m resolution. Landsat 8 OLI has eight bands with a 30 metres resolution, one panchromatic (15 metres), and two thermal bands having a resolution of 100 metres but resampled to 30 metres.

Table 2 List of spectral bands of Landsat 5, 7, and 8 (TM, ETM+, and OLI/TIRS).

Landsat 5 TM and Landsat 7 ETM+		**Landsat 8 OLI**	
Bands and wavelength (μm)	**Resolution**	**Bands and wavelength (μm)**	**Resolution**
Band 1 Blue (0.45-0.52)	30m	Band 1 Aerosol (0.43-0.45)	30m
Band 2 Green (0.52-0.61)	30m	Band 2 Blue (0.45-0.51)	30m
Band 3 Red (0.63-0.69)	30m	Band 3 Green (0.53-0.59)	30m
Band 4 NIR (0.76-0.90)	30m	Band 4 Red (0.64-0.67)	30m
Band 5 SWIR1 (1.55-1.75)	30m	Band 5 NIR (0.85-0.88)	30m
Band 6 Thermal (10.40-12.50)	(60)-30m	Band 6 SWIR1 (1.57-1.65)	30m
Band 7 SWIR 2 (2.08-2.35)	30m	Band 7 SWIR 2 (2.11-2.29)	30m
Band 8 Panchromatic (0.52-0.90) ETM+ only	15m	Band 8 Panchromatic (0.50-0.68)	15m
		Band 9 Cirrus (1.36-1.38)	30m
		Band 10 Thermal 1 (10.6-11.19)	(100)-30m
		Band 11 Thermal 2 (11.50-12.51)	(100)-30m

2.3. Methods for glacier mapping

2.3.1. Manual Delineation

Many studies have traditionally used manual digitisation to find and study the changes in the front position of glaciers through time (Carr et al. 2014, 2017; Howat and Eddy 2012; Moon and Joughin 2008), while some researchers have used manual digitisation to assess the accuracy of other semi-automated approaches to mapping (e.g., Alifu et al. 2015; Fischer et al. 2014; Paul et al. 2013; Shafique et al. 2018). Manual delineation is considered to be the most accurate method for glacier mapping (Albert 2002; Paul et al. 2017), but its accuracy depends on the analyst and it is time-consuming, especially when working on change assessment over a large region like the Arctic.

2.3.2. Index-based methods

Semi-automated methods such as Normalized Difference Snow Index (NDSI) and Band Ratio are easy to implement and can produce consistent results (Burns and Nolin 2014). In the band ratio method, the visible bands (green and red) or near-infrared band in the EM spectrum are divided by short SWIR which results in the "Ratio Image". In NDSI, the difference between visible (green or red) and SWIR bands is applied then divide with the addition of both bands resulting in a single band. These index-based methods utilise the different bands of the electromagnetic spectrum that make up the satellite image. Snow and ice are highly reflective in the

visible part of the electromagnetic spectrum, their reflectance starts to decrease in the near-infrared region, reaching nearly zero in the shortwave infrared (Jezek 2006) (see Figure 3). In both techniques, the resulting image shows high values over the glacier and low values over the non-glacier area such as rocks and vegetation (Raup et al. 2014). These high and low values assist to select the threshold which helps to create the binary mask that indicates glacier and non-glacier areas. Then glacier outline can be derived by converting the binary mask to vector.

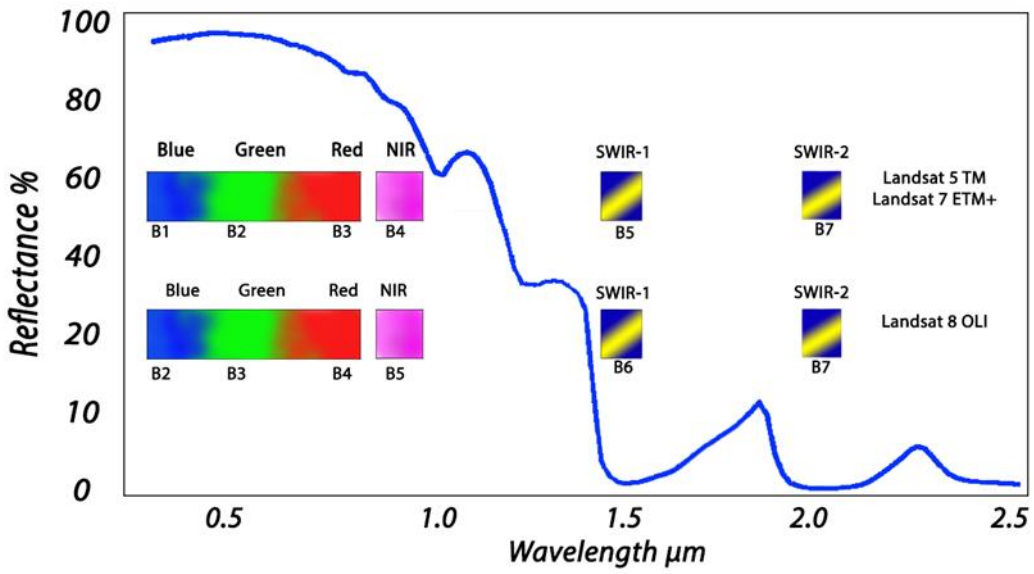

Figure 3: The spectral curve of snow/debris-free glacier with the band positions of Landsat (5,7,8), from visible to short wave infrared region (Shao et al. 2020).

Both Band Ratio and NDSI are well-established, fast, and robust methods for mapping clean glaciers over extensive areas (Paul et al. 2017). However, some difficulties are still present using these index-based methods. For example, mapping glaciers in the presence of lakes, clouds, shadow, and debris cover is known to cause

errors (Racoviteanu and Williams 2012). Band Ratio (visible/SWIR) is an effective method for mapping shadowed ice but tends to misclassify lakes (water bodies) as part of the glacier (Kääb et al. 2005; Paul et al. 2007). Band Ratio (NIR/SWIR) has also been used, but using NIR with SWIR is less effective in deep shadow (Burns and Nolin 2014). NDSI can provide more satisfactory results in the case of shaded ice (Racoviteanu, Arnaud, et al. 2008). The common problem of these techniques is when it comes to mapping debris cover glaciers, because NDSI and Band Ratio are using the multispectral response of ice to map glaciers but debris-covered glaciers have a similar reflectance to the surrounding terrain (Alifu et al. 2015). Therefore, a different approach is required to accurately map these systems.

2.3.3. Indices with morphometric parameters

Researchers have attempted to develop semi-automated methods for mapping using indices with morphometric parameters such as slope, aspect and curvature (e.g., Herreid and Pellicciotti 2020; Bhambri et al. 2011; Scherler et al. 2018; Bolch and Kamp 2006; Paul et al. 2004), while some have relied on manual delineation (Burns and Nolin 2014; Fischer et al. 2014). Paul et al. (2004) combined a multispectral classification technique with a DEM, showing that without the DEM, the method showed less promising results. Shafique et al. (2018) used NDSI with slope to delineate debris-covered glaciers. Ghosh et al. (2014) used Band Ratio with slope to map debris-covered glaciers. Although, combining slope (morphometric

parameters) with Band Ratio has proven useful and faster than the manual delineation of the glacier, it still requires manual editing (Ghosh et al. 2014).

Alifu et al. (2015) introduced a new method called “New Band Ratio” for mapping debris-covered glaciers. The common approach that was followed by researchers is to use a Digital Elevation Model (DEM) with indices (NDSI and Band Ratio) for mapping debris-covered glaciers, while this New Band Ratio method utilises the thermal, NIR, and SWIR (Thermal ÷ (NIR ÷ SWIR)) bands with the slope information obtained from a DEM. The thermal provides information about temperature changes on different surfaces, which helps in differentiating the debris-covered part of the glacier from other materials (Alifu et al. 2015). The thermal band can be used to differentiate between ice cover and debris-cover and increase the accuracy of the mapping. However, using only a thermal band for debris cover is limited, when the debris cover is thicker more than 40-50cm (Ranzi et al. 2004). Combining the thermal band with morphometric and multispectral data shows a promising result (Bolch et al. 2007), but manual editing will be still required for developing a semi-automated method for mapping debris-covered glaciers (Racoviteanu et al. 2008).

2.3.4. Machine learning techniques

There is a number of machine learning techniques that researchers have used for glacier mapping such as Support Vector Machine (SVM), Artificial Neural Network, (ANN), Convolutional Neural Network (CNN), Random Forest, Decision tree, spectral

angle mapper, and maximum likelihood (e.g., Khan et al. 2020; Kumar et al. 2020; Racoviteanu and Williams 2012; Robson et al. 2020).

Robson et al. (2020) used CNN and Object-Based Image Analysis (OBIA) to detect rock glaciers, finding that combining CNN with OBIA for mapping glaciers offers a promising result and leads to reduction of manual correction. Kumar et al. (2020) used the Maximum likelihood classifier to map glacier changes from 1987 to 2017 in Bhutan, and found the accuracy between 80% and 67.2%, and suggested that the higher spatial resolution of images can provide better accuracy. Khan et al. (2020) investigated three main machine learning classifiers for glacier mapping: Random Forest, SVM, and ANN, based on the three classes" glaciers", "debris-covered glaciers", and "non-glaciated area" splitting data into training (70%) and testing (30%) found that when compared random forest (Kappa: 0.95) performed better than ANN (Kappa: 0.92) and SVM (Kappa: 0.89). The OBIA approach has been used to map debris-covered glacier in the Manaslu region of Nepal and to compute decadal scale changes in glaciers in Hohe Tauern National Park in Austria by (Robson et al. 2015, 2016).

Most of these techniques are developed and tested for selected glaciers in a particular region. In the case of debris-covered glaciers, the developed method can be successful for that region but may not always be transferable to another region because of the distribution of debris-covered with diverse thicknesses (Bhambri et al. 2011). Most importantly, to map glacier changes over large areas at multiple

points in time, several satellite images are needed, and users must download and store each image locally on a laptop, desktop or local server. Processing large numbers of images on a desktop or laptop can be time-consuming, especially for large-scale mapping.

2.4. Glacier Inventory/outlines

The World Glacier Monitoring Service (WGMS) is an international organization, established in 1986 to monitor the world's glaciers. WGMS is based in Switzerland and Its primary goal is to collect and analyse data on the state of glaciers worldwide (WGMS 1989). The WGMS compiled the World Glacier Inventory (WGI), an inventory of glaciers at the global scale (Haeberli 1998; WGMS 1989). The World Glacier Inventory (WGI), a comprehensive database of glaciers around the world which is one of the main tasks of WGMS. The WGI contains information on the location, size, and other characteristics of over 200,000 glaciers worldwide (Eis 2020). The WGMS data, which is included in the WGI, has been used to better understand the state of the world's glaciers and the effects of climate change on them (Gärtner-Roer et al. 2019). . In addition, the WGMS collects standardised information on glacier area, volume, and mass changes (e.g., Zemp et al. 2013, 2009).

The increase in the number of earth observation satellites that are now available, coupled with sophisticated image processing software, led to the Global Land Ice

Measurements from Space (GLIMS) project. The aim of the GLIMS initiative is to improve our understanding of how glaciers and ice sheets are changing, and maintain an up-to-date inventory of glacier outlines (Raup et al. 2007). The central product of the GLIMS project is a glacier database that stores glacier outlines and key information such as size, elevation, and other glacier attributes. GLIMS outlines are freely accessible to the worldwide community via its website, https://www.glims.org/ (Racoviteanu et al. 2009; Raup et al. 2007).

The Randolph Glacier Inventory (RGI) is another global product that compiles glacier outlines and is supplementary to the GLIMS glacier database (Pfeffer et al. 2014). Despite these initiatives, multitemporal outlines of glaciers are still lacking for most parts of the world and researchers are still working on creating single and multi-temporal glacier outlines in various parts of the world to better understand how glaciers are responding to climate change in these regions. There are new glacier outlines generated for North Asia based on the NDSI method followed by manual editing using Landsat data (Earl and Gardner 2016). A Swiss glacier inventory for the year 2000 connected to the GLIMS project, was made using Landsat TM, ETM+, and ASTER imagery (Fischer et al. 2014; Paul et al. 2002).

A glacier inventory for the European Alps is also available derived from Landsat TM images from 2003 using the Band Ratio technique (Paul et al. 2011). Several glacier inventories are available for Norway including one for the Svartisen region that used mostly the Band Ratio technique to derive the mapping (Paul and Liss 2009),

additional inventories are also available forthe Jostedalsbreen region (Paul et al. 2011), and mainland Norway (Andreassen et al. 2012). Nuth et al., (2013) mapped new glacier outlines for Svalbard and Greenland using mostly Landsat images. Outlines of glaciers in southern Baffin Island, Canada were created by (Svoboda and Paul 2009) using ASTER data and Rastner et al. (2017) generated a new glacier inventory for Novaya Zemlya, Russian Arctic using the Band Ratio technique from Landsat 8 data.

Most of these glacier inventories provide glacier outlines at one point in time, meaning important multitemporal outlines are still lacking in most of the world, which impedes our understanding of how glaciers are changing through time in response to warming. These data are crucial for providing information to better understand the impacts of climate change, for modelling their future trajectories and quantifying their potential sea level contribution (Hock et al. 2019; Millan et al. 2022).

2.5. Conclusions

Given that the Arctic plays such an important role in the Earth's climate system by reflecting sunlight and trapping cold air, which helps to regulate global temperatures (Previdi et al. 2021). In recent years, Climate change has caused significant changes in the Arctic, including melting sea ice, glaciers and permafrost, which has resulted in rising sea levels (IPCC 2021). Arctic glaciers, ice caps, and the GrIS all contributed approximately 1.2mm to sea-level rise each year from 2003 to

2015 (Moon et al. 2019). These changes have far-reaching consequences not only for the Arctic region, but also for the rest of the world. The major research challenge for rapid monitoring of the Arctic will be to create a robust and automated methodology that can accurately create glaciers outlines through time at regional scale and to reduce the time of manual corrections. Such a tool would be of great benefit to the scientific community to allow continued assessment of the impacts that enhanced warming in the Pan-Arctic is having on the cryosphere. The main goal of this project is to develop are such an automated methodology and the detailed methodology is discussed in Chapter 3.

2.6. References

Aggarwal, V. Radha Krishna Murthy Shefali. 2004. 'Satellite Remote Sensing and GIS Applications in Agricultural Meteorology - Chp: Principles of Remote Sensing'. *Satellite Remote Sensing and GIS Applications in Agricultural Meteorology* 235.

Albert, Todd H. 2002. 'Evaluation of Remote Sensing Techniques for Ice-Area Classification Applied to the Tropical Quelccaya Ice Cap, Peru'. *Polar Geography* 26(3):210–26. doi: 10.1080/789610193.

Alifu, Haireti, Ryutaro Tateishi, and Brian Johnson. 2015. 'A New Band Ratio Technique for Mapping Debris-Covered Glaciers Using Landsat Imagery and a Digital Elevation Model'. *International Journal of Remote Sensing* 36(8):2063–75. doi: 10.1080/2150704X.2015.1034886.

Andreassen, Liss M., Solveig H. Winsvold, F. Paul, and J. E. Hausberg. 2012. *Inventory of Norwegian Glaciers*. Vol. 38.

Benn, Douglas, and David JA Evans. 2014. *Glaciers and Glaciation*. Routledge.

Bhambri, R., T. Bolch, and R. K. Chaujar. 2011. 'Mapping of Debris-Covered Glaciers in the Garhwal Himalayas Using ASTER DEMs and Thermal Data'. *International Journal of Remote Sensing* 32(23):8095–8119. doi: 10.1080/01431161.2010.532821.

Bolch, Tobias, Manfred Buchroithner, Andre Kunert, and Ulrich Kamp. 2007. 'Automated Delineation of Debris-Covered Glaciers Based on ASTER Data'. *Geoinformation in Europe (Proc. of 27th EARSel Symposium, 04-07 June 2007), Bozen, Italy.* (June):403–10.

Bolch, Tobias, and Ulrich Kamp. 2006. 'Glacier Mapping in High Mountains Using DEMs, Landsat and ASTER Data'. *Grazer Schriften Der Geographie Und Raumforschung* (1):37–48.

Burns, Patrick, and Anne Nolin. 2014. 'Using Atmospherically-Corrected Landsat Imagery to Measure Glacier Area Change in the Cordillera Blanca, Peru from 1987 to 2010'. *Remote Sensing of Environment* 140:165–78. doi: 10.1016/J.RSE.2013.08.026.

Campbell, James B., and Randolph H. Wynne. 2011. *Introduction to Remote Sensing*. Guilford Press.

CAP, News. n.d. 'Rivers Could Transform Transportation and Communications in South America'. Retrieved 26 March 2023 (https://www.caf.com/en/currently/news/2016/07/rivers-could-transform-transportation-and-communications-in-south-america/).

Carr, J. Rachel, Chris R. Stokes, and Andreas Vieli. 2017. 'Threefold Increase in Marine-Terminating Outlet Glacier Retreat Rates across the Atlantic Arctic: 1992–2010'. *Annals of Glaciology* 58(74):72–91. doi: 10.1017/aog.2017.3.

Carr, J. Rachel, Chris Stokes, and Andreas Vieli. 2014. 'Recent Retreat of Major Outlet Glaciers on Novaya Zemlya, Russian Arctic, Influenced by Fjord Geometry and Sea-Ice Conditions'. *Journal of Glaciology* 60(219):155–70. doi: 10.3189/2014JoG13J122.

Drusch, M., U. Del Bello, S. Carlier, O. Colin, V. Fernandez, F. Gascon, B. Hoersch, C. Isola, P. Laberinti, P. Martimort, A. Meygret, F. Spoto, O. Sy, F. Marchese, and P. Bargellini. 2012. 'Sentinel-2: ESA's Optical High-Resolution Mission for GMES Operational Services'. *Remote Sensing of Environment* 120:25–36. doi: 10.1016/j.rse.2011.11.026.

Earl, Lucas, and Alex Gardner. 2016. 'A Satellite-Derived Glacier Inventory for North Asia'. *Annals of Glaciology* 57(71):50–60. doi: 10.3189/2016AoG71A008.

Eis, Julia. 2020. 'Reconstructing Glacier Evolution Using a Flowline Model'.

Fischer, Mauro, Matthias Huss, Chloé Barboux, and Martin Hoelzle. 2014. 'The New Swiss Glacier Inventory SGI2010: Relevance of Using High-Resolution Source Data in Areas Dominated by Very Small Glaciers'. *Arctic, Antarctic, and Alpine Research* 46(4):933–45. doi: 10.1657/1938-4246-46.4.933.

Frank Paul, Andreas KÌÌb, Max Maisch, Tobias Kellenberger, Wilfried Haeberli. 2002. 'The New Remote-Sensing-Derived Swiss Glacier Inventory: I. Methods'. *Annals of Glaciology* 34(September 1985):362–66. doi: 10.3189/172756402781817473.

Gärtner-Roer, Isabelle, Samuel U. Nussbaumer, Fabia Hüsler, and Michael Zemp. 2019. 'Worldwide Assessment of National Glacier Monitoring and Future Perspectives'. *Mountain Research and Development* 39(2):A1–11. doi: 10.1659/MRD-JOURNAL-D-19-00021.1.

Ghosh, Swagata, Arvind C. Pandey, and Mahendra S. Nathawat. 2014. 'Mapping of Debris-Covered Glaciers in Parts of the Greater Himalaya Range, Ladakh, Western Himalaya, Using Remote Sensing and GIS'. *Journal of Applied Remote Sensing* 8(1):083579. doi: 10.1117/1.jrs.8.083579.

Haeberli, W. 1998. 'Historical Evolution and Operational Aspects of Worldwide Glacier Monitoring'. *Undefined*.

Hall, Dorothy K., R. S. Williams, K. A. Casey, N. E. DiGirolamo, and Z. Wan. 2006. 'Satellite-Derived, Melt-Season Surface Temperature of the Greenland Ice Sheet (2000-2005) and Its Relationship to Mass Balance'. *Geophysical Research Letters* 33(11):1–5. doi: 10.1029/2006GL026444.

Herreid, Sam, and Francesca Pellicciotti. 2020. 'The State of Rock Debris Covering Earth's Glaciers'. *Nature Geoscience* 13(9):621–27. doi: 10.1038/s41561-020-0615-0.

Hock, Regine, Andrew Bliss, Ben Marzeion, Rianne H. Giesen, Yukiko Hirabayashi, Matthias Huss, Valentina Radić, and Aimée B. A. Slangen. 2019. 'GlacierMIP – A Model Intercomparison of Global-Scale Glacier Mass-Balance Models and Projections'. *Journal of Glaciology* 65(251):453–67. doi: 10.1017/jog.2019.22.

Howat, Ian M., and Alex Eddy. 2012. 'Multi-Decadal Retreat of Greenland ' s Marine-Terminating Glaciers'. 57(203):389–96.

IPCC, 2021. 2021. *IPCC, 2021: Climate Change 2021: The Physical Science Basis. Contribution of Working Group I to the Sixth Assessment Report of the Intergovernmental Panel on Climate Change. [Masson-Delmotte, V., P. Zhai, A. Pirani, S.L. Connors, C. Péan, S. Berger, N. Caud, Y. Chen, L. Goldfarb, M.I. Gomis, M. Huang, K. Leitzell, E. Lonnoy, J.B.R. Matthews, T.K. Maycock, T. Waterfield, O. Yelekçi, R. Yu, and B. Zhou (Eds.)]. Cambridge University Press, Cambridge, United Kingdom and New York, NY, USA, In Press, Doi:10.1017/9781009157896.*

Jezek, Kenneth C. 2006. 'W.G. Rees 2006. Remote Sensing of Snow and Ice.' *Journal of Glaciology* 52(177):311–311. doi: 10.3189/172756506781828656.

Kääb, A., C. Huggel, L. Fischer, S. Guex, F. Paul, I. Roer, N. Salzmann, S. Schlaefli, K. Schmutz, D. Schneider, T. Strozzi, and Y. Weidmann. 2005. 'Remote Sensing of Glacier- and Permafrost-Related Hazards in High Mountains: An Overview'. *Natural Hazards and Earth System Science* 5(4):527–54. doi: 10.5194/nhess-5-527-2005.

Khan, Aftab Ahmed, Akhtar Jamil, Dostdar Hussain, Murtaza Taj, Gul Jabeen, and Muhammad Kamran Malik. 2020. 'Machine-Learning Algorithms for Mapping Debris-Covered Glaciers: The Hunza Basin Case Study'. *IEEE Access* 8:12725–34. doi: 10.1109/ACCESS.2020.2965768.

Kumar, Mithun, Ayad M. Fadhil Al-Quraishi, and Ismail Mondal. 2020. 'Glacier Changes Monitoring in Bhutan High Himalaya Using Remote Sensing Technology'. *Environmental Engineering Research* 26(1). doi: 10.4491/eer.2019.255.

Millan, Romain, Jérémie Mouginot, Antoine Rabatel, and Mathieu Morlighem. 2022. 'Ice Velocity and Thickness of the World's Glaciers'. *Nature Geoscience* 15(2):124–29. doi: 10.1038/s41561-021-00885-z.

Moon, Twila A., Irina Overeem, Matt Druckenmiller, Marika Holland, Henry Huntington, George Kling, Amy Lauren Lovecraft, Gifford Miller, Ted Scambos, Christina Schädel, Edward A. G. Schuur, Erin Trochim, Francis Wiese, Dee Williams, and Gifford Wong. 2019. 'The Expanding Footprint of Rapid Arctic Change'. *Earth's Future* 7(3):212–18. doi: 10.1029/2018EF001088.

Moon, Twila, and Ian Joughin. 2008. 'Changes in Ice Front Position on Greenland's Outlet Glaciers from 1992 to 2007'. *Journal of Geophysical Research: Earth Surface* 113(2):1–10. doi: 10.1029/2007JF000927.

Morris, Jennifer N., Alan J. Poole, and Andrew G. Klein. 2006. 'Retreat of Tropical Glaciers in Colombia and Venezuela from 1984 to 2004 as Measured from ASTER and Landsat Images'. (January 2006).

Ose, Kenji, Thomas Corpetti, and Laurent Demagistri. 2016. 'Multispectral Satellite Image Processing'. Pp. 58–124 in *Optical Remote Sensing of Land Surface: Techniques and Methods*. Elsevier Inc.

Paul, F., N. E. Barrand, S. Baumann, E. Berthier, T. Bolch, K. Casey, H. Frey, S. P. Joshi, V. Konovalov, R. Le Bris, N. Mölg, G. Nosenko, C. Nuth, A. Pope, A. Racoviteanu, P. Rastner, B. Raup, K. Scharrer, S. Steffen, and S. Winsvold. 2013. 'On the Accuracy of Glacier Outlines Derived from Remote-Sensing Data'. *Annals of Glaciology* 54(63):171–82. doi: 10.3189/2013AoG63A296.

Paul, F, H. Frey, and R. Le Bris. 2011. 'A New Glacier Inventory for the European Alps from Landsat TM Scenes of 2003: Challenges and Results'. *Annals of Glaciology* 52(59):144–52. doi: 10.3189/172756411799096295.

Paul, Frank, Liss M. Andreassen, and Solveig H. Winsvold. 2011. 'A New Glacier Inventory for the Jostedalsbreen Region, Norway, from Landsat TM Scenes of 2006 and Changes since 1966'. *Annals of Glaciology* 52(59):153–62. doi: 10.3189/172756411799096169.

Paul, Frank, Tobias Bolch, Kate Briggs, Andreas Kääb, Malcolm McMillan, Robert McNabb, Thomas Nagler, Christopher Nuth, Philipp Rastner, Tazio Strozzi, and Jan Wuite. 2017. 'Error Sources and Guidelines for Quality Assessment of Glacier Area, Elevation Change, and Velocity Products Derived from Satellite Data in the Glaciers_cci Project'. *Remote Sensing of Environment* 203:256–75. doi: 10.1016/j.rse.2017.08.038.

Paul, Frank, Christian Huggel, and Andreas Kääb. 2004. 'Combining Satellite Multispectral Image Data and a Digital Elevation Model for Mapping Debris-Covered Glaciers'. *Remote Sensing of Environment* 89(4):510–18. doi: https://doi.org/10.1016/j.rse.2003.11.007.

Paul, Frank, Andreas Kääb, and Wilfried Haeberli. 2007. 'Recent Glacier Changes in the Alps Observed by Satellite: Consequences for Future Monitoring Strategies'. *Global and Planetary Change* 56(1–2):111–22. doi: 10.1016/j.gloplacha.2006.07.007.

Paul, Frank, and M. Andreassen Liss. 2009. 'A New Glacier Inventory for the Svartisen Region, Norway, from Landsat ETM+ Data: Challenges and Change

Assessment'. *Journal of Glaciology* 55(192):607–18. doi: 10.3189/002214309789471003.

Paul, Frank, Solveig H. Winsvold, Andreas Kääb, Thomas Nagler, and Gabriele Schwaizer. 2016. 'Glacier Remote Sensing Using Sentinel-2. Part II: Mapping Glacier Extents and Surface Facies, and Comparison to Landsat 8'. *Remote Sensing* 8(7). doi: 10.3390/rs8070575.

Pettorelli, Nathalie, Henrike Schulte to Buehne, Aurélie Shapiro, and Paul Glover-Kapfer. 2018. 'Satellite Remote Sensing Conservation Technology 4 Satellite Remote Sensing'. *Conservation Technology Series WWF-UK* (4).

Pfeffer, W. Tad, Anthony A. Arendt, Andrew Bliss, Tobias Bolch, J. Graham Cogley, Alex S. Gardner, Jon Ove Hagen, Regine Hock, Georg Kaser, Christian Kienholz, Evan S. Miles, Geir Moholdt, Nico Mölg, Frank Paul, Valentina Radić, Philipp Rastner, Bruce H. Raup, Justin Rich, Martin J. Sharp, L. M. Andreassen, S. Bajracharya, N. E. Barrand, M. J. Beedle, E. Berthier, R. Bhambri, I. Brown, D. O. Burgess, E. W. Burgess, F. Cawkwell, T. Chinn, L. Copland, N. J. Cullen, B. Davies, H. De Angelis, A. G. Fountain, H. Frey, B. A. Giffen, N. F. Glasser, S. D. Gurney, W. Hagg, D. K. Hall, U. K. Haritashya, G. Hartmann, S. Herreid, I. Howat, H. Jiskoot, T. E. Khromova, A. Klein, J. Kohler, M. König, D. Kriegel, S. Kutuzov, I. Lavrentiev, R. Le Bris, X. Li, W. F. Manley, C. Mayer, B. Menounos, A. Mercer, P. Mool, A. Negrete, G. Nosenko, C. Nuth, A. Osmonov, R. Pettersson, A. Racoviteanu, R. Ranzi, M. A. Sarikaya, C. Schneider, O. Sigurdsson, P. Sirguey, C. R. Stokes, R. Wheate, G. J. Wolken, L. Z. Wu, and F. R. Wyatt. 2014. 'The Randolph Glacier Inventory: A Globally Complete Inventory of Glaciers'. *Journal of Glaciology* 60(221):537–52. doi: 10.3189/2014JoG13J176.

Previdi, Michael, Karen L. Smith, and Lorenzo M. Polvani. 2021. 'Arctic Amplification of Climate Change: A Review of Underlying Mechanisms'. *Environmental Research Letters* 16(9):093003. doi: 10.1088/1748-9326/ac1c29.

Racoviteanu, Adina E., Yves Arnaud, Mark W. Williams, and Julio Ordoñez. 2008. 'Decadal Changes in Glacier Parameters in the Cordillera Blanca, Peru, Derived from Remote Sensing'. *Journal of Glaciology* 54(186):499–510. doi: 10.3189/002214308785836922.

Racoviteanu, Adina E., Frank Paul, Bruce Raup, Siri Jodha Singh Khalsa, and Richard Armstrong. 2009. 'Challenges and Recommendations in Mapping of Glacier Parameters from Space: Results of the 2008 Global Land Ice Measurements from Space (GLIMS) Workshop, Boulder, Colorado, USA'. *Annals of Glaciology* 50(53):53–69. doi: 10.3189/172756410790595804.

Racoviteanu, Adina E., Mark W. Williams, and Roger G. Barry. 2008. 'Optical Remote Sensing of Glacier Characteristics: A Review with Focus on the Himalaya'. *Sensors* 8(5):3355–83. doi: 10.3390/s8053355.

Racoviteanu, Adina, and Mark W. Williams. 2012. 'Decision Tree and Texture Analysis for Mapping Debris-Covered Glaciers in the Kangchenjunga Area, Eastern Himalaya'. *Remote Sensing* 4(10):3078–3109. doi: 10.3390/rs4103078.

Ranzi, Roberta, Giovanna Grossi, Laura Iacovelli, and Stefan Taschner. 2004. 'Use of Multispectral ASTER Images for Mapping Debris-Covered Glaciers within the GLIMS Project'. *International Geoscience and Remote Sensing Symposium (IGARSS)* 2(October):1144–47. doi: 10.1109/igarss.2004.1368616.

Rastner, Philipp, Tazio Strozzi, and Frank Paul. 2017. 'Fusion of Multi-Source Satellite Data and DEMs to Create a New Glacier Inventory for Novaya Zemlya'. *Remote Sensing* 9(11):1–18. doi: 10.3390/rs9111122.

Raup, Bruce H., Liss M. Andreassen, Tobias Bolch, Suzanne Bevan, and Bruce H. Raup. 2014. 'Remote Sensing of Glaciers'.

Raup, Bruce, Adina Racoviteanu, Siri Jodha Singh Khalsa, Christopher Helm, Richard Armstrong, and Yves Arnaud. 2007. 'The GLIMS Geospatial Glacier Database: A New Tool for Studying Glacier Change'. *Global and Planetary Change* 56(1–2):101–10. doi: 10.1016/j.gloplacha.2006.07.018.

Robson, Benjamin Aubrey, Tobias Bolch, Shelley MacDonell, Daniel Hölbling, Philipp Rastner, and Nicole Schaffer. 2020. 'Automated Detection of Rock Glaciers Using Deep Learning and Object-Based Image Analysis'. *Remote Sensing of Environment* 250. doi: 10.1016/j.rse.2020.112033.

Robson, Benjamin Aubrey, Daniel Hölbling, Christopher Nuth, Tazio Strozzi, and Svein Olaf Dahl. 2016. 'Decadal Scale Changes in Glacier Area in the Hohe Tauern National Park (Austria) Determined by Object-Based Image Analysis'. *Remote Sensing* 8(1). doi: 10.3390/rs8010067.

Robson, Benjamin Aubrey, Christopher Nuth, Svein Olaf Dahl, Daniel Hölbling, Tazio Strozzi, and Pål Ringkjøb Nielsen. 2015. 'Automated Classification of Debris-Covered Glaciers Combining Optical, SAR and Topographic Data in an Object-Based Environment'. *Remote Sensing of Environment* 170:372–87. doi: 10.1016/j.rse.2015.10.001.

Sahu, Rakesh, and R. D. Gupta. 2020. 'Glacier Mapping and Change Analysis in Chandra Basin, Western Himalaya, India during 1971–2016'. *International Journal of Remote Sensing* 41(18):6914–45. doi: 10.1080/01431161.2020.1752412.

Scherler, Dirk, Hendrik Wulf, and Noel Gorelick. 2018. 'Global Assessment of Supraglacial Debris-Cover Extents'. *Geophysical Research Letters* 45(21):11,798-11,805. doi: 10.1029/2018GL080158.

Shafique, Muhammad, Baber Faiz, Alam Sher Bacha, and Saleem Ullah. 2018. 'Evaluating Glacier Dynamics Using Temporal Remote Sensing Images: A Case Study

of Hunza Valley, Northern Pakistan'. *Environmental Earth Sciences* 77(5):1–11. doi: 10.1007/s12665-018-7365-y.

Shao, Donghang, Wenbo Xu, Hongyi Li, Jian Wang, and Xiaohua Hao. 2020. 'Modeling Snow Surface Spectral Reflectance in a Land Surface Model Targeting Satellite Remote Sensing Observations'. *Remote Sensing* 12(18):3101. doi: 10.3390/rs12183101.

Shukla, A., R. P. Gupta, and M. K. Arora. 2010. 'Delineation of Debris-Covered Glacier Boundaries Using Optical and Thermal Remote Sensing Data'. *Remote Sensing Letters* 1(1):11–17. doi: 10.1080/01431160903159316.

Svoboda, Felix, and Frank Paul. 2009. 'A New Glacier Inventory on Southern Baffin Island, Canada, from ASTER Data: I. Applied Methods, Challenges and Solutions'. *Annals of Glaciology* 50(53):11–21. doi: 10.3189/172756410790595912.

Tammemagi, Hans. 2012. 'Five National Parks That Honour First Nations'. *The Tyee*. Retrieved 26 March 2023 (https://thetyee.ca/Life/2012/08/04/Canadas-Five-Best-Parks/).

Taschner, S., and Roberto Ranzi. 2002. 'Comparing the Opportunities of LANDSAT-TM and ASTER Data for Monitoring a Debris Covered Glacier in the Italian Alps within the GLIMS Project'. Pp. 1044–46 vol.2 in *International Geoscience and Remote Sensing Symposium (IGARSS)*. Vol. 2.

Théau, Jérôme. 2008. 'Temporal Resolution'. Pp. 1150–51 in *Encyclopedia of GIS*. Springer US.

WGMS. 1989. 'World Glacier Inventory – Status 1988'. *Haeberli, W., Bösch, H., Scherler, K., Østrem, G. and Wallén, C. C. (Eds.), IAHS (ICSI) / UNEP / UNESCO, World Glacier Monitoring Service, Zurich, Switzerland* 458.

Young, Nicholas E., Ryan S. Anderson, Stephen M. Chignell, Anthony G. Vorster, Rick Lawrence, and Paul H. Evangelista. 2017. 'A Survival Guide to Landsat Preprocessing'. *Ecology* 98(4):920–32. doi: 10.1002/ecy.1730.

Zemp, M., M. Hoelzle, and W. Haeberli. 2009. 'Six Decades of Glacier Mass-Balance Observations: A Review of the Worldwide Monitoring Network'. *Annals of Glaciology* 50(50):101–11. doi: 10.3189/172756409787769591.

Zemp, M., E. Thibert, M. Huss, D. Stumm, C. Rolstad Denby, C. Nuth, S. U. Nussbaumer, G. Moholdt, A. Mercer, C. Mayer, P. C. Joerg, P. Jansson, B. Hynek, A. Fischer, H. Escher-Vetter, H. Elvehøy, and L. M. Andreassen. 2013. 'Reanalysing Glacier Mass Balance Measurement Series'. *The Cryosphere* 7(4):1227–45. doi: 10.5194/tc-7-1227-2013.

Zhang, Qifei, Yaning Chen, Zhi Li, Yupeng Li, Yanyun Xiang, and Wei Bian. 2019. 'Glacier Changes from 1975 to 2016 in the Aksu River Basin, Central Tianshan

Mountains'. *Journal of Geographical Sciences* 29(6):984–1000. doi: 10.1007/s11442-019-1640-z.

Chapter 3

Glacier area changes in Novaya Zemlya from 1986-89 to 2019-21 using object-based image analysis in Google Earth Engine

Cite this article:

Ali A, Dunlop P, Coleman S, Kerr D, McNabb RW, Noormets R (2023). Glacier area changes in Novaya Zemlya from 1986–89 to 2019–21 using object-based image analysis in Google Earth Engine. Journal of Glaciology 1–12.

https://doi.org/10.1017/jog.2023.18

3.1. Abstract

Climate change has had a significant impact on glacier recession, particularly in the Arctic, where glacier meltwater is an important contributor to global sea-level rise. Therefore, it is important to accurately quantify glacier recession within this sensitive region. In this study, we mapped 480 glaciers in Novaya Zemlya, Russian Arctic, using object-based image analysis applied to multispectral Landsat satellite imagery in Google Earth Engine to quantify the area changes between 1986-89 to 2019-21. The results show that in 1986-89, the total glacierized area was 22,990±301 km^2, in 2000-01 the area was 22,525±308 km^2, and by 2019-21 the glacier area had reduced to 21,670±292 km^2, representing a total 5.73% reduction in glacier area between 1986-89 and 2019-21. Higher glacier area loss was observed on the Barents Sea coast (7.1%), compared to the Kara (4.1%), reflecting previously observed differences in warming trends. The accuracy of the automatically generated outlines of each layer (1986-89, 2000-01, and 2019-21) was evaluated by comparing with manually corrected outlines (reference data) using random sampling, resulting in an overall accuracy estimate of between 96% and 97% compared to the reference data. This automated approach in Google Earth Engine is a promising tool for rapidly mapping glacier change that reduces the amount of time required to generate accurate glacier outlines.

Key words

Landsat, Glaciers, object-based image analysis, Google Earth Engine

3.2. Introduction

Glaciers distinct from the Antarctic and Greenland Ice Sheets are one of the key elements of the cryosphere and are major freshwater reservoirs (Millan et al. 2022). As a result of climate change, these large freshwater stores are now melting at a fast rate, increasing global sea levels (Hugonnet et al. 2021; Zemp et al. 2019). After thermal expansion, glaciers and ice sheets are the largest contributors to sea-level rise in the 21st century (IPCC 2021). With millions of people around the world living within a few kilometres of the coast, future sea level rise has the potential to displace populations across the globe (Kulp and Strauss 2019).

Over the last few decades the rate of temperature increase in the Arctic has been estimated to be more than twice as high as anywhere else in the world (Schädel et al. 2018; You et al. 2021), with a recent study estimating Arctic warming to be as much a four times higher since 1979 (Rantanen et al. 2022). In the Arctic, mountain glaciers, ice caps, and the Greenland Ice Sheet (GrIS) have all retreated over the past 100 years and have started to retreat faster since 2000 (AMAP 2017). Combined, Arctic glaciers, ice caps, and the GrIS contributed approximately 1.2mm to sea level rise each year from 2003 to 2015 (Moon et al. 2019).

Given the importance of glaciers in the Arctic and their potential to impact large parts of the world, it is necessary to develop automated methods that can easily monitor regional glacier changes and provide a clear understanding of the climate change impacts on Arctic glaciers. To monitor changes over such an expansive and

largely inaccessible region like the Arctic, satellite remote sensing is an ideal tool as it can be used to map large glacierized areas relatively quickly (e.g., Winsvold et al. 2014).

Several techniques have been used for glacier mapping based on remote sensing data, such as manual delineation (e.g., Albert 2002), Band Ratio (e.g., Bolch et al. 2010), Normalized Difference Snow Index (NDSI) (Hall et al. 1995), object-based image analysis (e.g., Robson et al. 2015, 2016), and supervised learning-based classification (e.g. Maximum likelihood, Support Vector Machines, and Random Forest; Khan et al. 2020; Kumar et al. 2020; Nijhawan et al. 2016). Of these methods, manual delineation is considered to be the most accurate (Albert 2002; Alifu et al. 2015; Paul et al. 2017), but this method is both time-consuming and potentially more susceptible to operator bias compared to more automated approaches. Both Band Ratio and NDSI are well-established, fast, and robust methods for mapping debris-free glaciers ice over extensive areas (Paul et al. 2015). However, some difficulties are still present in using these index-based methods, for example mapping glaciers in the presence of lakes, clouds, shadow, and debris cover.

Band Ratio with visible and Shortwave Infrared (SWIR) bands from Landsat imagery (red/SWIR1) is an effective method for mapping shadowed ice but tends to misclassify lakes (water bodies) as part of the glacier (Kääb et al. 2005; Paul et al. 2007). Band Ratio with Near Infrared (NIR) and SWIR (NIR/SWIR1) have also been used, but using NIR with SWIR is less effective in areas with dark shadows (Burns

and Nolin 2014). NDSI can provide more satisfactory results in the case of shaded ice, but fails to differentiate glacier ice from pro-glacial lakes (Racoviteanu et al. 2008). Supervised learning based classification techniques may have limited applicability over large regions because of the longer processing time (Racoviteanu et al. 2009).

Glacier outlines are an important data source that not only tell us the size of the glacier, but importantly are used for estimating ice volume (Millan et al. 2022), and glacier mass changes (Zemp et al. 2019), or predicting sea level rise (Hock et al. 2019). The Randolph Glacier Inventory (RGI) is a global inventory of glaciers, and it is supplementary to the Global Land Ice Measurements from Space (GLIMS) database (RGI Consortium 2017). GLIMS is a digital database that contains glacier outlines and is a cooperative effort of worldwide institutes (Raup et al. 2007), available at https://www.glims.org/. However, for most glaciers around the world, outlines are only available at a single point in time which limits its use for understanding the long-term impacts of climate change for glaciers in many regions.

In order to map glacier changes over large areas over multiple points in time, multiple satellite images are needed. To do this mapping locally, users must download and store each image, with file sizes ranging from ~200 MB for complete Landsat 4-5 scenes, to ~1 GB for Sentinel-2 or Landsat 8 and 9 scenes. Processing large images on a desktop or laptop computer can be resource-intensive, which provides an additional cost barrier for large-scale mapping efforts. More recently,

cloud-based platforms such as Google Earth Engine (Gorelick et al. 2017) have enabled users to forgo the time and costs of downloading, storing, and processing images locally, which has greatly expanded the possibilities for large-scale analysis in a number of fields (e.g., Lea 2018; Mahdianpari et al. 2019; Zhang et al. 2020).

In this study, a method is developed using the Google Earth Engine cloud-based platform using an object-based image analysis approach to map and generate glacier outlines automatically. We use this method to generate multi-temporal outlines of glaciers on Novaya Zemlya, Russian Arctic. The main goals of this study are: i) to develop an automated method to map glaciers by leveraging the computational power and extensive data catalogue of Google Earth Engine; ii) to map the glaciers of Novaya Zemlya at multiple points in time; iii) to compare the derived area changes to mass losses (Hugonnet et al. 2021); and iv) to evaluate the accuracy of the method using manually-corrected outlines.

3.3. Study Area

The Russian Arctic consists of three main regions: Franz Josef Land, Severnaya Zemlya, and Novaya Zemlya, which lies north of the Russian mainland between the Barents and Kara Seas (Grant et al. 2009). According to the RGI 6.0, the glacier-covered area of Severnaya Zemlya is 16,701 km^2, for Franz-Josef Land it is 12,762 km^2 and for Novaya Zemlya it is 22,128 km^2 (RGI Consortium, 2017). The most prominent feature of Novaya Zemlya is the large ice cap on the northern island (Severny Island), whereas the southern part of the archipelago (Yuzhny Island) is

dominated by a small valley and mountain glaciers (Melkonian et al. 2016). The ice cap on the northern side of Novaya Zemlya is approximately 400 km long and has a maximum elevation of 1,600 m above sea level (a.s.l.), with the southern part of Novaya Zemlya reaching 1,340 m a.s.l. (Rastner et al. 2017).

Novaya Zemlya (Figure 4) has three different types of glaciers: the main ice cap's large outlet glaciers are mostly marine-terminating, while most of the glaciers that are separated from the main ice cap are land-terminating, with a small number of lake terminating glaciers (Rastner et al. 2017). According to the RGI 6.0, Novaya Zemlya has a total of 480 glaciers: 38 marine-terminating glaciers, 424 land-terminating glaciers, and 18 lake-terminating glaciers.

Glacier melt is influenced by different climate drivers such as, temperature, precipitation, solar radiation, wind, oceanic influences and atmospheric circulation as well as topography of glaciers (Benn & Evans, 2014). Melting of different types of glaciers, such as land, lake, and marine-terminating glaciers, may vary with these climate drivers in distinct regions.

Marine-terminating glaciers are glaciers that flow into the ocean and are influenced by both atmospheric and oceanic conditions. Warm ocean waters interact with the glacier terminus, which can accelerate melting, causing the glacier to thin and retreat rapidly (e.g., Kochtitzky & Copland, 2022). Marine-terminating glaciers also

undergo and often experience calving, where large chunks of ice break off from the glacier's terminus, that contribute to area reduction.

Lake-terminating glaciers are glaciers that terminate in a lake. Like with marine-terminating glaciers, water temperature affects the rate of melting at the glacier terminus (Sugiyama et al., 2021). Warmer lake waters can enhance melting and contribute to area reduction. Changes in lake dynamics, including its size, depth, and water circulation patterns, can also impact the glaciers area change (e.g., Tsutaki et al., 2011).

Land-terminating glaciers are glaciers that terminate on land, typically in mountainous regions (King et al. 2018). Some land-terminating glaciers may have a layer of debris (rocks, sediment) on their surface, that reduces melting and potentially stabilizing the glacier.

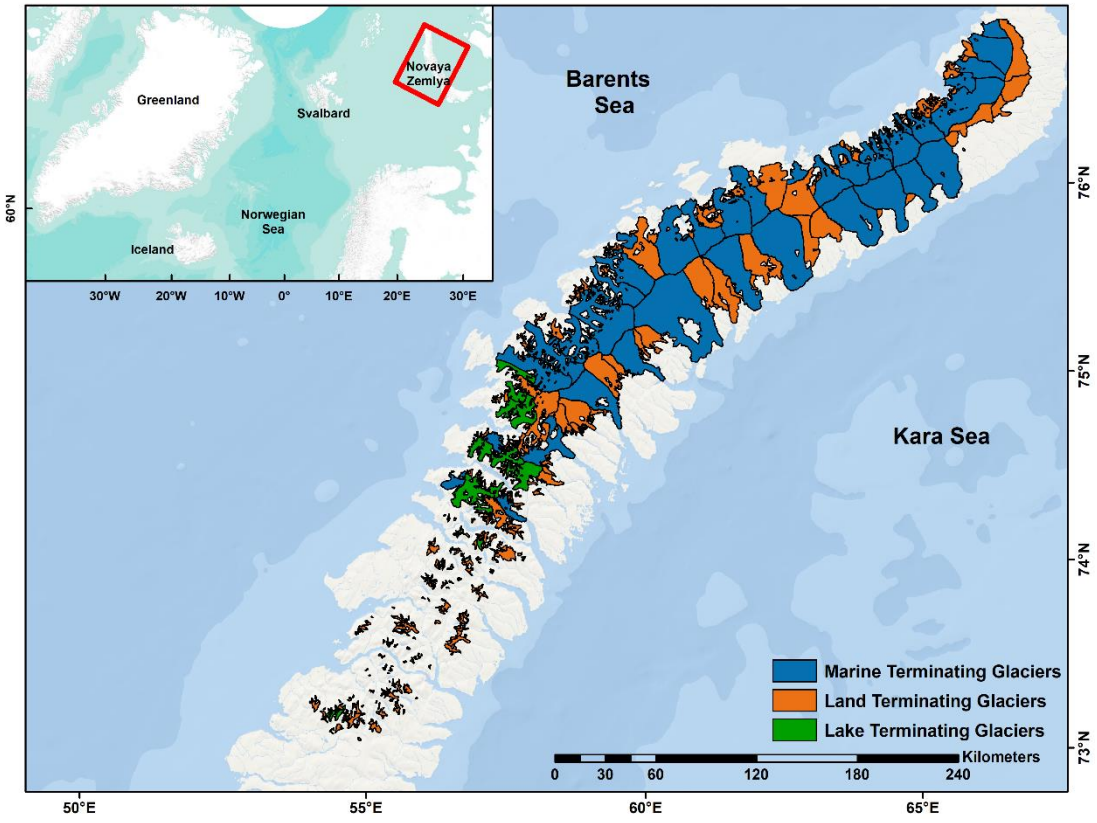

Figure 4: The study area of Novaya Zemlya, with glaciers outlines from RGI 6.0 shown. The ESRI World Ocean and World Terrain base maps are used in the background.

3.4. Data and method

3.4.1. Data

Landsat data have proven to be an effective asset for glacier mapping, and for creating multi-temporal outlines of glaciers due to their large swath width, multispectral capabilities, and long temporal record of capturing images over 5 decades (e.g., Nuth et al. 2013). A total of sixteen images from Landsat 5 Thematic Mapper (TM), Landsat 7 Enhanced Thematic Mapper Plus (ETM+), and Landsat 8 Operational Land Imager (OLI) are used in this study (Table 3), divided into three

time periods: 1986-89, 2000-01, and 2019-21. The images used were carefully selected with minimal cloud cover.

Landsat is a collaborative effort of the USGS and NASA and has been continuously observing the Earth from 1972 until the present day (Masek et al. 2020). The USGS provides Landsat products in three categories: real-time (RT), Tier 1, and Tier 2 which are stored in Collection 1 or 2. Tier 1 images have the best quality, and are considered suitable for time-series analysis (Masek et al. 2020), while Tier 2 images have issues with geometric correction but are still usable. In this study, we use orthorectified Level-2 (surface reflectance) images (Tier 1) from Collection 1 for mapping glaciers in Novaya Zemlya. Some studies have used raw radiance or Digital Number (DN) values for glacier mapping with no atmospheric or topographic correction (Alifu et al. 2015; Paul et al. 2002). However, surface reflectance data are essential for systematic analysis, particularly in highly automated approaches (Hemati et al. 2021).

Table 3: Details of images that are used in this study.

S. No	Satellite	Date (DD/MM/YYYY)	WRS-2 Path/Row	Google Earth Engine Image IDs
01	Landsat 5	26/07/1986	174/6	LANDSAT/LT05/C01/T1_SR/LT05_174006_19860726
02	Landsat 5	03/08/1987	177/6	LANDSAT/LT05/C01/T1_SR/LT05_177006_19870803
03	Landsat 5	06/08/1989	179/6	LANDSAT/LT05/C01/T1_SR/LT05_179006_19890806
04	Landsat 5	06/08/1989	179/7	LANDSAT/LT05/C01/T1_SR/LT05_179007_19890806
05	Landsat 5	06/08/1989	179/8	LANDSAT/LT05/C01/T1_SR/LT05_179008_19890806
06	Landsat 7	25/08/2000	174/6	LANDSAT/LE07/C01/T1_SR/LE07_174006_20000825

07	Landsat 7	31/07/2000	175/6	LANDSAT/LE07/C01/T1_SR/LE07_175006_20000731
08	Landsat 7	12/08/2000	179/6	LANDSAT/LE07/C01/T1_SR/LE07_179006_20000812
09	Landsat 7	12/08/2000	179/7	LANDSAT/LE07/C01/T1_SR/LE07_179007_20000812
10	Landsat 7	08/08/2001	178/8	LANDSAT/LE07/C01/T1_SR/LE07_178008_20010808
11	Landsat 8	20/08/2019	176/5	LANDSAT/LC08/C01/T1_SR/LC08_176005_20190820
12	Landsat 8	20/08/2019	176/6	LANDSAT/LC08/C01/T1_SR/LC08_176006_20190820
13	Landsat 8	23/08/2021	178/7	LANDSAT/LC08/C01/T1_SR/LC08_178007_20210823
14	Landsat 8	18/08/2020	180/6	LANDSAT/LC08/C01/T1_SR/LC08_180006_20200818
15	Landsat 8	19/09/2020	180/7	LANDSAT/LC08/C01/T1_SR/LC08_180007_20200919
16	Landsat 8	19/09/2020	180/8	LANDSAT/LC08/C01/T1_SR/LC08_180008_20200919

3.4.2. Method: Object Based Image Analysis

Google Earth Engine is a cloud-based remote sensing platform with planetary-scale analysis capabilities that contains a multi-petabyte catalogue of satellite imagery and geospatial datasets, making Google Earth Engine one of the most powerful remote sensing analysis tools available for analysing change datasets (Gorelick et al. 2017). Using Google Earth Engine, we developed an object-based image analysis approach for classifying imagery, instead of a simpler pixel-based approach. Pixel-based classification focuses on individual pixels and neglects additional contextual information contained in surrounding pixels that could be used to increase the accuracy such as the spatial relationship with surrounding pixels, size of objects, texture, and shape that object-based image analysis incorporates (Blaschke 2010).

The method was initially developed using a single Landsat 8 OLI/TIRS image before being applied to the other image sets for the whole of Novaya Zemlya to map glacier

changes. This study utilizes six bands from visible to SWIR (OLI Bands 2-7), and one thermal infrared band (TIR1, TIRS Band 10) as input layers for image segmentation (Figure 5). The visible to SWIR bands have 30m resolution. The TIR1 band was originally collected with 100m resolution, but Google Earth Engine automatically resampled this using a cubic convolution method to 30m.

In the object-based image analysis approach, segmentation is an important step that groups similar pixels into a cluster or image objects (Ren and Malik 2003). Pixel-based classification can result in so-called “salt and pepper” noise, and segmentation helps to reduce this effect in the final classification (Mahdianpari et al. 2019). To reduce noise in the images, a one-sigma Gaussian filter of radius 2 was applied before segmentation (Xue et al. 2018).

Google Earth Engine mainly supports three image segmentation techniques for remote sensing: simple non-iterative clustering, k-means, and G-means (Liu et al. 2018). We use simple non-iterative clustering (Achanta and Süsstrunk 2017), which is an improved version of simple linear clustering, to segment the Landsat image (Figure 6B). The important parameters of simple non-iterative clustering are compactness, connectivity, seeds or grid size, and neighbourhood size. The compactness parameter defines the smoothness of the clusters, which affects cluster shape (Shafizadeh-Moghadam et al. 2021). A compactness value of zero removes spatial distance weighting, meaning that clusters are created based only on spectral characteristics. The connectivity parameter deals with adjacent objects,

with a connectivity of 4 corresponding to only orthogonal neighbours, and a connectivity of 8 corresponding to orthogonal and diagonal neighbours. The seed/size parameter determines the initial location or spacing of the cluster centres, and neighbourhood size is used to avoid boundary artifacts between tiles (Tassi and Vizzari 2020). In this study, the parameters compactness = 0, connectivity = 4, seed grid spacing = 15 pixels, and neighbourhood size = 128 pixels were selected by repeated iteration and visual evaluation.

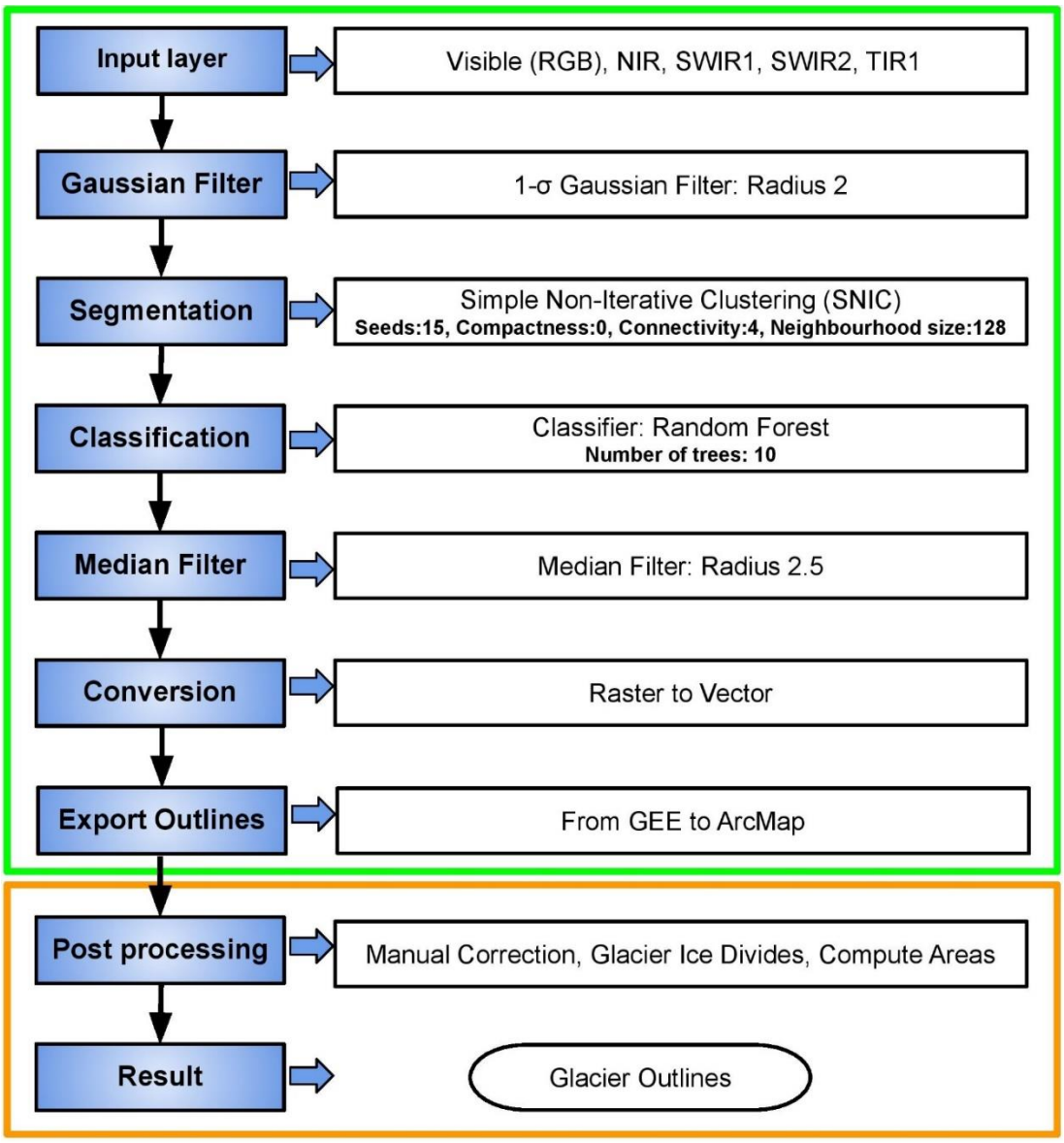

Figure 5: Workflow of the method for creating glacier outlines in Google Earth Engine. The green box shows the automated steps in Google Earth Engine, while orange shows the post-processing steps in ArcMap 10.5.1.

The Random Forest classifier was implemented in Google Earth Engine for the classification of the segmented images. The Random Forest algorithm is a supervised machine learning algorithm that combines the output of multiple decision trees to produce a single result (Kulkarni and Lowe 2016). For image

classification, Random Forest is the most widely used machine learning algorithm in Google Earth Engine (Amani et al. 2020). Random Forest is robust, easy to implement, capable of dealing with high dimensionality, and can reduce the risk of overfitting (Nery et al. 2016; Praticò et al. 2021).

In this study, the Random Forest algorithm using ten trees was trained on manually selected samples of “glacier” and “non-glacier” throughout the scene, and the segments were classified into two main classes: “glacier” and “non-glacier”. The “glacier” class includes ice, debris-covered ice, and moraines, while the non-glacier class includes water, vegetation, sea-ice, bare land and seasonal snow patches. To train the classifier, we used a total of 728 samples for the 1986-89 images, including 365 glacier samples and 363 non-glacier samples. For the 2000-01 images, we used 317 glacier and 303 non-glacier samples, and for the 2019-21 images we used 339 glacier and 367 non-glacier samples.

Finally, a median filter with radius 2.5 was applied to reduce noise in the classified image, and then the classified image was converted from raster to vector to create glacier outlines (Figure 6C). The automated glacier outlines were exported from Google Earth Engine to ArcMap 10.5.1 for post processing. As a final step, each glacier was examined to see if manual correction was required, and manual corrections were made where necessary. Finally, the linked glacier outlines were separated using the internal boundaries of the RGI version 6.0, to enable examination of the changes in each glacier.

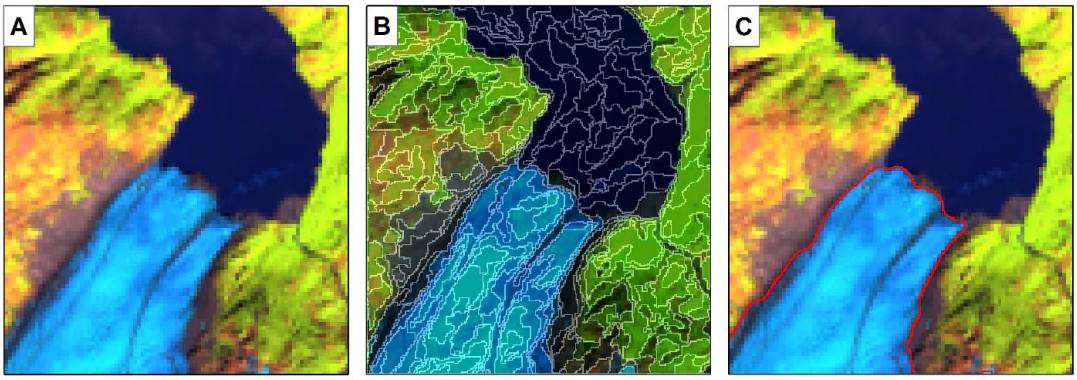

Figure 6: The process of generating outlines using an object-based image analysis approach in Google Earth Engine: (a) a false color composite of a Landsat 8 image (OLI Bands SWIR1, NIR, and Red); (b) the result of simple non-iterative clustering segmentation; (c) the final glacier outline, overlain on the original image.

3.4.2.1. Accuracy and Uncertainty

The temporal nature by which satellite images are captured, invariably means that images of the same area are captured during different conditions and there can be seasonal variations that can impact on image quality. These variations can be illumination differences, cloud cover, or shadows cast over the target feature; for glacier mapping, snow patches can remain on the ground which are spectrally similar to snow covered glaciers. Therefore, it is important to understand the capabilities of the method when utilising images from different times and to assess how accurate the glacier areas are computed using this automated methodology without manual corrections. Therefore, to determine the uncertainty in the glacier area, two approaches were used: random sampling and buffer analysis.

3.4.2.2. Uncertainty by random sampling

To assess the accuracy of the automated outlines from each period, random samples were generated for each class in ArcMap 10.5.1, using manually corrected outlines as reference data. The random samples were separated into two classes, "glacier" and "non-glacier," with an equal number of samples for each class. In total, 1,998 samples for each class were taken for the 1986-89 outlines, 1,971 samples from each class for the 2000-01 outlines and 1,937 samples from each class for the 2019-21 outlines. These points were intersected with the automatically generated outlines and the reference data, and confusion matrices were created (Table 4).

Table 4 Confusion matrices of each layer generated based on random sampling.

1986-89		**Reference Data**				
		Glacier	Non-glacier	Total	User's accuracy	Kappa
Classified	Glacier	1973	100	2073	95.1%	0.93
	Non-glacier	25	1898	1923	98.7%	
	Total	1998	1998	3996		
	Producer's accuracy	98.7%	94.9%			
2000-01		**Reference Data**				
		Glacier	Non-glacier	Total	User's accuracy	Kappa
Classified	Glacier	1954	140	2094	93.3%	0.92
	Non-glacier	17	1831	1848	99.0%	
	Total	1971	1971	3942		
	Producer's accuracy	99.1%	92.8%			
2019-21		**Reference Data**				
		Glacier	Non-glacier	Total	User's accuracy	Kappa
Classified	Glacier	1917	115	2032	94.3%	0.93

	Non-glacier	20	1822	1842	98.9%
	Total	1937	1937	3874	
	Producer's accuracy	98.9%	94.0%		

3.4.2.3. Uncertainty using buffer analysis

To assess the area uncertainty of the manually-corrected outlines, a buffer of ±30m was applied to each manually corrected layer. In the absence of suitable reference data, the buffer approach is typically employed to determine accuracy using a literature-derived uncertainty value (±0.5 or 1 pixel) (Granshaw and Fountain 2006; Paul et al. 2017). The uncertainty in the glacier area was determined by calculating the buffered area of each layer. The high, low, and area ± uncertainty values for each period are shown in Table 5.

Table 5 Computed areas (in km^2) of each layer based on the ±30 m buffer.

Time period	High	Low	Area
1986-89	23291	22689	22990 ± 301
2000-01	22833	22217	22525 ± 308
2019-21	21962	21378	21670 ± 292

3.5. Results

In 1986-89, the total glacierized region of Novaya Zemlya was 22,990±301 km^2, in 2000-01 the area was 22,525±308 km^2, and by 2019-21 the glacier area was reduced to 21,670±292 km^2. Of the 480 glaciers mapped, 142 are greater than 10 km^2, 262 glaciers are between 1 to 10 km^2, and 76 glaciers are smaller than 1 km^2. This glacier inventory includes three terminus types: 38 marine-terminating, 424 land-

terminating, and 18 lake-terminating glaciers. The marine-terminating glaciers cover the largest glacier area (14,448±137 km^2), followed by the land-terminating glaciers covering 7,299±94 km^2, and the lake-terminating glaciers that cover 1,241±16 km^2.

The overall accuracy for each layer was calculated using the confusion matrices (Table 4). The 1986-89 layer showed 96.8% overall accuracy, the 2000-01 layer had 96.0% accuracy, and the 2019-21 layer had 96.5% accuracy. The details of producer's and user's accuracy are mentioned in Table 4. The producer's accuracy varies between 92.8% and 98.9%, the user's accuracy ranges between 93.3% and 99.0%, and the kappa coefficient is greater or equal to 0.92 for all three layers.

It is also important to assess how accurate the automatically-generated glacier areas are, using the information displayed in Table 4. Table 6 compares the manually estimated glacier areas with the unbiased estimates of glacier area for each time period, calculated following the methods described by Olofsson et al. (2013). The comparison of manual and automated area estimates shows that besides 2000-01, the manual and automated area estimates overlap within the uncertainty bands. When compared to 1986-89 and 2000-01, the manual area estimates shows that the area loss nearly doubled between 2000-01 and 2019-21, whereas the automatic estimate shows the opposite. Additionally, the automated estimate of the area

changes between 2000-01 and 2019-21 has a larger uncertainty (±624 km^2) than the estimated change (-441 km^2) (Table 6).

Table 6: The total area (in km^2) of glaciers computed manually corrected outlines (± 1 pixel buffer), both including and excluding glaciers that surged, and the automatically generated outlines (± 95% confidence interval)

	Manual		Change (from previous)		Automated	Change (from previous)
	All	Non-Surge	All	Non-Surge		
1986-89	22,990 ± 301	22,049 ± 301			22,930±470	
2000-01	22,525 ± 308	21,578 ± 308	-465 ± 430	-470 ± 430	21,762±435	-1,168 ± 640
2019-21	21,670 ± 292	20,756 ± 292	-855 ± 424	-821 ± 424	21,321±448	-441 ± 624

3.5.1. Glacier area changes

To calculate area changes, we use the manually-corrected glacier outlines. Between 1986-89 and 2019-2021, glaciers in Novaya Zemlya showed a 5.7% reduction in total area. Glacier retreat rates increased by 1.7% from 2000-01 to 2019-21 (-3.7%), compared to 1986-89 to 2000-01 (-2%). These changes in glacier area were not constant across glacier terminus type (land, lake, and marine-terminating). From 1986-89 to 2019-21, land-terminating glaciers lost 580±130 km^2 (7.9%), lake-terminating glaciers lost 106±21 km^2 (9.9%), and marine-terminating glaciers lost 580±263 km^2 (4.4%) of glacierized area, see Figure 7.

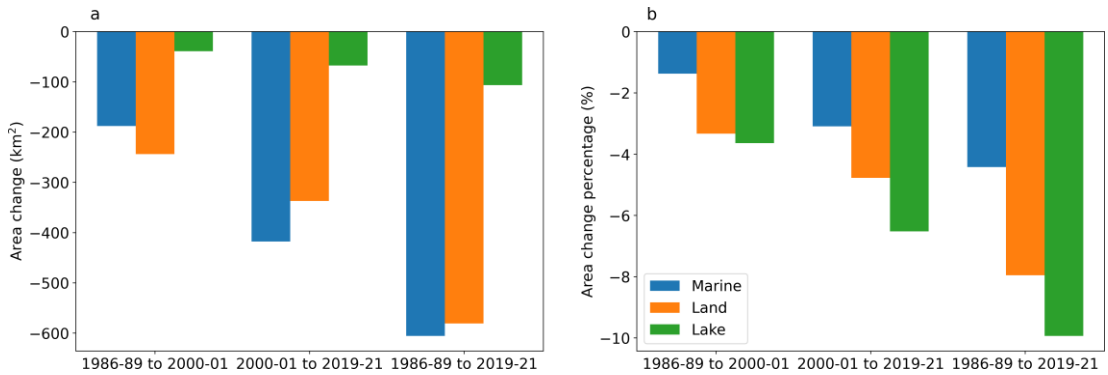

Figure 7: The total area changes for lake, marine, and land-terminating glaciers in both km^2 (a) and percent area (b).

Figure 8a depicts the area lost for each glacier from 1986-89 to 2000-01 and Figure 8b shows the loss of each glacier from 2000-01 to 2019-21, while Figure 7c and Figure 8d show the area loss of each glacier as a percentage. Only 41 glaciers larger than 200 km^2 are responsible for nearly half (49.5%) of the area loss in the region, and 272 glaciers are responsible for 84% of the total glacier area loss. Because of the larger area of these glaciers, however, the total percentage loss for these 272 glaciers is less than 25%.

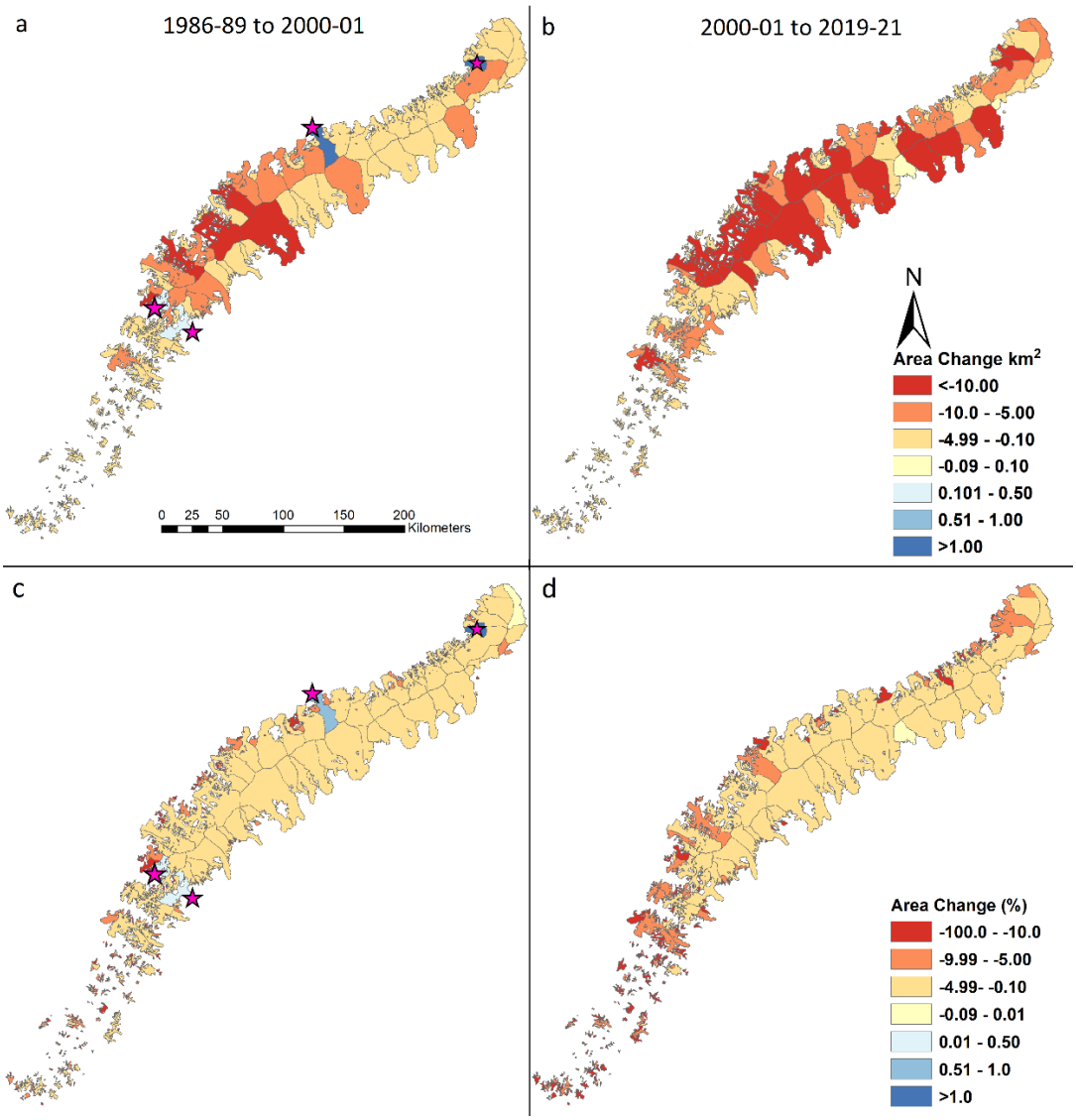

Figure 8: Area changes of Novaya Zemlya glaciers, (a) from 1986-89 to 2000-01 and (b) 2000-01 to 2019-21 in km^2, and (c) from 1986-89 to 2000-01 and (d) 2000-01 to 2019-21 as a percent. Stars in a and c show glaciers that surged during the 1986-89 and 2000-01 period.

Figure 9 shows the percent area change vs glacier area based on terminus type. Figure 9b depicts 38 marine-terminating glaciers that cover the majority of the glacierized region (14,448±137 km^2) in Novaya Zemlya, Figure 9a shows 18 lake-terminating glaciers which cover 1,241±16 km^2, while Figure 9c shows 424 land-

terminating glaciers covering 7,299±94 km^2. Between 1986-89 and 2019-21, three land-terminating glaciers have completely disappeared, and 18 glaciers retreated more than 60%, while a further 57 glaciers retreated between 40% and 60%.

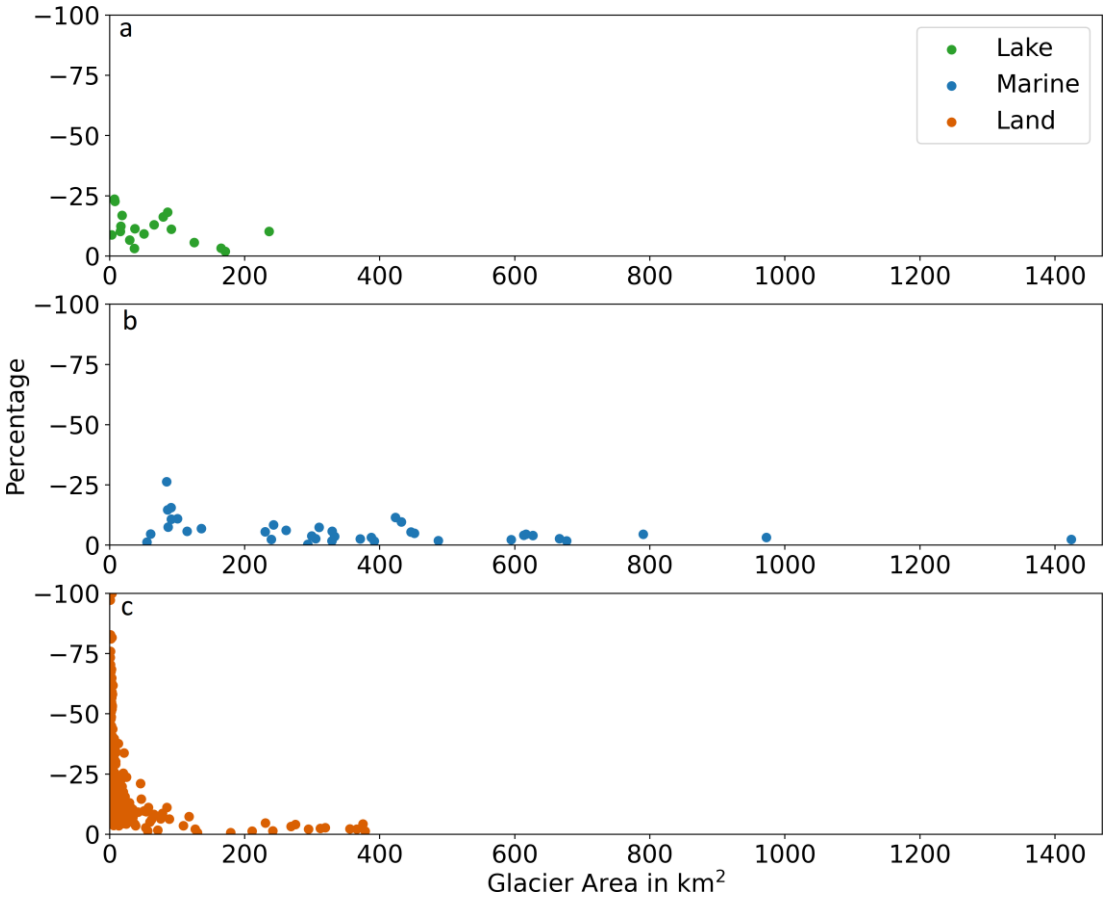

Figure 9: Percent area change vs glacier area for each glacier from 1986-89 to 2019-21, for (a) lake-terminating, (b) marine-terminating, and (c) land-terminating glaciers.

3.6. Discussion

3.6.1. Glacier retreat

As reported in elsewhere (e.g., Kochtitzky and Copland 2022; Sharp et al. 2014), It is clear that glaciers are retreating across the Arctic. This study shows that all glaciers in Novaya Zemlya have been retreated at various rates from 0.3% to 100%, with a few examples of surging glaciers captured in the analysis (Figure 8a, 8c). Although the area loss of glaciers differed by each glacier type in Novaya Zemlya. Carr et al. (2017) found that the retreat rate of marine-terminating glaciers is higher than that of land-terminating glaciers, which is corroborated by our results (Figure 10). However, land-terminating glaciers did not experience the same increase in retreat rate as lake and marine-terminating glaciers in 2000-01 to 2019-21. The retreat rates of land-terminating glaciers increased by 1.4% between 2000-01 and 2019-21 relative to that between 1986-89 to 2000-01, whereas the retreat rates of lake and marine-terminating glaciers increased by 2.8% and 1.7%, respectively.

Like the rest of the Arctic, Novaya Zemlya is warming faster than the rest of the world, with both surface air and sea surface temperatures increasing rapidly on both the Barents and Kara Sea coasts (e.g., Kohnemann et al. 2017; Isaksen et al. 2022). In particular, Isaksen et al. (2022) found that 2m surface air temperature warming was higher on the Barents Sea side of Novaya Zemlya (1.5–2.0 ˚C/decade between 1981-2020) compared to the Kara Sea side (1.0–1.5 ˚C/decade). These

changes are driven in part by a decrease in Sea Ice Concentration (SIC) in the region (Yamagami et al. 2022), with the drop in SIC over the Barents Sea nearly twice as high compared to the Kara Sea (Kumar et al. 2021). Consistent with these studies, our observations show that glaciers terminating on the Barents Sea coast of Novaya Zemlya retreated faster than glaciers terminating on the Kara Sea coast Figure 10, a pattern that remains consistent across glacier terminus type (Figure 11). Barents Sea glaciers lost a total area of 843.4 km^2 (-7.3%) between 1986-89 and 2019-21, while glaciers on the Kara Sea lost 448.9 km^2 (-4.2%).

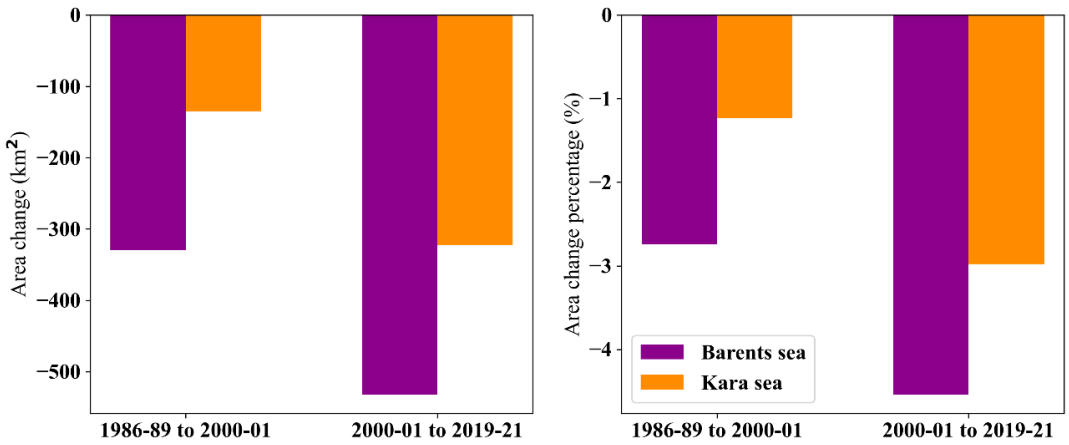

Figure 10 Area change for glaciers on the Barents Sea vs Kara Sea (a) in km^2 and (b) as a percentage.

Examination based on terminus type shows that all three types of glaciers are retreating more on the Barents Sea side than those terminating on Kara Sea side (Figure 11). Carr et al. (2014) observed a similar pattern of higher retreat on the Barents Sea coast than the Kara Sea between 1992 and 2010. Marine and lake-terminating glaciers are retreating faster on both sides, in both time periods of the

study, although land-terminating glacier retreat is slowing down at the Barents Sea from 2000-01 to 2019-21 compared to 1986-89 and 2000-01.

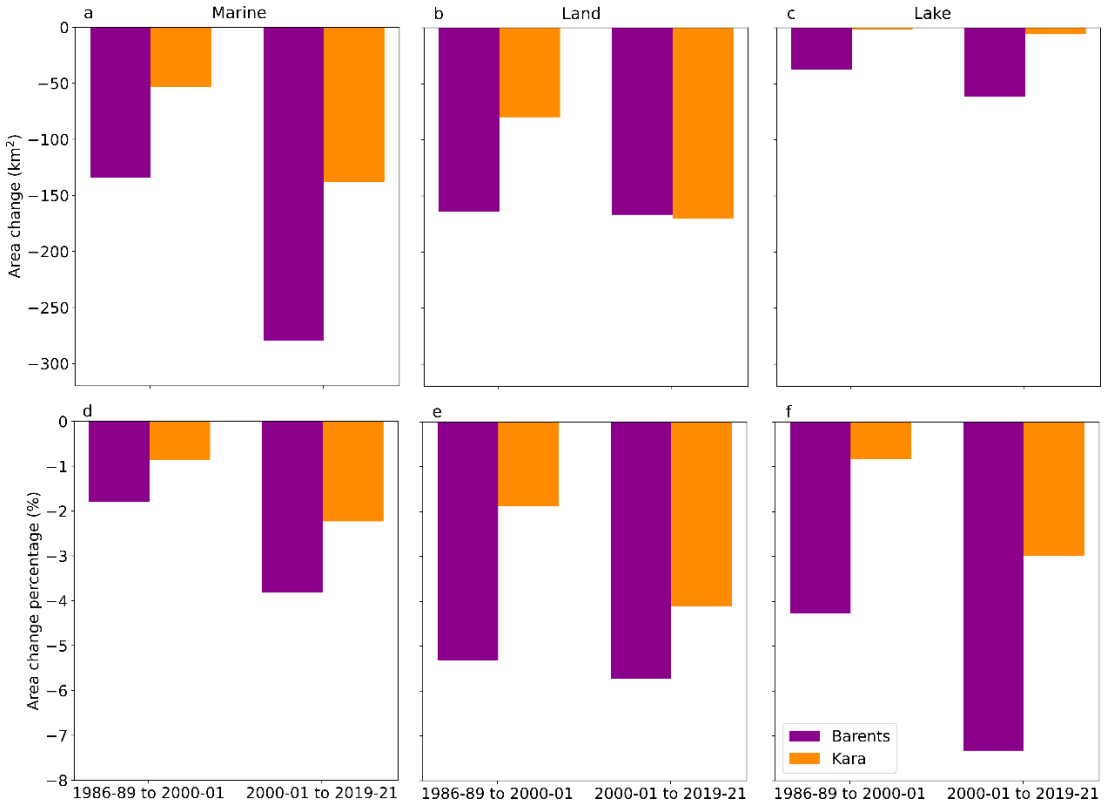

Figure 11: Area change of marine (a, d), land (b, e) and lake-terminating (c, f) glaciers on the Barents Sea vs Kara Sea, in km^2 (a-c) and percent area (d-f).

All three types of glaciers: lake, marine, and land-terminating glaciers have lost more glacier area from 2000-01 to 2019-21 than 1986-89 to 2000-01; although, during the period 1986-89 to 2000-01, three marine-terminating glaciers and one lake-terminating glacier surged. Two of the same glaciers were identified by (Carr et al. 2017), and one was identified by (Grant et al. 2009). This study identified one additional glacier surge (RGI ID: RGI60-09.00070) that increased the area of the glacier by 3.26 km^2, and showed terminus advance by up to 1.31 km by 2000-01

compared to 1986-89 (Figure 12). During 1986-89 to 2000-01, all four surged glaciers increased in area by 0.6% (+5.8 km^2), however during the second time period (2000-01 to 2019-21), the same glaciers retreated and showed a strongly negative change in area of -3.4% (-32.6 km^2), with a net area loss between 1986-89 and 2019-21 for each glacier. These four glaciers were excluded from the area change analysis.

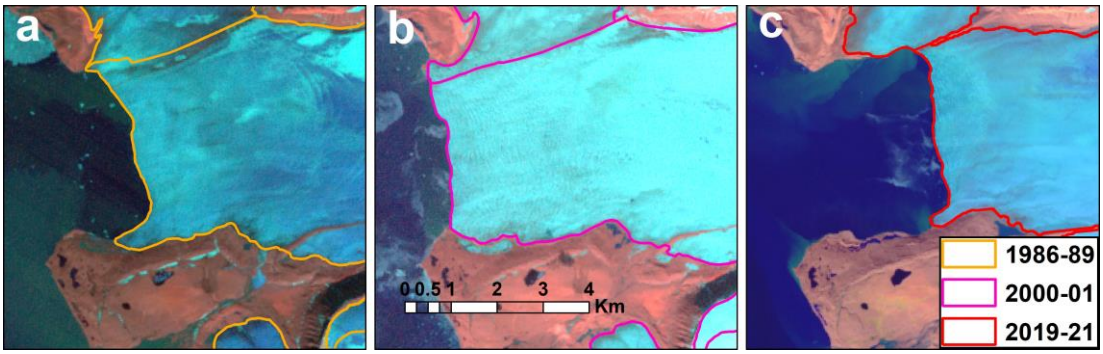

Figure 12: Time series of Landsat images showing Pavlov Glacier (RGI60-09.00070) in (a) 1986-07-26, (b) 2000-07-31, and (c) 2019-08-20, showing a clear advance associated with a surge between 1986 and 2000.

3.6.2. Comparison of glacier area loss with mass balance loss

Comparing glacier area changes with geodetic mass balances obtained from Hugonnet et al. (2021) for the period 2000-2020 shows that marine-terminating glaciers lost area (3.1%) as well as mass (-0.25 m a^{-1}) and lake-terminating glaciers lost a total of 6.5% area while also showing greater mass loss (-0.42 m a^{-1}) compared to land and marine terminating glaciers (Figure 13). However, land-terminating glaciers show a slightly different pattern than lake and marine-terminating glaciers

(Figure 13), with land-terminating glaciers losing a substantial amount of area (4.7%) with less substantial mass loss (-0.18 m a^{-1}).

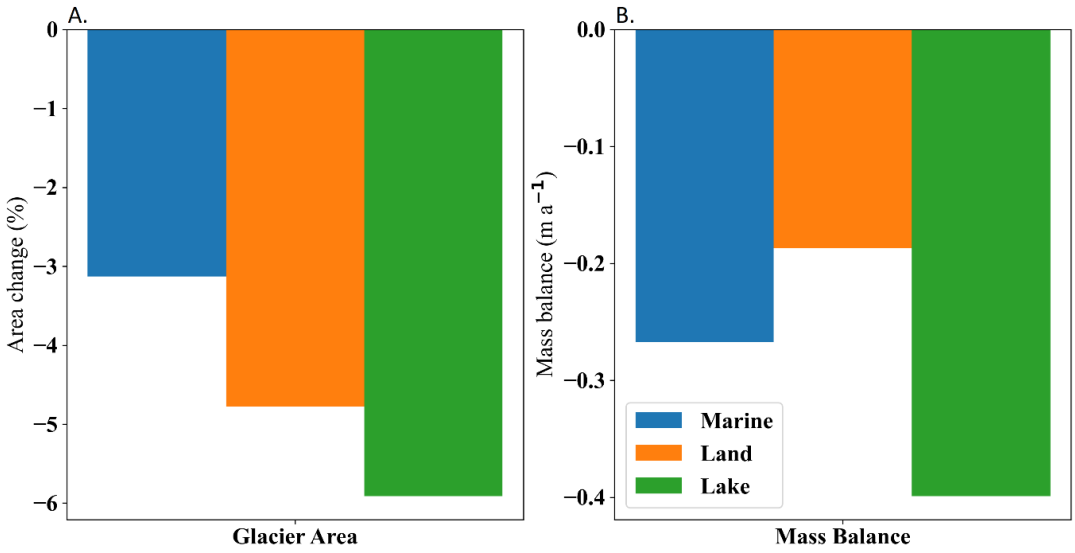

Figure 13: (a) Percent area change (2000-01 to 2019-21) and (b) area-averaged mass change (2000-2020) from Hugonnet et al. (2021) for each glacier type.

Figure 14 depicts a comparison of each glacier area loss with its mass loss. The results indicate that lake-terminating glaciers lost more area than land and marine-terminating glaciers (Figure 13), with a more negative mass balance (Figure 14). Ciracì et al. (2018) found that marine-terminating glaciers are losing mass faster than glaciers terminating on land. Almost the same trend can be seen in marine-terminating glaciers, with a more negative area-averaged mass balance for marine-terminating glaciers compared to land-terminating glaciers (Figure 14), because marine and lake-terminating glaciers lose mass via frontal ablation and land-terminating glaciers do not. Land-terminating glaciers showed least mass loss compared to marine and lake-terminating glaciers, as seen in the total mass loss of

land-terminating glaciers (Figure 13). In terms of relative area change, however, land-terminating glaciers showed a stronger decrease in area compared to marine-terminating glaciers.

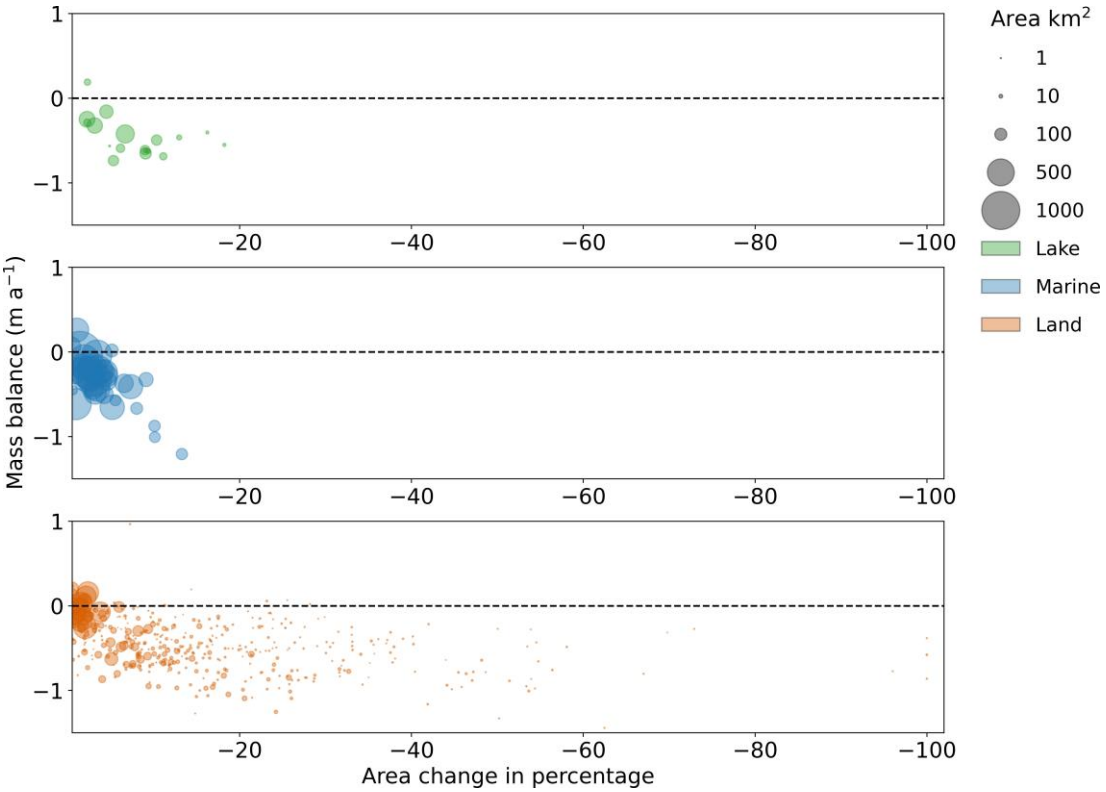

Figure 14: Area-averaged mass change (2000-2020) from Hugonnet et al. (2021) vs percent area change (2000-01 to 2019-21) for each glacier.

3.6.3. Methodology framework in Google Earth Engine

Rastner et al. (2013) compared object-based image analysis with pixel-based classification using the Red/SWIR band ratio technique, demonstrating that object-based image analysis performed better than pixel-based classification and reduced the time needed for manual corrections, despite the longer processing time required.

The 16 Level-2 products used in this study total 9.10 GB as distributed by USGS Earth Explorer. Downloading the files via the USGS Bulk Download Web Application took approximately 15 minutes, even on a fast internet connection. In comparison, running the script to generate outlines for a single image on Google Earth Engine and exporting the outlines took approximately one minute.

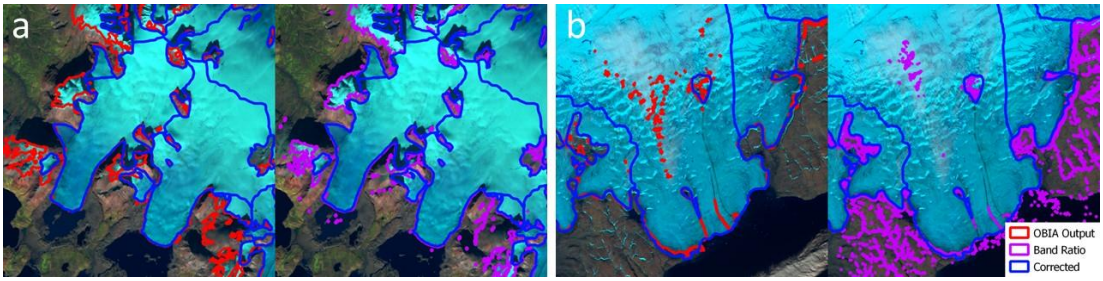

Figure 15: Comparison between object-based image analysis, Band Ratio, and Corrected outlines for two different sites in Novaya Zemlya.

In addition to the time saved by forgoing downloading and processing the images locally, the object-based image analysis method implemented on Google Earth Engine reduced the amount of manual correction needed when compared to the Red/SWIR1 band ratio method. Figure 15 compares the object-based image analysis output to the manually-corrected outlines, as well as the output of the Red/SWIR1 band ratio using a threshold of 2.0, following (Rastner et al. 2017). Both outputs clearly require manual correction, with large areas of seasonal snow captured by both methods in the area shown in Figure 15a, but the band ratio output captures a large area of seasonal and perennial snow patches (Figure 15b) that is not captured by the object-based image analysis output. In addition, both methods have

misclassified areas of thin cloud cover, shown in the middle of Figure 15b, as well as areas with larger medial moraines.

In this study, the Google Earth Engine object-based image analysis approach removes the time required for downloading, extracting, and storing the images, is easily applicable to other regions, and reduces the amount of manual correction required, compared with pixel-based methods. This method, however, may not be effective for mapping debris-covered glaciers, or areas covered by fresh snow or thin cloud cover. To address these issues, other approaches that have used object-based image analysis have included additional datasets such as digital elevation models and terrain slope or coherence derived from synthetic aperture radar (SAR) images (Robson et al. 2015, 2016). Unfortunately, many of these products are not yet available in Google Earth Engine, though the possibility exists for users to upload and make use of these additional datasets in their workflows.

3.7. Conclusion

This study presents a new object-based image analysis methodology, implemented in Google Earth Engine, for rapid and accurate glacier mapping. The software framework designed in Google Earth Engine utilises multi-temporal Landsat satellite imagery, and the outlines generated showed an accuracy of between 96% and 97% when compared to a manually-corrected reference dataset. This demonstrates that our methodology is a powerful, robust tool for accurate and rapid mapping of

glaciers changes on regional scale that reducing the time required of manual correction and can be applied to other glacierized regions. Utilizing this automated approach, we created outlines of glaciers on Novaya Zemlya for three different time periods: 1986-89, 2000-01, and 2019-21. This important dataset is essential for understanding the impact of climate change on glaciers and could be used to estimate ice volume and mass change.

This method allowed for a comprehensive analysis of the changes that occurred in Novaya Zemlya glaciers between 1986-1989 and 2019-21. Over this time period, glaciers in Novaya Zemlya lost a total area of 1,319±419 km^2 (5.7%), with three glaciers disappearing entirely. The results clearly demonstrate that all glaciers in Novaya Zemlya are responding to the impacts of climatic warming in the Arctic. With the exception of four glaciers that surged between 1986-89 to 2000-01, all glaciers in the study area retreated between 1986-89 and 2019-21, and even those four glaciers have retreated since 2000-01.

Our analysis indicates there are regional variations in how glaciers are responding to oceanic warming in this part of the Arctic, with more loss observed from glaciers that terminate on the Barents Seaside of Novaya Zemlya compared to those that terminate on the Kara Sea-side. In comparison, results showed that land-terminating glaciers retreated less between 2000-01 and 2019-21 compared to 1986-89 to 2000-01, while the retreat rate of marine-terminating glaciers increased from 2000-01 to 2019-21, relative to 1986-89 to 2000-01. While marine-terminating

glaciers, which cover the majority of Novaya Zemlya, lost more area than land and lake-terminating glaciers, lake-terminating glaciers showed a larger percentage loss than the land and marine-terminating glaciers.

Detailed regional studies of glacier behaviour across the Arctic are important for understanding the decadal responses and the likely trajectory of Arctic glaciers in a warming world. Given their potential contribution to global sea levels, it is important to map and understand the scale of change accurately and to provide tools for rapid assessment at regional scales. Platforms such as Google Earth Engine, combined with the expansive Landsat archive and approaches such as Object-Based Image Analysis, help provide these tools.

3.8. References

Albert, Todd H. 2002. 'Evaluation of Remote Sensing Techniques for Ice-Area Classification Applied to the Tropical Quelccaya Ice Cap, Peru'. *Polar Geography* 26(3):210–26. doi: 10.1080/789610193.

Alifu, Haireti, Ryutaro Tateishi, and Brian Johnson. 2015. 'A New Band Ratio Technique for Mapping Debris-Covered Glaciers Using Landsat Imagery and a Digital Elevation Model'. *International Journal of Remote Sensing* 36(8):2063–75. doi: 10.1080/2150704X.2015.1034886.

Amani, Meisam, Arsalan Ghorbanian, Seyed Ali Ahmadi, Mohammad Kakooei, Armin Moghimi, S. Mohammad Mirmazloumi, Sayyed Hamed Alizadeh Moghaddam, Sahel Mahdavi, Masoud Ghahremanloo, Saeid Parsian, Qiusheng Wu, and Brian Brisco. 2020. 'Google Earth Engine Cloud Computing Platform for Remote Sensing Big Data Applications: A Comprehensive Review'. *IEEE Journal of Selected Topics in Applied Earth Observations and Remote Sensing* 13:5326–50. doi: 10.1109/JSTARS.2020.3021052.

AMAP. 2017. *Snow, Water, Ice and Permafrost in the Arctic (SWIPA) 2017. Arctic Monitoring and Assessment Programme (AMAP), Oslo, Norway. ISBN: 978-82-7971-101-8*.

Benn, Douglas, and David J. A. Evans. 2014. *Glaciers and Glaciation, 2nd Edition*. Routledge.

Blaschke, T. 2010. 'Object Based Image Analysis for Remote Sensing'. *ISPRS Journal of Photogrammetry and Remote Sensing* 65(1):2–16. doi: 10.1016/j.isprsjprs.2009.06.004.

Bolch, Tobias, Brian Menounos, and Roger Wheate. 2010. 'Landsat-Based Inventory of Glaciers in Western Canada, 1985-2005'. *Remote Sensing of Environment* 114(1):127–37. doi: 10.1016/j.rse.2009.08.015.

Burns, Patrick, and Anne Nolin. 2014. 'Using Atmospherically-Corrected Landsat Imagery to Measure Glacier Area Change in the Cordillera Blanca, Peru from 1987 to 2010'. *Remote Sensing of Environment* 140:165–78. doi: 10.1016/j.rse.2013.08.026.

Carr, J. Rachel, Heather Bell, Rebecca Killick, and Tom Holt. 2017. 'Exceptional Retreat of Novaya Zemlya's Marine-Terminating Outlet Glaciers between 2000 and 2013'. *The Cryosphere* 11(5):2149–74. doi: 10.5194/tc-11-2149-2017.

Carr, J. Rachel, Chris Stokes, and Andreas Vieli. 2014. 'Recent Retreat of Major Outlet Glaciers on Novaya Zemlya, Russian Arctic, Influenced by Fjord Geometry and

Sea-Ice Conditions'. *Journal of Glaciology* 60(219):155–70. doi: 10.3189/2014JoG13J122.

Ciracì, Enrico, Isabella Velicogna, and Tyler Sutterley. 2018. *Mass Balance of Novaya Zemlya Archipelago, Russian High Arctic, Using Time-Variable Gravity from GRACE and Altimetry Data from ICESat and Cryosat-2*.

Consortium, R. G. I. 2017. 'Randolph Glacier Inventory 6.0 - A Dataset of Global Glacier Outlines: Version 6.0. Technical Report, Global Land Ice Measurments from Space, Boulder, Colorado, USA. Digital Media'. doi: 10.7265/n5-rgi-60.

Gorelick, Noel, Matt Hancher, Mike Dixon, Simon Ilyushchenko, David Thau, and Rebecca Moore. 2017. 'Google Earth Engine: Planetary-Scale Geospatial Analysis for Everyone'. *Remote Sensing of Environment* 202(2016):18–27. doi: 10.1016/j.rse.2017.06.031.

Granshaw, Frank, and Andrew Fountain. 2006. 'Glacier Change (1958-1998) in the North Cascades National Park Complex, Washington, USA'. *Journal of Glaciology* 52:251–56. doi: 10.3189/172756506781828782.

Grant, Katie L., Chris R. Stokes, and Ian S. Evans. 2009. 'Identification and Characteristics of Surge-Type Glaciers on Novaya Zemlya, Russian Arctic'. *Journal of Glaciology* 55(194):960–72. doi: 10.3189/002214309790794940.

Hall, Dorothy K., George A. Riggs, and Vincent V. Salomonson. 1995. 'Development of Methods for Mapping Global Snow Cover Using Moderate Resolution Imaging Spectroradiometer Data'. *Remote Sensing of Environment* 54(2):127–40. doi: https://doi.org/10.1016/0034-4257(95)00137-P.

Hemati, MohammadAli, Mahdi Hasanlou, Masoud Mahdianpari, and Fariba Mohammadimanesh. 2021. 'A Systematic Review of Landsat Data for Change Detection Applications: 50 Years of Monitoring the Earth'. *Remote Sensing* 13(15):2869. doi: 10.3390/rs13152869.

Hock, Regine, Andrew Bliss, Ben Marzeion, Rianne H. Giesen, Yukiko Hirabayashi, Matthias Huss, Valentina Radić, and Aimée B. A. Slangen. 2019. 'GlacierMIP – A Model Intercomparison of Global-Scale Glacier Mass-Balance Models and Projections'. *Journal of Glaciology* 65(251):453–67. doi: 10.1017/jog.2019.22.

Hugonnet, Romain, Robert McNabb, Etienne Berthier, Brian Menounos, Christopher Nuth, Luc Girod, Daniel Farinotti, Matthias Huss, Ines Dussaillant, Fanny Brun, and Andreas Kääb. 2021. 'Accelerated Global Glacier Mass Loss in the Early Twenty-First Century'. *Nature* 592(7856):726–31. doi: 10.1038/s41586-021-03436-z.

IPCC. 2021. 'Climate Change 2021: The Physical Science Basis. Contribution of Working Group I to the Sixth Assessment Report of the Intergovernmental Panel on Climate Change [Masson-Delmotte, V., P. Zhai, A. Pirani, S.L. Connors, C. Péan, S.

Berger, N. Caud, Y. Chen, L. Goldfarb, M.I. Gomis, M. Huang, K. Leitzell, E. Lonnoy, J.B.R. Matthews, T.K. Maycock, T. Waterfield, O. Yelekçi, R. Yu, and B. Zhou (Eds.)]. Cambridge University Press. In Press.' (September):43.

Isaksen, Ketil, Øyvind Nordli, Boris Ivanov, Morten A. Ø. Køltzow, Signe Aaboe, Herdis M. Gjelten, Abdelkader Mezghani, Steinar Eastwood, Eirik Førland, Rasmus E. Benestad, Inger Hanssen-Bauer, Ragnar Brækkan, Pavel Sviashchennikov, Valery Demin, Anastasiia Revina, and Tatiana Karandasheva. 2022. 'Exceptional Warming over the Barents Area'. *Scientific Reports* 12(1):9371. doi: 10.1038/s41598-022-13568-5.

Kääb, A., C. Huggel, L. Fischer, S. Guex, F. Paul, I. Roer, N. Salzmann, S. Schlaefli, K. Schmutz, D. Schneider, T. Strozzi, and Y. Weidmann. 2005. 'Remote Sensing of Glacier- and Permafrost-Related Hazards in High Mountains: An Overview'. *Natural Hazards and Earth System Science* 5(4):527–54. doi: 10.5194/nhess-5-527-2005.

Khan, Aftab Ahmed, Akhtar Jamil, Dostdar Hussain, Murtaza Taj, Gul Jabeen, and Muhammad Kamran Malik. 2020. 'Machine-Learning Algorithms for Mapping Debris-Covered Glaciers: The Hunza Basin Case Study'. *IEEE Access* 8:12725–34. doi: 10.1109/ACCESS.2020.2965768.

King, Owen, Amaury Dehecq, Duncan Quincey, and Jonathan Carrivick. 2018. 'Contrasting Geometric and Dynamic Evolution of Lake and Land-Terminating Glaciers in the Central Himalaya'. *Global and Planetary Change* 167:46–60. doi: 10.1016/j.gloplacha.2018.05.006.

Kochtitzky, William, and Luke Copland. 2022a. 'Retreat of Northern Hemisphere Marine-Terminating Glaciers, 2000–2020'. *Geophysical Research Letters* 49(3):e2021GL096501. doi: 10.1029/2021GL096501.

Kochtitzky, William, and Luke Copland. 2022b. 'Retreat of Northern Hemisphere Marine-Terminating Glaciers, 2000–2020'. *Geophysical Research Letters* 49(3):e2021GL096501. doi: 10.1029/2021GL096501.

Kohnemann, Svenja H. E., Günther Heinemann, David H. Bromwich, and Oliver Gutjahr. 2017. 'Extreme Warming in the Kara Sea and Barents Sea during the Winter Period 2000–16'. *Journal of Climate* 30(22):8913–27. doi: 10.1175/JCLI-D-16-0693.1.

Kulkarni, Arun, and Barrett Lowe. 2016. 'Random Forest Algorithm for Land Cover Classification'. *Computer Science Faculty Publications and Presentations*.

Kulp, Scott A., and Benjamin H. Strauss. 2019. 'New Elevation Data Triple Estimates of Global Vulnerability to Sea-Level Rise and Coastal Flooding'. *Nature Communications* 10(1). doi: 10.1038/s41467-019-12808-z.

Kumar, Avinash, Juhi Yadav, and Rahul Mohan. 2021. 'Spatio-Temporal Change and Variability of Barents-Kara Sea Ice, in the Arctic: Ocean and Atmospheric Implications'. *Science of The Total Environment* 753:142046.

Kumar, Mithun, Ayad M. Fadhil Al-Quraishi, and Ismail Mondal. 2020. 'Glacier Changes Monitoring in Bhutan High Himalaya Using Remote Sensing Technology'. *Environmental Engineering Research* 26(1). doi: 10.4491/eer.2019.255.

Lea, James M. 2018. 'The Google Earth Engine Digitisation Tool (GEEDiT) and the Margin Change Quantification Tool (MaQiT) – Simple Tools for the Rapid Mapping and Quantification of Changing Earth Surface Margins'. *Earth Surface Dynamics* 6(3):551–61. doi: 10.5194/esurf-6-551-2018.

Liu, Xiaoping, Guohua Hu, Yimin Chen, Xia Li, Xiaocong Xu, Shaoying Li, Fengsong Pei, and Shaojian Wang. 2018. 'High-Resolution Multi-Temporal Mapping of Global Urban Land Using Landsat Images Based on the Google Earth Engine Platform'. *Remote Sensing of Environment* 209:227–39. doi: 10.1016/j.rse.2018.02.055.

Mahdianpari, Masoud, Bahram Salehi, Fariba Mohammadimanesh, Saeid Homayouni, and Eric Gill. 2019. 'The First Wetland Inventory Map of Newfoundland at a Spatial Resolution of 10 m Using Sentinel-1 and Sentinel-2 Data on the Google Earth Engine Cloud Computing Platform'. *Remote Sensing* 11(1):43. doi: 10.3390/rs11010043.

Masek, Jeffrey G., Michael A. Wulder, Brian Markham, Joel McCorkel, Christopher J. Crawford, James Storey, and Del T. Jenstrom. 2020. 'Landsat 9: Empowering Open Science and Applications through Continuity'. *Remote Sensing of Environment* 248:111968. doi: 10.1016/j.rse.2020.111968.

Melkonian, Andrew K., Michael J. Willis, Matthew E. Pritchard, and Adam J. Stewart. 2016. 'Recent Changes in Glacier Velocities and Thinning at Novaya Zemlya'. *Remote Sensing of Environment* 174:244–57. doi: 10.1016/j.rse.2015.11.001.

Millan, Romain, Jérémie Mouginot, Antoine Rabatel, and Mathieu Morlighem. 2022. 'Ice Velocity and Thickness of the World's Glaciers'. *Nature Geoscience* 15(2):124–29. doi: 10.1038/s41561-021-00885-z.

Moon, Twila A., Irina Overeem, Matt Druckenmiller, Marika Holland, Henry Huntington, George Kling, Amy Lauren Lovecraft, Gifford Miller, Ted Scambos, Christina Schädel, Edward A. G. Schuur, Erin Trochim, Francis Wiese, Dee Williams, and Gifford Wong. 2019. 'The Expanding Footprint of Rapid Arctic Change'. *Earth's Future* 7(3):212–18. doi: 10.1029/2018EF001088.

Nery, Thayse, Rohan Sadler, Maria Solis-Aulestia, Ben White, Maksym Polyakov, and Morteza Chalak. 2016. 'Comparing Supervised Algorithms in Land Use and Land Cover Classification of a Landsat Time-Series'. Pp. 5165–68 in *2016 IEEE International Geoscience and Remote Sensing Symposium (IGARSS)*.

Nijhawan, Rahul, Pradeep Garg, and Praveen Thakur. 2016. 'A Comparison of Classification Techniques for Glacier Change Detection Using Multispectral Images'. *Perspectives in Science* 8:377–80. doi: 10.1016/j.pisc.2016.04.080.

Nuth, C., J. Kohler, M. König, A. Von Deschwanden, J. O. Hagen, A. Kääb, G. Moholdt, and R. Pettersson. 2013. 'Decadal Changes from a Multi-Temporal Glacier Inventory of Svalbard'. *Cryosphere* 7(5):1603–21. doi: 10.5194/tc-7-1603-2013.

Paul, Frank, Tobias Bolch, Kate Briggs, Andreas Kääb, Malcolm McMillan, Robert McNabb, Thomas Nagler, Christopher Nuth, Philipp Rastner, Tazio Strozzi, and Jan Wuite. 2017. 'Error Sources and Guidelines for Quality Assessment of Glacier Area, Elevation Change, and Velocity Products Derived from Satellite Data in the Glaciers_cci Project'. *Remote Sensing of Environment* 203:256–75. doi: 10.1016/j.rse.2017.08.038.

Paul, Frank, Tobias Bolch, Andreas Kääb, Thomas Nagler, Christopher Nuth, Killian Scharrer, Andrew Shepherd, Tazio Strozzi, Francesca Ticconi, Rakesh Bhambri, Etienne Berthier, Suzanne Bevan, Noel Gourmelen, Torborg Heid, Seongsu Jeong, Matthias Kunz, Tom Rune Lauknes, Adrian Luckman, John Peter Merryman Boncori, Geir Moholdt, Alan Muir, Julia Neelmeijer, Melanie Rankl, Jeffrey VanLooy, and Thomas Van Niel. 2015. 'The Glaciers Climate Change Initiative: Methods for Creating Glacier Area, Elevation Change and Velocity Products'. *Remote Sensing of Environment* 162:408–26. doi: 10.1016/j.rse.2013.07.043.

Paul, Frank, Andreas Kääb, and Wilfried Haeberli. 2007. 'Recent Glacier Changes in the Alps Observed by Satellite: Consequences for Future Monitoring Strategies'. *Global and Planetary Change* 56(1–2):111–22. doi: 10.1016/j.gloplacha.2006.07.007.

Praticò, Salvatore, Francesco Solano, Salvatore Di Fazio, and Giuseppe Modica. 2021. 'Machine Learning Classification of Mediterranean Forest Habitats in Google Earth Engine Based on Seasonal Sentinel-2 Time-Series and Input Image Composition Optimisation'. *Remote Sensing* 13(4):586. doi: 10.3390/rs13040586.

Racoviteanu, Adina E., Frank Paul, Bruce Raup, Siri Jodha Singh Khalsa, and Richard Armstrong. 2009. 'Challenges and Recommendations in Mapping of Glacier Parameters from Space: Results of the 2008 Global Land Ice Measurements from Space (GLIMS) Workshop, Boulder, Colorado, USA'. *Annals of Glaciology* 50(53):53–69. doi: 10.3189/172756410790595804.

Racoviteanu, Adina E., Mark W. Williams, and Roger G. Barry. 2008. 'Optical Remote Sensing of Glacier Characteristics: A Review with Focus on the Himalaya'. *Sensors* 8(5):3355–83. doi: 10.3390/s8053355.

Rantanen, Mika, Alexey Yu Karpechko, Antti Lipponen, Kalle Nordling, Otto Hyvärinen, Kimmo Ruosteenoja, Timo Vihma, and Ari Laaksonen. 2022. 'The Arctic

Has Warmed Nearly Four Times Faster than the Globe since 1979'. *Communications Earth & Environment* 3(1):1–10. doi: 10.1038/s43247-022-00498-3.

Rastner, Philipp, Tobias Bolch, Claudia Notarnicola, and Frank Paul. 2014. 'A Comparison of Pixel- and Object-Based Glacier Classification with Optical Satellite Images'. *IEEE Journal of Selected Topics in Applied Earth Observations and Remote Sensing* 7(3):853–62. doi: 10.1109/JSTARS.2013.2274668.

Rastner, Philipp, Tazio Strozzi, and Frank Paul. 2017. 'Fusion of Multi-Source Satellite Data and DEMs to Create a New Glacier Inventory for Novaya Zemlya'. *Remote Sensing* 9(11):1–18. doi: 10.3390/rs9111122.

Raup, Bruce H., Liss M. Andreassen, Tobias Bolch, Suzanne Bevan, and Bruce H. Raup. 2014. 'Remote Sensing of Glaciers'.

Raup, Bruce, Adina Racoviteanu, Siri Jodha Singh Khalsa, Christopher Helm, Richard Armstrong, and Yves Arnaud. 2007. 'The GLIMS Geospatial Glacier Database: A New Tool for Studying Glacier Change'. *Global and Planetary Change* 56(1–2):101–10. doi: 10.1016/j.gloplacha.2006.07.018.

Ren and Malik. 2003. 'Learning a Classification Model for Segmentation'. Pp. 10–17 vol.1 in *Proceedings Ninth IEEE International Conference on Computer Vision*.

Robson, Benjamin Aubrey, Daniel Hölbling, Christopher Nuth, Tazio Strozzi, and Svein Olaf Dahl. 2016. 'Decadal Scale Changes in Glacier Area in the Hohe Tauern National Park (Austria) Determined by Object-Based Image Analysis'. *Remote Sensing* 8(1). doi: 10.3390/rs8010067.

Robson, Benjamin Aubrey, Christopher Nuth, Svein Olaf Dahl, Daniel Hölbling, Tazio Strozzi, and Pål Ringkjøb Nielsen. 2015. 'Automated Classification of Debris-Covered Glaciers Combining Optical, SAR and Topographic Data in an Object-Based Environment'. *Remote Sensing of Environment* 170:372–87. doi: 10.1016/j.rse.2015.10.001.

Schädel, Christina, Charles D. Koven, David M. Lawrence, Gerardo Celis, Anthony J. Garnello, Jack Hutchings, Marguerite Mauritz, Susan M. Natali, Elaine Pegoraro, Heidi Rodenhizer, Verity G. Salmon, Meghan A. Taylor, Elizabeth E. Webb, William R. Wieder, and Edward AG Schuur. 2018. 'Divergent Patterns of Experimental and Model-Derived Permafrost Ecosystem Carbon Dynamics in Response to Arctic Warming'. 13(10):105002. doi: 10.1088/1748-9326/aae0ff.

Shafizadeh-Moghadam, Hossein, Morteza Khazaei, Seyed Kazem Alavipanah, and Qihao Weng. 2021. 'Google Earth Engine for Large-Scale Land Use and Land Cover Mapping: An Object-Based Classification Approach Using Spectral, Textural and Topographical Factors'. *GIScience & Remote Sensing* 58(6):914–28. doi: 10.1080/15481603.2021.1947623.

Sharp, Martin, David O. Burgess, Fiona Cawkwell, Luke Copland, James A. Davis, Evelyn K. Dowdeswell, Julian A. Dowdeswell, Alex S. Gardner, Douglas Mair, Libo Wang, Scott N. Williamson, Gabriel J. Wolken, and Faye Wyatt. 2014. 'Remote Sensing of Recent Glacier Changes in the Canadian Arctic'. Pp. 205–28 in *Global Land Ice Measurements from Space*, *Springer Praxis Books*, edited by J. S. Kargel, G. J. Leonard, M. P. Bishop, A. Kääb, and B. H. Raup. Berlin, Heidelberg: Springer.

Sugiyama, Shin, Masahiro Minowa, Yasushi Fukamachi, Shuntaro Hata, Yoshihiro Yamamoto, Tobias Sauter, Christoph Schneider, and Marius Schaefer. 2021. 'Subglacial Discharge Controls Seasonal Variations in the Thermal Structure of a Glacial Lake in Patagonia'. *Nature Communications* 12:6301. doi: 10.1038/s41467-021-26578-0.

Tassi, Andrea, and Marco Vizzari. 2020. 'Object-Oriented LULC Classification in Google Earth Engine Combining SNIC, GLCM, and Machine Learning Algorithms'. *Remote Sensing* 12(22):3776. doi: 10.3390/rs12223776.

Tsutaki, Shun, Daisuke Nishimura, Takeshi Yoshizawa, and Shin Sugiyama. 2011. 'Changes in Glacier Dynamics under the Influence of Proglacial Lake Formation in Rhonegletscher, Switzerland'. *Annals of Glaciology* 52(58):31–36. doi: 10.3189/172756411797252194.

Wilfried Haeberli Frank Paul, Tobias Kellenberger, Andreas KÌÌb, Max Maisch. 2002. 'The New Remote-Sensing-Derived Swiss Glacier Inventory: I. Methods'. *Annals of Glaciology* 34(September 1985):362–66. doi: 10.3189/172756402781817473.

Winsvold, S. H., L. M. Andreassen, and C. Kienholz. 2014. 'Glacier Area and Length Changes in Norway from Repeat Inventories'. *Cryosphere* 8(5):1885–1903. doi: 10.5194/tc-8-1885-2014.

Xue, Xingyu, Zhoulu Yu, Shaochun Zhu, Qiming Zheng, Melanie Weston, Ke Wang, Muye Gan, and Hongwei Xu. 2018. 'Delineating Urban Boundaries Using Landsat 8 Multispectral Data and VIIRS Nighttime Light Data'. *Remote Sensing* 10(5):799. doi: 10.3390/rs10050799.

Yamagami, Yoko, Masahiro Watanabe, Masato Mori, and Jun Ono. 2022. 'Barents-Kara Sea-Ice Decline Attributed to Surface Warming in the Gulf Stream'. *Nature Communications* 13(1):3767. doi: 10.1038/s41467-022-31117-6.

You, Qinglong, Ziyi Cai, Nick Pepin, Deliang Chen, Bodo Ahrens, Zhihong Jiang, Fangying Wu, Shichang Kang, Ruonan Zhang, Tonghua Wu, Pengling Wang, Mingcai Li, Zhiyan Zuo, Yanhong Gao, Panmao Zhai, and Yuqing Zhang. 2021. 'Warming Amplification over the Arctic Pole and Third Pole: Trends, Mechanisms and Consequences'. *Earth-Science Reviews* 217:103625. doi: 10.1016/j.earscirev.2021.103625.

Zemp, M., M. Huss, E. Thibert, N. Eckert, R. McNabb, J. Huber, M. Barandun, H. Machguth, S. U. Nussbaumer, I. Gärtner-Roer, L. Thomson, F. Paul, F. Maussion, S. Kutuzov, and J. G. Cogley. 2019. 'Global Glacier Mass Changes and Their Contributions to Sea-Level Rise from 1961 to 2016'. *Nature* 568(7752):382–86. doi: 10.1038/s41586-019-1071-0.

Zhang, Xiao, Liangyun Liu, Changshan Wu, Xidong Chen, Yuan Gao, Shuai Xie, and Bing Zhang. 2020. 'Development of a Global 30 m Impervious Surface Map Using Multisource and Multitemporal Remote Sensing Datasets with the Google Earth Engine Platform'. *Earth System Science Data* 12(3):1625–48. doi: 10.5194/essd-12-1625-2020.

Chapter 4

Decadal glacier area changes in the Arctic and high latitudes using object-based image analysis in Google Earth Engine

Asim Ali[1], Paul Dunlop[1], Sonya Coleman[2], Dermot Kerr[2], Robert W McNabb[1], and Riko Noormets[3]

[1]School of Geography and Environmental Sciences, Ulster University, UK

[2]School of Computing, Engineering, and Intelligent Systems, Ulster University, UK

[3]School of Marine, Geology, and Geophysics, University Centre in Svalbard

4.1. Abstract

Climate change has had a significant impact on glacier recession worldwide, with melting ice sheets and glaciers contributing disproportionately to global sea-level rise. To better understand the impact of climate change on glaciers in the Arctic and high latitudes, observations of temporal changes in glacier extent are necessary. Currently such large-scale observations are not available due to the large effort required to accurately map glacier areas over very large areas. In this study, we mapped 1723 glaciers in Baffin Island, Canadian Arctic, Qeqertarsuaq (Disko Island), Greenland and Kenai, Alaska, using Object-Based Image Analysis (OBIA) applied to multispectral Landsat satellite imagery in Google Earth Engine (GEE) to quantify glacier area change over three decades. Over the period 1985-86 to 2019-21, Baffin glaciers lost 452±227 km^2 (6.6%), Disko glaciers lost 456±168 km^2 (23.6%), and the Kenai glaciers showed a 196±84 km^2 (25.7%) decline in the total area. Based on ERA5 reanalysis data, Disko (1.7 °C) shows the highest temperature increase between 2001 and 2019, followed by Baffin (1.1 °C) and Kenai (1 °C), when compared to between 1985 and 2001. The results also showed that glacier area loss also increased in 2000-02 to 2019-21 in all three regions, compared 1985-86 to 2000-02. During 1985-86 and 2019-21, a total of 70 glaciers have completely retreated, including 69 on Disko and one in Kenai

Key words

4.2. Introduction

The Arctic cryosphere is an important component of the earth's system that stores freshwater, influences sea-level, and results in net cooling of the earth's surface (Olsen et al. 2011). However, the Arctic has experienced some of the most rapid warming of any region on earth over the last few decades (e.g., Schädel et al. 2018; You et al. 2021). According to a recent study by Rantanen et al. (2022), warming in the Arctic has been four times greater than the rest of world since 1979. As result of climate change, mountain glaciers, ice caps, and the Greenland Ice Sheet (GrIS) have all receded in the Arctic over the last century (AMAP 2017). These vast freshwater reservoirs are rapidly melting, and raising global sea levels (Hugonnet et al. 2021; Zemp et al. 2019).

Millions of people live within a few kilometres of the coast, and future sea level rise could start forcing communities worldwide to relocate (Kulp and Strauss 2019). In the 21st century, glaciers and ice sheets are the largest contributor to global sea-level rise (IPCC 2021). As glaciers have such a large impact and have the potential to affect a large portion of the world, it is important to closely monitor regional glacier changes and gain a clear understanding of the impact of climate change on these systems. Remote sensing is an ideal tool for monitoring changes in huge glacierized regions that are largely inaccessible like the Arctic (e.g. Winsvold et al. 2014).

Glaciers are climatically controlled systems that grow and decay in response to temperature and precipitation changes, making them one of the best indicators of climate change (e.g., Bosson et al. 2019). Continuous monitoring of glaciers by mapping glacier outlines across different time-frames can be a useful tool to help quantify glacier changes and predict their future evolution (Haeberli 2004; Huss 2012). Glacier outlines are essential for this task, as they are used to estimate ice volume (Millan et al. 2022), calculate glacier mass changes (e.g., Zemp et al. 2019), and are important for predicting sea level rise (Hock et al. 2019).

Several important digital glacier inventories are available that have glacier outlines for different parts of the work. However, it is important that these are updated regularly for assessing the impacts of climate change on glaciers over long times scales (Sorg et al. 2012). Global Land Ice Measurements from Space (GLIMS) is a digital database that stores glacier outlines, accessible globally at https://www.glims.org/, where users can explore and download glacier outlines (Raup et al. 2007). However, for most glaciers worldwide, outlines are only available at a single point in time, limiting their use for understanding the long-term effects of climate change on glaciers.

In this study, we apply a newly developed Object-Based Image Analysis (OBIA) approach to map and generate glacier outlines automatically using a framework developed in Google Earth Engine (GEE) by Ali et al. (2023). This automated method is used to generate multi-temporal outlines of glaciers in three regions: Baffin,

Canadian Arctic; Disko, Greenland; and the Kenai Peninsula, Alaska. The main goals of this study are : i) to map glacier area changes across three different regions at multiple points in time; ii) to evaluate changes in temperature with changes in glacier area; iii) to compare the derived area changes to mass losses (Hugonnet et al. 2021); and iv) to assess the accuracy of the method using manually-corrected outlines in different glacierized regions.

4.3. Study Area

To understand the impacts of climate change on glaciers in the Arctic and high latitudes this study focused on three different regions; including two in the Arctic: Baffin Island (Canadian Arctic), Disko Island (Greenland), and one in the Kenai Peninsula, Alaska (Figure 16). A total of 1723 glaciers were chosen from the Randolph Glacier inventory (RGI) version 6.0 (RGI Consortium 2017): 748 glaciers on Disko (RGI Area: 1869 km^2); 523 glaciers on Baffin (7054 km^2); and 452 glaciers on the Kenai Peninsula (638 km^2).

The Canadian Arctic Archipelago is located north of mainland Canada and is the world's largest region of land ice outside of the Greenland and Antarctica ice sheets (Sharp et al. 2014). The average annual temperature on Baffin can be as low as -20°C in the north and -6°C in the south, with extreme low temperatures reaching -50°C (Peter and Maxwell 2015). Annual precipitation on Baffin Island varies from 400mm on the southern part of the island to less than 100mm in the centre (Strozzi et al. 2017).

Disko (Greenlandic: Qeqertarsuaq) is the largest island in Greenland, located off the west coast. The average monthly temperature ranges from -12 °C in February to +7 °C in July (Friberg et al. 2001). The coldest record from 1991 to 2020 is -40.5 °C, set in March 1993 while the highest temperature ever recorded was 21.7 °C in July 2017 (Greenland Climate, 2020).

The Kenai Peninsula is situated between the Cook Inlet and the Gulf of Alaska in south-central Alaska (Yang et al. 2020). It generally has a maritime climate with a mean annual temperature of 1.1 °C and 485mm of precipitation (Berg et al. 2006). The warmest month in Kenai is July, with an average high of 17°C and low of 10°C, and the coldest month is January, with an average low of -11°C and high of -4°C.

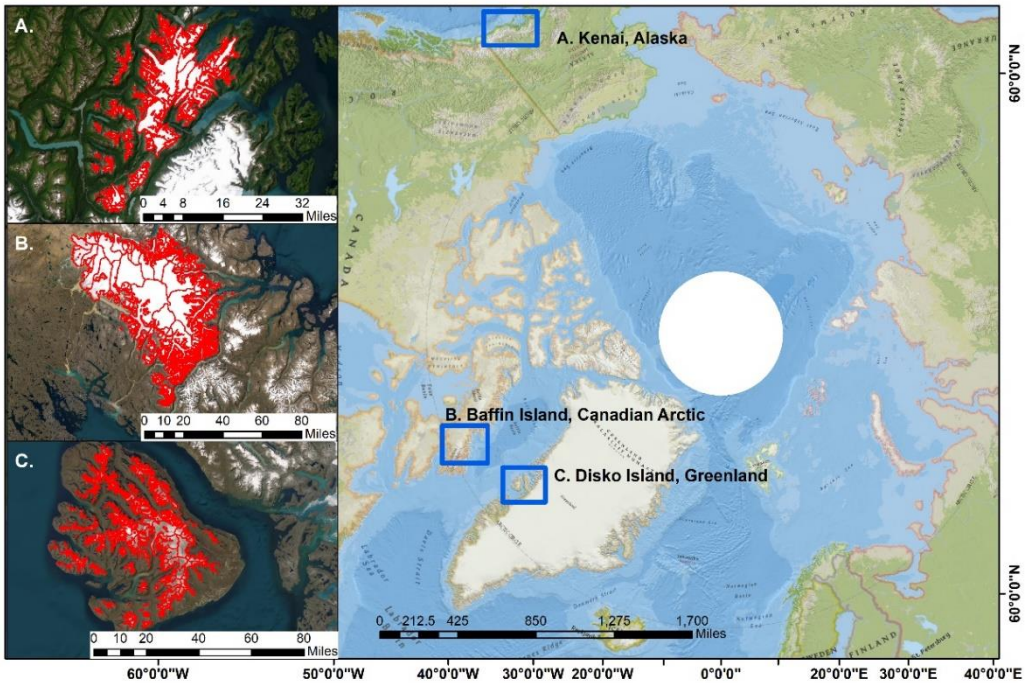

Figure 16 The three study areas: A. Kenai, Alaska; B. Baffin, Canada; and C. Disko, Greenland. Red polygons show the RGI 6.0 outlines of the glaciers selected for the study.

4.4. Data and Methods

4.4.1. Data

Landsat is a joint project of the United States Geological Survey (USGS) and National Aeronautics and Space Administration (NASA) that has been continuously monitoring the Earth since 1972 (Rocchio et al. 2018). Landsat satellite data has shown to be a useful asset for glacier mapping due to its large swath width of about 185 km that can capture a large area in single pass, long temporal record of capturing images, and multispectral capabilities that can acquire data in several bands (e.g., Hemati et al. 2021). Several bands are useful for glacier mapping because glaciers have distinct spectral signatures in specific bands that can be used to differentiate them from surrounding areas. In this study, the images were carefully selected in GEE during the summer-time period (July-September) with minimal cloud cover, including three images of Landsat 5 Thematic Mapper (TM), four Landsat 7 Enhanced Thematic Mapper Plus (ETM+) images, and four Landsat 8 Operational Land Imager (OLI) images (Table 7).

The USGS creates data in three categories: real-time (RT), Tier 1, and Tier 2, which are stored in Collection 1 or 2. Tier 1 images have the highest quality and are suited for time-series analysis (Masek et al. 2020), while Tier 2 images have geometric correction issues but are still good quality images. Some studies have used digital number or raw radiance data without atmospheric correction to map glaciers (e.g., Alifu et al. 2015; Paul et al. 2002). However, surface reflectance data is necessary

for systematic analysis, especially in highly automated approaches (Hemati et al. 2021). In this study, we use Collection 1, Tier 1, Level 2 surface reflectance products.

In this study, we also used ERA5 reanalysis data for computing temperature changes over the selected regions from 1985 to 2019. ERA5 is the fifth generation of reanalysis data produced by the European Centre for Medium-Range Weather Forecasts (ECMWF) (Copernicus Climate Change Service 2019). ERA5 provides global coverage of various meteorological variables, including temperature, precipitation, wind speed, humidity, and atmospheric pressure (e.g., Vanella et al. 2022).

Table 7: Details of images that are used in this study.

Satellite	Date (DD/MM/YYYY)	WRS-2 Path/Row	GEE Image IDs
Baffin, Canadian Arctic			
Landsat 5	19/08/1985	18/13	LANDSAT/LT05/C01/T1_SR/LT05_018013_19850819
Landsat 7	13/08/2000	17/13	LANDSAT/LE07/C01/T1_SR/LE07_017013_20000813
Landsat 7	01/08/2002	19/13	LANDSAT/LE07/C01/T1_SR/LE07_019013_20020801
Landsat 8	25/07/2020	19/13	LANDSAT/LC08/C01/T1_SR/LC08_019013_20200725
Landsat 8	30/07/2021	17/13	LANDSAT/LC08/C01/T1_SR/LC08_017013_20210730
Disko, Greenland			
Landsat 5	03/09/1985	11/11	LANDSAT/LT05/C01/T1_SR/LT05_011011_19850903
Landsat 7	29/08/2001	12/11	LANDSAT/LE07/C01/T1_SR/LE07_012011_20010829
Landsat 8	01/09/2019	11/11	LANDSAT/LC08/C01/T1_SR/LC08_011011_20190901
Kenai, Alaska			
Landsat 5	28/07/1986	67/18	LANDSAT/LT05/C01/T1_SR/LT05_067018_19860728

Landsat 7	01/08/2002	67/18	LANDSAT/LE07/C01/T1_SR/LE07_067018_20020801
Landsat 8	18/08/2019	67/18	LANDSAT/LC08/C01/T1_SR/LC08_067018_20190808

4.4.2. Method: Object based image analysis in Google Earth Engine

Google Earth Engine is a powerful cloud-based remote sensing analysis tool that has planetary-scale analysis capabilities and a multi-petabyte imagery library (Gorelick et al. 2017). Object Based Image Analysis incorporates contextual information from neighbouring pixels, the size and shape of objects, and texture during classification, whereas pixel-based classification focuses on individual pixels (Blaschke 2010). In this study, we use an Object-based Image Analysis approach in Google Earth Engine to map glacier changes developed byAli et al. (2023). We provide a brief summary of the approach used below, with full details of the methodology available in Ali et al. (2023).

Segmentation is an important step in the OBIA approach as it groups similar pixels into clusters or image objects (Ren and Malik 2003). As input layers for image segmentation, this study uses the visible green and red, near infrared, shortwave infrared, and thermal bands. Before segmentation, a one-sigma Gaussian filter with radius 2 pixels was applied to reduce noise in the images (Xue et al. 2018). We use the simple non-iterative clustering technique, an improved version of simple linear clustering, to segment the Landsat image (Achanta and Süsstrunk 2017).

To classify the image objects, we trained a Random Forest classifier with 10 trees on manually selected samples of "glacier" and "non-glacier" classes distributed

throughout the scene. To train the classifier, we used approximately 100 “glacier” and 100 “non-glacier” samples per image. The Random Forest classifier is the most widely used machine learning algorithm in GEE (Amani et al. 2020), it is robust, and can handle high dimensionality, reducing the risk of overfitting (Nery et al. 2016; Praticò et al. 2021). After classification, a median filter with a radius of 2.5 was used to reduce noise in the classified image, which was then converted from raster to vector to create glacier outlines.

The automated glacier outlines were exported from GEE to ArcGIS 10.5.1 for post-processing. Each glacier was examined to determine whether manual correction was required, and manual corrections were made where needed. Finally, the linked glacier outlines were separated using the RGI's internal boundaries, which enabled analysis of changes for each glacier.

To have a better understanding of the glacier area changes, we also used ERA5 reanalysis data in the Google Earth Engine platform to calculate the average yearly temperature for each region. The ERA5 data can be accessed through the Google Earth Engine interface, making it a valuable tool for analysis. We exported the temperature data from Google Earth Engine and used the Matplotlib library to produce a figure depicting the temperature changes from 1985 to 2019 for each region.

4.4.2.1. Accuracy and Uncertainty

Satellite-capture images during different conditions can have differences in illumination, issues with cloud cover or shadows over the target feature, all of which can have impact on automated classification and image quality. The three regions used in this study have seasonal variations, different climatic regimes and as well different topographic settings. So, it is important to understand the capabilities of the method when utilising images from different times and in different locations. To determine the uncertainty of the mapped glacier area, two approaches were used these were random sampling and buffer analysis.

4.4.2.2. Uncertainty by random sampling

Random samples were generated to assess the accuracy of the automated outlines from each time period, and reference datasets were created based on the manually corrected outlines of each layer. The random samples were divided into two classes, "glacier" and "non-glacier," with an equal number of samples in each class, using the manually corrected outlines as reference data. The confusion matrix was created by comparing the classification for the automated outlines and the reference data. The details of producer's accuracy, user's accuracy and misclassified samples of each layer are given in Table 8.

Table 8 Confusion matrices of each layer in Baffin, Disko, and Kenai generated based on random sampling.

		Reference Data			
	Baffin: Layer 1985	**Glacier**	**Non-glacier**	**Total**	**User's accuracy**
Classified	Glacier	1784	38	1822	97.9%
	Non-glacier	35	1781	1816	98.0%
	Total	1819	1819	3638	
	Producer's accuracy	98.0%	97.9%		
	Layer 2000-02	Glacier	Non-glacier	Total	User's accuracy
	Glacier	1725	28	1753	98.4%
	Non-glacier	56	1753	1809	96.9%
	Total	1781	1781	3562	
	Producer's accuracy	96.8%	98.4%		
	Layer 2020-21	Glacier	Non-glacier	Total	User's accuracy
	Glacier	1659	19	1678	98.8%
	Non-glacier	49	1689	1738	97.1%
	Total	1708	1708	3416	
	Producer's accuracy	97.1%	98.8%		
	Disko: Layer 1985	Glacier	Non-glacier	Total	User's accuracy
Classified	Glacier	929	26	955	97.2%
	Non-glacier	31	934	965	96.7%
	Total	960	960	1920	
	Producer's accuracy	96.7%	97.2%		
	Layer 2001	Glacier	Non-glacier	Total	User's accuracy
	Glacier	677	25	702	96.4%
	Non-glacier	27	679	706	96.1%
	Total	704	704	1408	
	Producer's accuracy	96.1%	96.4%		
	Layer 2019	Glacier	Non-glacier	Total	User's accuracy
	Glacier	636	11	647	98.3%
	Non-glacier	41	666	707	94.2%
	Total	677	677	1354	
	Producer's accuracy	93.9%	98.3%		
	Kenai: Layer 1986	Glacier	Non-glacier	Total	User's accuracy
Classified	Glacier	698	50	748	93.3%
	Non-glacier	35	683	718	95.1%
	Total	733	733	1466	
	Producer's accuracy	95.2%	93.1%		
	Layer 2002	Glacier	Non-glacier	Total	User's accuracy
	Glacier	623	34	657	94.8%
	Non-glacier	51	640	691	92.6%
	Total	674	674	1348	
	Producer's accuracy	92.4%	94.9%		
	Layer 2019	Glacier	Non-glacier	Total	User's accuracy

Glacier	618	2	620	99.6%
Non-glacier	35	651	686	94.8%
Total	653	653	1306	
Producer's accuracy	94.6%	99.6%		

4.4.2.3. Uncertainty using buffer analysis.

A ±30m buffer was applied to assess the area uncertainty of each manual corrected outline. In the absence of appropriate reference data, the buffer approach is commonly used to determine accuracy using a literature-derived uncertainty value (±0.5 or 1 pixel) (Granshaw and Fountain 2006; Paul et al. 2017). The buffered area of each layer in Baffin, Dikso, and Kenai was used to calculate the uncertainty in the glacier area, and Table 9 shows the high, low, and area with ± uncertainty values for each time period.

Table 9 Computed areas (in km^2) of each layer based on the ±30 m buffer.

Baffin	**High**	**Low**	**Area**
1985	7369	7053	7211±158
2000-02	7213	6887	7050±163
2020-21	6922	6596	6759±163
Disko			
1985	2056	1802	1929±127
2001	1896	1642	1769±127
2019	1582	1362	1472±110
Kenai			
1986	824	704	764±60
2002	768	642	705±63
2019	627	509	568±59

4.5. Results

The overall accuracy for each layer in Baffin, Disko, and Kenai was calculated using the confusion matrices in Table 8, showing an overall accuracy of between 93.7%

and 98% in three different regions. Baffin showed an overall accuracy between 97.6% and 98.0%, Disko has an accuracy range from 96.1% to 97%, and Kenai has an accuracy between 93.7% and 97.1%. Table 10 displays the overall accuracy and kappa coefficient of the method in each area for each layer.

Table 10 Overall accuracy and kappa coefficient of each layer of Baffin, Disko, and Kenai based on random sampling.

	1985-86		2000-02		2019-21	
Regions	**Percentage**	**Kappa**	**Percentage**	**Kappa**	**Percentage**	**Kappa**
Baffin	97.9	0.96	97.6	0.95	98.0	0.96
Disko	97.0	0.94	96.3	0.92	96.1	0.92
Kenai	94.2	0.88	93.7	0.87	97.1	0.94

Table 8 provides the detailed information of the producer and user accuracy. The producer accuracy of all layers varies between 93.1% to 99.6%, while the user accuracy ranges from 93.3% to 99.6%, and kappa coefficient is between 0.87 and 0.96. The Kappa Coefficient values range from -1 to 1, indicating how well classification and reference data agree. The producer accuracy assesses how accurately the reference pixels were identified, whereas the user accuracy measures how well the map depicts what is actually on the ground.

4.5.1. Glacier Area change

Between 1985-86 and 2019-21, the glaciers on Baffin lost a total of 452±227 km^2 (6.6%) glacierized area, while Disko glaciers showed a 456±168 km^2 (23.6%) reduction, and Kenai glaciers area decreased by 196±84 km^2 (25.7%). The area loss of glaciers was greater in the second time period of the study (2000-02 to 2019-21) compared to the first time period (1985-86 to 2000-02). From 1985-86 to 2000-02,

glaciers on Baffin lost 2.2% area, Disko glaciers lost 8.2%, and Kenai lost 7.7%. From 2000-02 to 2019-21 the area loss of each region nearly doubled, to 4.1% for glaciers on Baffin, 16.7% on Disko, and 19.5% in the Kenai Peninsula (Figure 17).

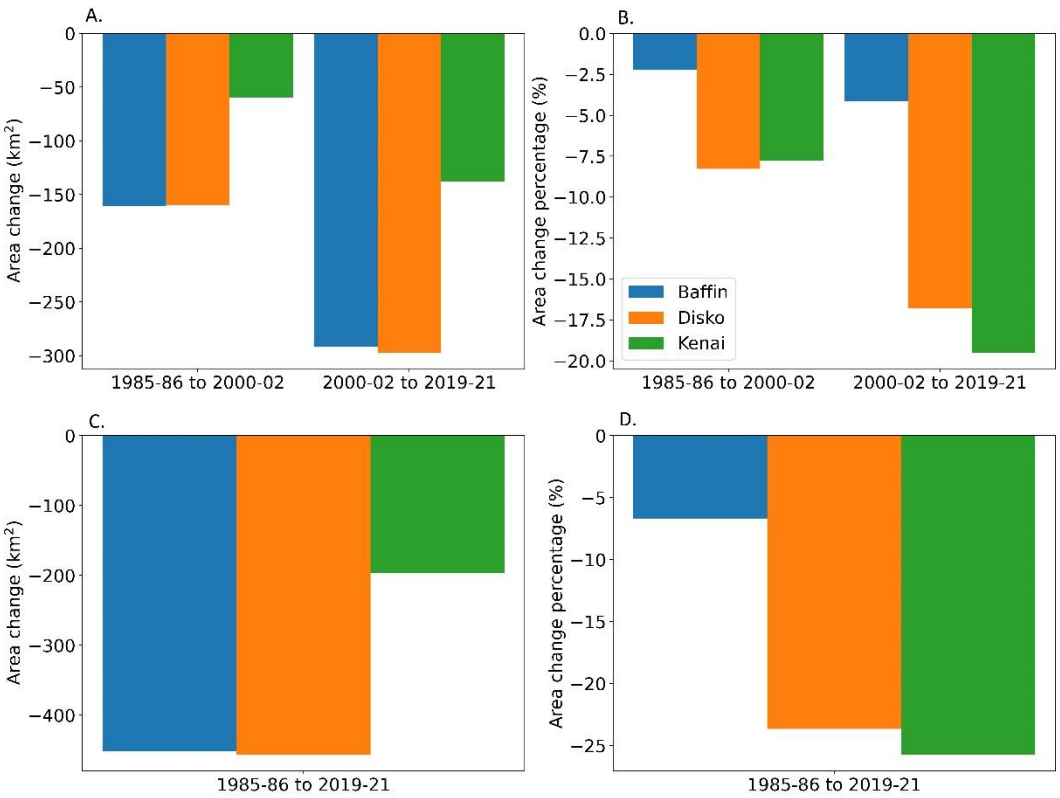

Figure 17 The total area loss of Baffin, Disko, and Kenai glaciers from 1985-86 to 2000-02 and 2000-02 to 2019-21, in both area and percent area. A and C shows the area loss of glacier in km^2 while B and D show the area loss in percentage.

Figure 18 depicts the total area change of each glacier as a percentage for two time periods: 1985-86 to 2000-02 and 2000-02 to 2019-21. Sixteen glaciers on Baffin, five glaciers on Disko, and four glaciers on Kenai have lost more than $5km^2$ of their total area, while in percentage the same sixteen glaciers on Baffin shows the loss from 2% to 13%, five glaciers on Disko lost between 10% and 52%, and four glaciers on Kenai lost from 10% to 28%. During the period of this study, a total of 70 glaciers

have completely retreated, sixty-nine glaciers of these are on Disko and the other glacier is in Kenai.

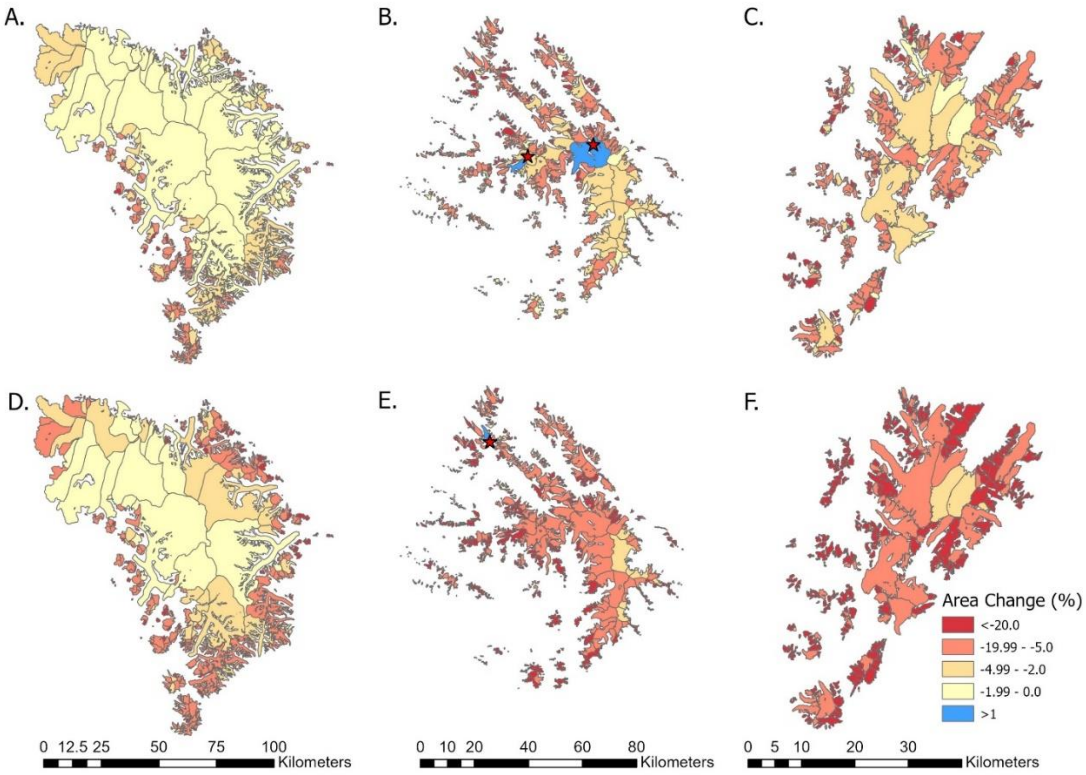

Figure 18 Represent the glacier area changes from 1985-86 to 2000-02 (A, B, and C) and between 2000-02-2019-21 (D, E, and F). (A-D) shows Baffin, (B-E) Disko, and (C-F) Kenai Alaska. The stars in B and E represent the surged glaciers.

4.6. Discussion

4.6.1. Glacier area changes

Glaciers, ice caps, and the Greenland Ice Sheet (GrIS) have all retreated in the Arctic over the last century and have started to retreat faster since 2000 (AMAP 2017). The same trend has been observed in this study in Baffin, Disko, and Kenai. Baffin glaciers loss increased by 1.9 percentage points in 2000-02 to 2019-21, while in

Disko (8.5 percentage points) and Kenai (11.7 percentage points) the area lost increased by double compared to 1985-86 to 2019-21. The same trend has also been observed in Novaya Zemlya, where glacier area loss increased by 1.7 percentage points from 2000-01 to 2019-21 compared to 1986-89 to 2000-01 (Ali et al. 2023) (Figure 19).

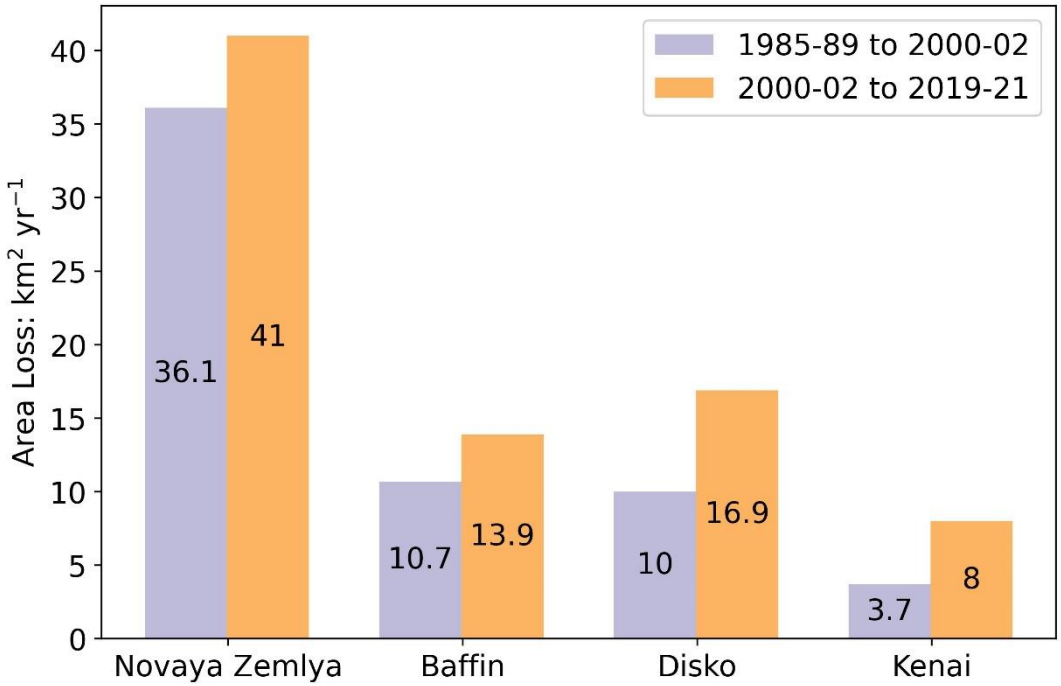

Figure 19 Area loss of four regions in km^2 per year between two time periods. Data for Novaya Zemlya from Ali et al. (2023).

A total of 70 glaciers have entirely retreated, and many more are on the verge of disappearing: sixteen glaciers on Baffin, 165 glaciers on Disko, and thirty-seven glaciers in Kenai have lost more than 80% of their total area (Figure 20). Although these glaciers are small in size (< 2 km^2), their combined area (73.5 km^2) declined to 8.3 km^2 between 1985-89 and 2019-21.

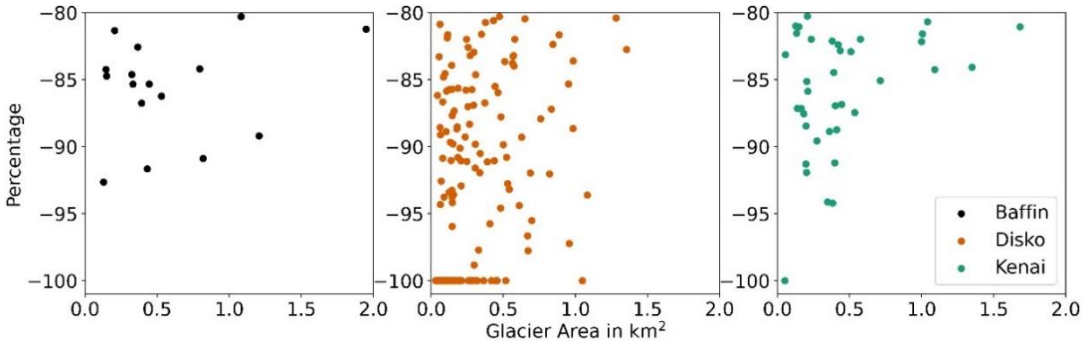

Figure 20 Representing the glaciers that have been retreated more than 80% of their areas during 1985-86 and 2019-21, x-axis shows the area of glacier from 1985-86

4.6.2. Evaluating temperature with glacier area changes

Between 1985 and 2019, the lowest temperature at Baffin ranged from -15.1 °C to -9 °C, the highest at Kenai varied from -2.1°C to 3.2°C, Novaya Zemlya temperature varies from -8.9 °C to -6.9 °C and Disko temperature ranged between -8.9°C and -3.9°C (Figure 21). During the second time period (2000-02-2019-21) of the study, the glacier area loss increased by almost double, and the average temperatures rose by 2 °C in Novaya Zemlya, 1.1 °C in Baffin, 1.7 °C in Disko, and Kenai by 1 °C compared to 1985 and 2001.

Across all four areas, Kenai is the warmest region (Figure 21,22), showing a higher percentage loss of area (Figure 17). Novaya Zemlya experienced a higher increase in annually average temperature but shows a lower percentage area loss (5.7%), due to the smallest increase in summer (May-Sep) average temperature with respect to other three areas (Figure 22).

The total loss of Baffin glacierized area in km^2 (452±227 km^2) is not substantially different from Disko (456±168 km^2), but Disko shows a higher percentage loss of

23.6% area while Baffin lost 6.6%. However, Disko is a warmer region than Baffin, and experienced a larger increase in annually averaged temperature as well as in summer average temperature in 2000-02 to 2019-21 compared to 1985-86 to 2000-02.

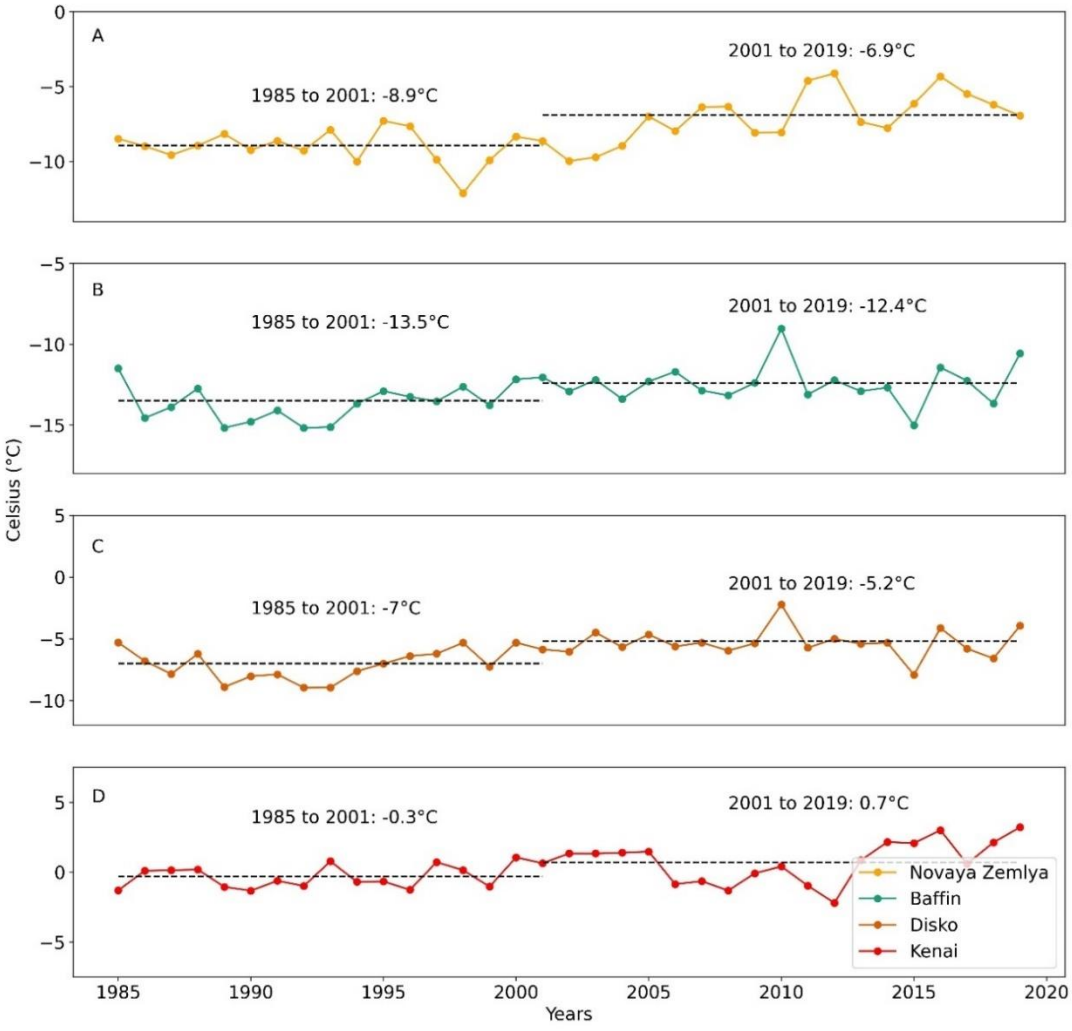

Figure 21 Annually average temperature of Baffin, Disko, and Kenai. The dashed line represents the average temperature of the study time periods.

Computing the annual average precipitation would provide a more thorough understanding of glacier area changes in these regions. However, it is important to note that snowfall requires temperatures to be close or below freezing, less than 0

degrees Celsius. However, during the summer months, the average temperature in Kenai and Disko exceeds 0 degrees Celsius, resulting in rain instead of snow. So, accurately computing the precipitation in these four areas becomes challenging due to the variability of data across time periods in different regions.

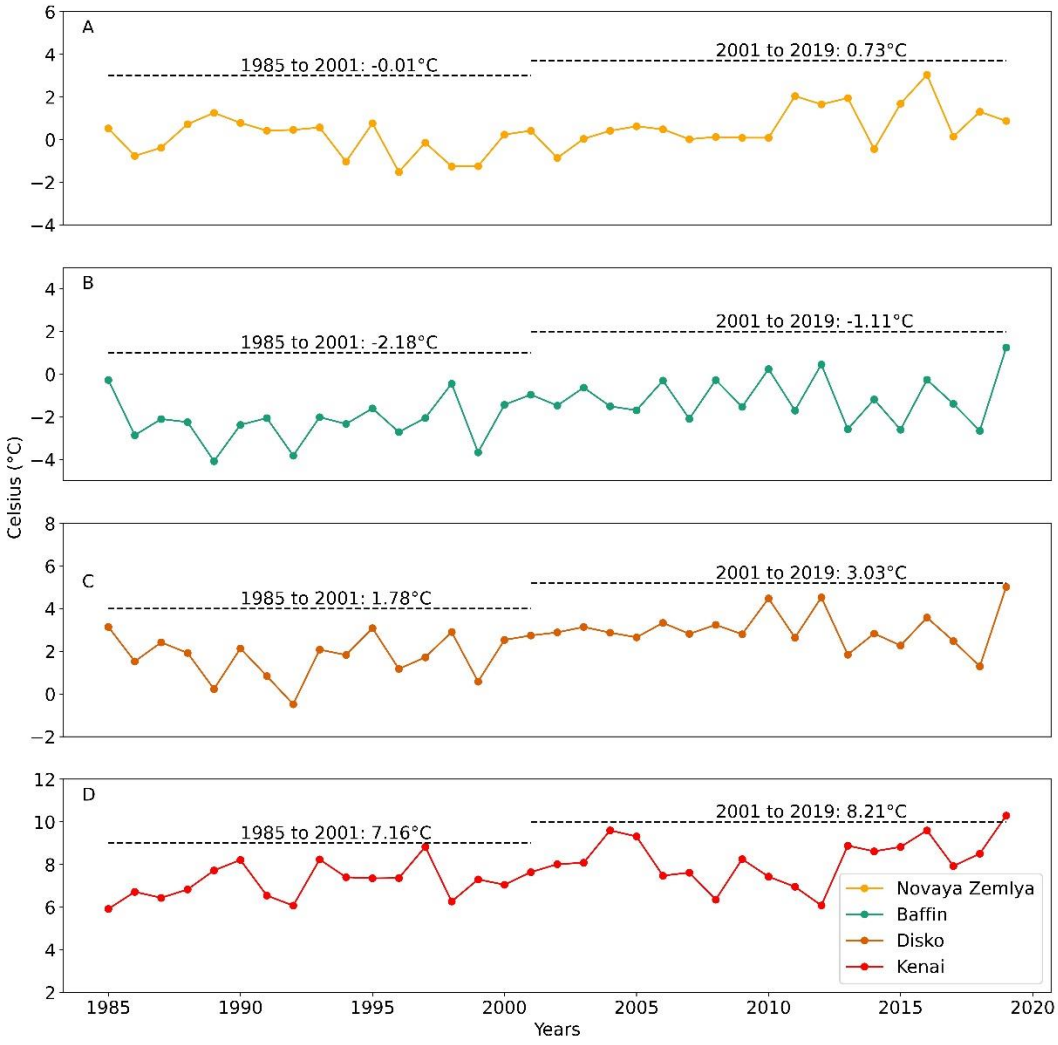

Figure 22 Summer months (May-September) average temperature of Baffin, Disko, and Kenai. The dashed line represents the average temperature of the study time periods.

4.6.3. Comparison of glacier area loss with mass balance

Comparing glacier area changes on Novaya Zemlya, Baffin, Disko, and Kenai with geodetic mass balances obtained from for the period 2000–2020 reveals that Kenai represents the highest loss of both area (19.4%) and as well as mass balance (0.89 m a^{-1}), while Novaya Zemlya glaciers lost the least amount of both area (3.7%) and mass balance (0.24 m a^{-1}). In contrast to Novaya Zemlya, Disko, and Kenai, Baffin has a slightly different pattern, losing a total of 4.1% of glacier area while experiencing a substantial increase in mass loss (0.67 m a^{-1}) relative to other regions (Figure 23).

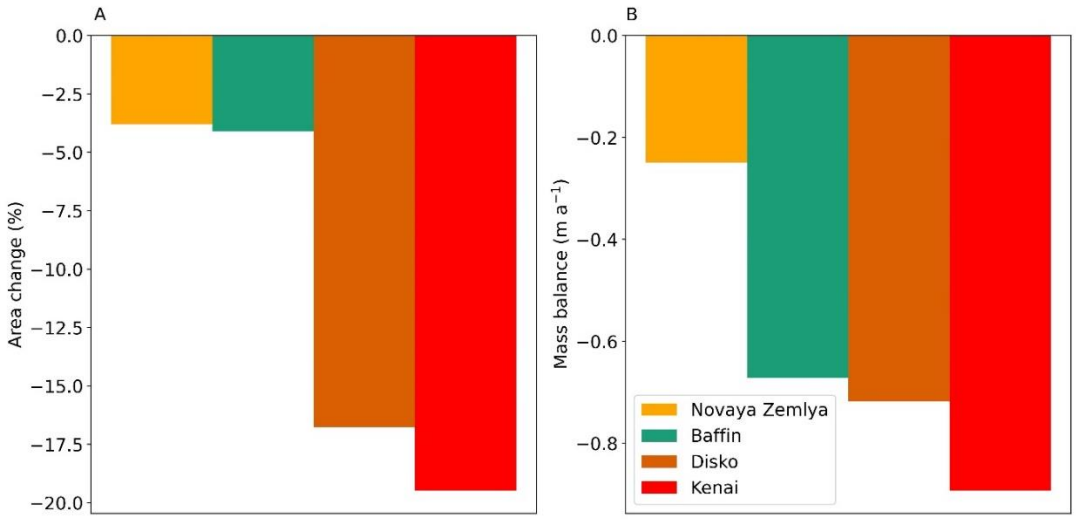

Figure 23 (A) shows total glacier area change (2000-02 to 2019-21) and (B) represent area-averaged mass change (2000-2020) from (Hugonnet et al. 2021).

4.7. Conclusion

This study used an OBIA method in GEE, utilizing multi-temporal Landsat satellite images for rapid and accurate glacier mapping in three different regions: Baffin, Canada, Disko, Greenland, and the Kenai Peninsula, Alaska. The automatically

generated outlines showed an accuracy between 93% and 98% when compared with manually corrected outlines. The results demonstrate that OBIA in GEE is a powerful, robust tool for precise and fast mapping of glacier changes on a regional scale, decreasing the time required for manual correction.

The OBIA framework in GEE enabled a comprehensive analysis of the decadal changes of 1273 glaciers from 1985-86 to 2019-21, showing that the selected glaciers on Baffin lost a total of 452±227 Km^2 (-6.6%) area, glaciers on Disko lost 456±168 km^2 (-23.6%), and the selected glaciers in the Kenai Peninsula lost 196±84 km^2 (-25.7%).

The findings showed that in 2000-02 to 2019-21 the glaciers in Kenai and Disko lost increased more than double compared to 1985-86 to 2000-02, while glaciers' area lost in Baffin increased from 2.2% to 4.1%. Our analysis also shows that there are complicated regional variations in how glaciers are responding to warming in different parts of the Arctic, with the increase of 1 °C temperature Kenai lost more glacierized region than Baffin and Disko in the second time period of the study, while Disko experienced the highest increased of temperature of 1.7 °C which causes a substantial amount of area lost.

4.8. References

Achanta, Radhakrishna, and Sabine Süsstrunk, eds. 2017. 'Superpixels and Polygons Using Simple Non-Iterative Clustering'. *30Th Ieee Conference On Computer Vision And Pattern Recognition (Cvpr 2017)*. doi: 10.1109/Cvpr.2017.520.

Ali, Asim, Paul Dunlop, Sonya Coleman, Dermot Kerr, Robert W. McNabb, and Riko Noormets. 2023. 'Glacier Area Changes in Novaya Zemlya from 1986-89 to 2019-21 Using Object-Based Image Analysis in Google Earth Engine'. *Journal of Glaciology 1–12*. doi: 10.1017/jog.2023.18.

Alifu, Haireti, Ryutaro Tateishi, and Brian Johnson. 2015. 'A New Band Ratio Technique for Mapping Debris-Covered Glaciers Using Landsat Imagery and a Digital Elevation Model'. *International Journal of Remote Sensing* 36(8):2063–75. doi: 10.1080/2150704X.2015.1034886.

Amani, Meisam, Arsalan Ghorbanian, Seyed Ali Ahmadi, Mohammad Kakooei, Armin Moghimi, S. Mohammad Mirmazloumi, Sayyed Hamed Alizadeh Moghaddam, Sahel Mahdavi, Masoud Ghahremanloo, Saeid Parsian, Qiusheng Wu, and Brian Brisco. 2020. 'Google Earth Engine Cloud Computing Platform for Remote Sensing Big Data Applications: A Comprehensive Review'. *IEEE Journal of Selected Topics in Applied Earth Observations and Remote Sensing* 13:5326–50. doi: 10.1109/JSTARS.2020.3021052.

AMAP. 2017. *Snow, Water, Ice and Permafrost in the Arctic (SWIPA) 2017. Arctic Monitoring and Assessment Programme (AMAP), Oslo, Norway. ISBN: 978-82-7971-101-8*.

Berg, Edward E., J. David Henry, Christopher L. Fastie, Andrew D. De Volder, and Steven M. Matsuoka. 2006. 'Spruce Beetle Outbreaks on the Kenai Peninsula, Alaska, and Kluane National Park and Reserve, Yukon Territory: Relationship to Summer Temperatures and Regional Differences in Disturbance Regimes'. *Forest Ecology and Management* 227(3):219–32. doi: 10.1016/j.foreco.2006.02.038.

Blaschke, T. 2010. 'Object Based Image Analysis for Remote Sensing'. *ISPRS Journal of Photogrammetry and Remote Sensing* 65(1):2–16. doi: 10.1016/j.isprsjprs.2009.06.004.

Bosson, J. B., M. Huss, and E. Osipova. 2019. 'Disappearing World Heritage Glaciers as a Keystone of Nature Conservation in a Changing Climate'. *Earth's Future* 7(4):469–79. doi: 10.1029/2018EF001139.

Climate, Greenland. n.d. 'Greenland Climate: Average Weather, Temperature, Precipitation'. Retrieved 1 March 2023 (https://www.climatestotravel.com/climate/greenland).

Consortium, R. G. I. 2017. 'Randolph Glacier Inventory 6.0 - A Dataset of Global Glacier Outlines: Version 6.0. Technical Report, Global Land Ice Measurments from Space, Boulder, Colorado, USA. Digital Media'. doi: 10.7265/n5-rgi-60.

Copernicus Climate Change Service. 2019. 'ERA5-Land Monthly Averaged Data from 1950 to Present. Copernicus Climate Change Service (C3S) Climate Data Store (CDS). DOI: 10.24381/Cds.68d2bb30'.

Friberg, Nikolai, Alexander M. Milner, Lars M. Svendsen, Claus Lindegaard, and Søren Erik Larsen. 2001. 'Macroinvertebrate Stream Communities along Regional and Physico-Chemical Gradients in Western Greenland'. *Freshwater Biology* 46(12):1753–64. doi: 10.1046/j.1365-2427.2001.00857.x.

Gorelick, Noel, Matt Hancher, Mike Dixon, Simon Ilyushchenko, David Thau, and Rebecca Moore. 2017. 'Google Earth Engine: Planetary-Scale Geospatial Analysis for Everyone'. *Remote Sensing of Environment* 202(2016):18–27. doi: 10.1016/j.rse.2017.06.031.

Granshaw, Frank, and Andrew Fountain. 2006. 'Glacier Change (1958-1998) in the North Cascades National Park Complex, Washington, USA'. *Journal of Glaciology* 52:251–56. doi: 10.3189/172756506781828782.

Haeberli, Wilfried. 2004. 'Glaciers and Ice Caps: Historical Background and Strategies of World-Wide Monitoring'. Pp. 559–78 in *Mass Balance of the Cryosphere: Observations and Modelling of Contemporary and Future Changes*, edited by A. J. Payne and J. L. Bamber. Cambridge: Cambridge University Press.

Hemati, MohammadAli, Mahdi Hasanlou, Masoud Mahdianpari, and Fariba Mohammadimanesh. 2021. 'A Systematic Review of Landsat Data for Change Detection Applications: 50 Years of Monitoring the Earth'. *Remote Sensing* 13(15):2869. doi: 10.3390/rs13152869.

Hock, Regine, Andrew Bliss, Ben Marzeion, Rianne H. Giesen, Yukiko Hirabayashi, Matthias Huss, Valentina Radić, and Aimée B. A. Slangen. 2019. 'GlacierMIP – A Model Intercomparison of Global-Scale Glacier Mass-Balance Models and Projections'. *Journal of Glaciology* 65(251):453–67. doi: 10.1017/jog.2019.22.

Hugonnet, Romain, Robert McNabb, Etienne Berthier, Brian Menounos, Christopher Nuth, Luc Girod, Daniel Farinotti, Matthias Huss, Ines Dussaillant, Fanny Brun, and Andreas Kääb. 2021. 'Accelerated Global Glacier Mass Loss in the Early Twenty-First Century'. *Nature* 592(7856):726–31. doi: 10.1038/s41586-021-03436-z.

Humlum, Ole. 1996. 'Origin of Rock Glaciers: Observations from Mellemfjord, Disko, Central West Greenland'. *Permafrost and Periglacial Processes* 7(4):361–80. doi: 10.1002/(SICI)1099-1530(199610)7:4<361::AID-PPP227>3.0.CO;2-4.

Huss, M. 2012. ‘Extrapolating Glacier Mass Balance to the Mountain-Range Scale: The European Alps 1900–2100’. *The Cryosphere* 6(4):713–27. doi: 10.5194/tc-6-713-2012.

given-i=Peter, family=Adam, and family=J. Dunbar given-i=Maxwell. 2015. ‘Arctic Archipelago’. Retrieved 25 October 2022 (www.thecanadianencyclopedia.ca/en/article/arctic-archipelago).

IPCC, 2021. 2021. *IPCC, 2021: Climate Change 2021: The Physical Science Basis. Contribution of Working Group I to the Sixth Assessment Report of the Intergovernmental Panel on Climate Change. [Masson-Delmotte, V., P. Zhai, A. Pirani, S.L. Connors, C. Péan, S. Berger, N. Caud, Y. Chen, L. Goldfarb, M.I. Gomis, M. Huang, K. Leitzell, E. Lonnoy, J.B.R. Matthews, T.K. Maycock, T. Waterfield, O. Yelekçi, R. Yu, and B. Zhou (Eds.)]. Cambridge University Press, Cambridge, United Kingdom and New York, NY, USA, In Press, Doi:10.1017/9781009157896.*

Kulp, Scott A., and Benjamin H. Strauss. 2019. ‘New Elevation Data Triple Estimates of Global Vulnerability to Sea-Level Rise and Coastal Flooding’. *Nature Communications* 10(1). doi: 10.1038/s41467-019-12808-z.

Masek, Jeffrey G., Michael A. Wulder, Brian Markham, Joel McCorkel, Christopher J. Crawford, James Storey, and Del T. Jenstrom. 2020. ‘Landsat 9: Empowering Open Science and Applications through Continuity’. *Remote Sensing of Environment* 248:111968. doi: 10.1016/j.rse.2020.111968.

Millan, Romain, Jérémie Mouginot, Antoine Rabatel, and Mathieu Morlighem. 2022. ‘Ice Velocity and Thickness of the World’s Glaciers’. *Nature Geoscience* 15(2):124–29. doi: 10.1038/s41561-021-00885-z.

Nery, Thayse, Rohan Sadler, Maria Solis-Aulestia, Ben White, Maksym Polyakov, and Morteza Chalak. 2016. ‘Comparing Supervised Algorithms in Land Use and Land Cover Classification of a Landsat Time-Series’. Pp. 5165–68 in *2016 IEEE International Geoscience and Remote Sensing Symposium (IGARSS)*.

Olsen, M. S., T. V. Callaghan, J. D. Reist, L. O. Reiersen, D. Dahl-Jensen, M. A. Granskog, B. Goodison, G. K. Hovelsrud, M. Johansson, R. Kallenborn, J. Key, A. Klepikov, W. Meier, J. E. Overland, T. D. Prowse, M. Sharp, W. F. Vincent, and J. Walsh. 2011. ‘The Changing Arctic Cryosphere and Likely Consequences: An Overview’. *AMBIO* 40(1):111–18. doi: 10.1007/s13280-011-0220-y.

Paul, Frank, Tobias Bolch, Kate Briggs, Andreas Kääb, Malcolm McMillan, Robert McNabb, Thomas Nagler, Christopher Nuth, Philipp Rastner, Tazio Strozzi, and Jan Wuite. 2017. ‘Error Sources and Guidelines for Quality Assessment of Glacier Area, Elevation Change, and Velocity Products Derived from Satellite Data in the Glaciers_cci Project’. *Remote Sensing of Environment* 203:256–75. doi: 10.1016/j.rse.2017.08.038.

Praticò, Salvatore, Francesco Solano, Salvatore Di Fazio, and Giuseppe Modica. 2021. 'Machine Learning Classification of Mediterranean Forest Habitats in Google Earth Engine Based on Seasonal Sentinel-2 Time-Series and Input Image Composition Optimisation'. *Remote Sensing* 13(4):586. doi: 10.3390/rs13040586.

Rantanen, Mika, Alexey Yu Karpechko, Antti Lipponen, Kalle Nordling, Otto Hyvärinen, Kimmo Ruosteenoja, Timo Vihma, and Ari Laaksonen. 2022. 'The Arctic Has Warmed Nearly Four Times Faster than the Globe since 1979'. *Communications Earth & Environment* 3(1):1–10. doi: 10.1038/s43247-022-00498-3.

Raup, Bruce, Adina Racoviteanu, Siri Jodha Singh Khalsa, Christopher Helm, Richard Armstrong, and Yves Arnaud. 2007. 'The GLIMS Geospatial Glacier Database: A New Tool for Studying Glacier Change'. *Global and Planetary Change* 56(1):101–10. doi: 10.1016/j.gloplacha.2006.07.018.

Ren and Malik. 2003. 'Learning a Classification Model for Segmentation'. Pp. 10–17 vol.1 in *Proceedings Ninth IEEE International Conference on Computer Vision*.

Rocchio, Laura E. P., Peggy Connot, Steve Young, Kate Ramsayer, Linda Owen, Michelle Bouchard, and Christopher Barnes. 2018. *Landsat Benefiting Society for Fifty Years*. *Federal Government Series*. NASA.

Schädel, Christina, Charles D. Koven, David M. Lawrence, Gerardo Celis, Anthony J. Garnello, Jack Hutchings, Marguerite Mauritz, Susan M. Natali, Elaine Pegoraro, Heidi Rodenhizer, Verity G. Salmon, Meghan A. Taylor, Elizabeth E. Webb, William R. Wieder, and Edward AG Schuur. 2018. 'Divergent Patterns of Experimental and Model-Derived Permafrost Ecosystem Carbon Dynamics in Response to Arctic Warming'. 13(10):105002. doi: 10.1088/1748-9326/aae0ff.

Sharp, Martin, David O. Burgess, Fiona Cawkwell, Luke Copland, James A. Davis, Evelyn K. Dowdeswell, Julian A. Dowdeswell, Alex S. Gardner, Douglas Mair, Libo Wang, Scott N. Williamson, Gabriel J. Wolken, and Faye Wyatt. 2014. 'Remote Sensing of Recent Glacier Changes in the Canadian Arctic'. Pp. 205–28 in *Global Land Ice Measurements from Space*, *Springer Praxis Books*, edited by J. S. Kargel, G. J. Leonard, M. P. Bishop, A. Kääb, and B. H. Raup. Berlin, Heidelberg: Springer.

Sorg, Annina, Tobias Bolch, Markus Stoffel, Olga Solomina, and Martin Beniston. 2012. 'Climate Change Impacts on Glaciers and Runoff in Tien Shan (Central Asia)'. *Nature Climate Change* 2(10):725–31. doi: 10.1038/nclimate1592.

Strozzi, Tazio, Frank Paul, Andreas Wiesmann, Thomas Schellenberger, and Andreas Kääb. 2017. 'Circum-Arctic Changes in the Flow of Glaciers and Ice Caps from Satellite SAR Data between the 1990s and 2017'. *Remote Sensing* 9(9). doi: 10.3390/rs9090947.

Vanella, Daniela, Giuseppe Longo-Minnolo, Oscar Rosario Belfiore, Juan Miguel Ramírez-Cuesta, Salvatore Pappalardo, Simona Consoli, Guido D'Urso, Giovanni

Battista Chirico, Antonio Coppola, Alessandro Comegna, Attilio Toscano, Riccardo Quarta, Giuseppe Provenzano, Matteo Ippolito, Alessandro Castagna, and Claudio Gandolfi. 2022. 'Comparing the Use of ERA5 Reanalysis Dataset and Ground-Based Agrometeorological Data under Different Climates and Topography in Italy'. *Journal of Hydrology: Regional Studies* 42:101182. doi: 10.1016/j.ejrh.2022.101182.

Wilfried Haeberli Frank Paul, Tobias Kellenberger, Andreas KÌÌb, Max Maisch. 2002. 'The New Remote-Sensing-Derived Swiss Glacier Inventory: I. Methods'. *Annals of Glaciology* 34(September 1985):362–66. doi: 10.3189/172756402781817473.

Winsvold, S. H., L. M. Andreassen, and C. Kienholz. 2014. 'Glacier Area and Length Changes in Norway from Repeat Inventories'. *Cryosphere* 8(5):1885–1903. doi: 10.5194/tc-8-1885-2014.

Xue, Xingyu, Zhoulu Yu, Shaochun Zhu, Qiming Zheng, Melanie Weston, Ke Wang, Muye Gan, and Hongwei Xu. 2018. 'Delineating Urban Boundaries Using Landsat 8 Multispectral Data and VIIRS Nighttime Light Data'. *Remote Sensing* 10(5):799. doi: 10.3390/rs10050799.

Yang, Ruitang, Regine Hock, Shichang Kang, Donghui Shangguan, and Wanqin Guo. 2020. 'Glacier Mass and Area Changes on the Kenai Peninsula, Alaska, 1986–2016'. *Journal of Glaciology* 66(258):603–17. doi: 10.1017/jog.2020.32.

Yde, Jacob C., and N. Tvis Knudsen. 2007. '20th-Century Glacier Fluctuations on Disko (Qeqertarsuaq), Greenland'. *Annals of Glaciology* 46:209–14. doi: 10.3189/172756407782871558.

You, Qinglong, Ziyi Cai, Nick Pepin, Deliang Chen, Bodo Ahrens, Zhihong Jiang, Fangying Wu, Shichang Kang, Ruonan Zhang, Tonghua Wu, Pengling Wang, Mingcai Li, Zhiyan Zuo, Yanhong Gao, Panmao Zhai, and Yuqing Zhang. 2021. 'Warming Amplification over the Arctic Pole and Third Pole: Trends, Mechanisms and Consequences'. *Earth-Science Reviews* 217:103625. doi: 10.1016/j.earscirev.2021.103625.

Zemp, M., M. Huss, E. Thibert, N. Eckert, R. McNabb, J. Huber, M. Barandun, H. Machguth, S. U. Nussbaumer, I. Gärtner-Roer, L. Thomson, F. Paul, F. Maussion, S. Kutuzov, and J. G. Cogley. 2019. 'Global Glacier Mass Changes and Their Contributions to Sea-Level Rise from 1961 to 2016'. *Nature* 568(7752):382–86. doi: 10.1038/s41586-019-1071-0.

Chapter 5

Mapping glacier area changes in the Arctic and high latitudes using satellite remote sensing.

Asim Ali[1], Paul Dunlop[1], Sonya Coleman[2], Dermot Kerr[2], Robert W McNabb[1], and Riko Noormets[3]

[1]School of Geography and Environmental Sciences, Ulster University, UK
[2]School of Computing, Engineering, and Intelligent Systems, Ulster University, UK
[3]School of Marine, Geology, and Geophysics, University Centre in Svalbard

This paper has been submitted to Journal of Maps

5.1. Abstract

Glaciers have been retreating over the last century as a result of climate change, particularly in the Arctic, causing sea levels to rise, affecting coastal communities and potentially changing global weather and climate patterns. Therefore, it is important to understand the impact of climate change on glaciers and accurately quantify glacier area changes in the Arctic and at high latitudes. In this study, we mapped 2203 glaciers in Novaya Zemlya (Russian Arctic), Baffin Island (Canadian Arctic), Disko Island, (Greenland) and Kenai (Alaska), using Object-Based Image Analysis (OBIA) applied to multispectral Landsat satellite imagery in Google Earth Engine (GEE) to quantify the glacier area changes over three decades. Between 1985-86 and 2019-21, the results show that the overall glacier area loss in Novaya Zemlya is 1319±419 km^2 (5.7%), 452±227 km^2 (6.6%) in Baffin, 457±168 km^2 (23.6%) in Disko Island and 196±84 km^2 (25.7%) in Kenai. A total of seventy-three glaciers have completely disappeared including sixty-nine on Disko Island, three in Novaya Zemlya and one in Kenai. Based on a random sampling approach, the method showed an estimated accuracy between 93% and 98% with the reference data indicating that this method has the potential for rapid glacier mapping that can be easily used in other glacierized regions.

Key words

Landsat, Glaciers, OBIA, Google Earth Engine

5.2. Introduction

The cryosphere is a key component of the global climate system, and as temperatures continue to rise, the cryosphere continues to shrink, leading to a number of significant impacts (IPCC 2021). In particular, melting glaciers are a major concern, as they contribute to sea level rise, coastal erosion, hazards such as avalanches and glacial floods in mountainous regions and the disruption of essential fresh water supplies (Ding et al. 2021).

Glaciers in the Arctic region play a vital role in the global climate system by reflecting sunlight and trapping cold air, which helps to regulate global temperatures (Previdi et al. 2021). Over the last few decades, the Arctic is warming faster than any other region in the world, a phenomenon known as Arctic amplification (e.g., Dai et al. 2019). Positive feedback mechanisms, such as ice-albedo feedback, where sea ice melts and more sunlight are absorbed by the darker ocean, lead to further warming (Screen and Simmonds 2010). Additionally, changes in atmospheric and oceanic circulation patterns, and increases in greenhouse gas concentrations in the atmosphere are all factors that contribute to Arctic Amplification (Dai et al. 2019). As a result of these processes, studies have reported that the Arctic is warming twice or more than twice as much as anywhere else in the world (Schädel et al. 2018; You et al. 2021), with a recent study estimating that the Arctic has been warming nearly four times faster than the rest of the world (Rantanen et al. 2022) .

In the Arctic, glaciers, ice caps, and the Greenland Ice Sheet have all retreated in the past 100 years and are starting to retreat faster since 2000 causing changes in the surface albedo and global sea level rise (AMAP 2017). Glaciers, snow cover, and sea ice are expected to decrease throughout this century, which means that more incoming solar radiation will be absorbed by open water and land, leading to increased melting and heating across the Arctic (IPCC 2019).

The Global Land Ice Measurements from Space (GLIMS) initiative provides a global database of glacier outlines, mostly derived from satellite imagery (Raup et al. 2007). Glacier outlines are an important dataset, especially outlines of the same glaciers mapped over time, and are necessary for assessing the impact of climate change. However, mapped outlines are only available at a single point in time for most of the World's glaciers, which limits their use for understanding the long-term impacts of climate change.

Given the importance of glaciers to the Arctic region, multi-temporal glacier outlines are necessary to provide a clear understanding of the climate change impacts on Arctic glaciers. In this study, we used a satellite remote sensing approach in Google Earth Engine (GEE) to create multi-temporal outlines of glaciers in different Arctic regions, providing a valuable dataset that can be used to rapidly assess the impacts of climate change, to estimate glacier mass changes, and to predict glacier contributions to sea level rise (e.g Hock et al. 2019; Zemp et al. 2019).

5.3. Study Area

This study focused on four different regions within the Arctic and at high latitudes: Novaya Zemlya (Russian Arctic), Baffin Island (Canadian Arctic), Disko Island (Greenland), and the Kenai Peninsula (Alaska) (Figure 16). A total of 2203 glaciers were selected for mapping using the Randolph Glacier Inventory (RGI) version 6.0. According to the RGI 6.0, there are 480 glaciers on Novaya Zemlya measuring 22128 km^2, 748 glaciers of Disko Island measuring 1869 km^2, 523 glaciers on Baffin Island measuring 7054 km^2, and 452 glaciers in Kenai Alaska covering an area of 638 km^2 (RGI Consortium 2017).

Novaya Zemlya is located north of Russia's mainland, between the Barents and Kara Seas (Figure 24). The Canadian Arctic Archipelago, which is the largest land ice region outside of the Greenland and Antarctic ice sheets, is located north of mainland Canada (Figure 24), while Disko Island (Greenlandic: Qeqertarsuaq) is the largest island in Greenland, located off the west coast. The Kenai Peninsula is located in south-central Alaska, between the Cook Inlet and the Gulf of Alaska (Figure 24). The four study regions were chosen because they are spread widely within the Arctic and high latitudes and can provide representative insights on the impacts that pan-Arctic warming is have on glacier recession.

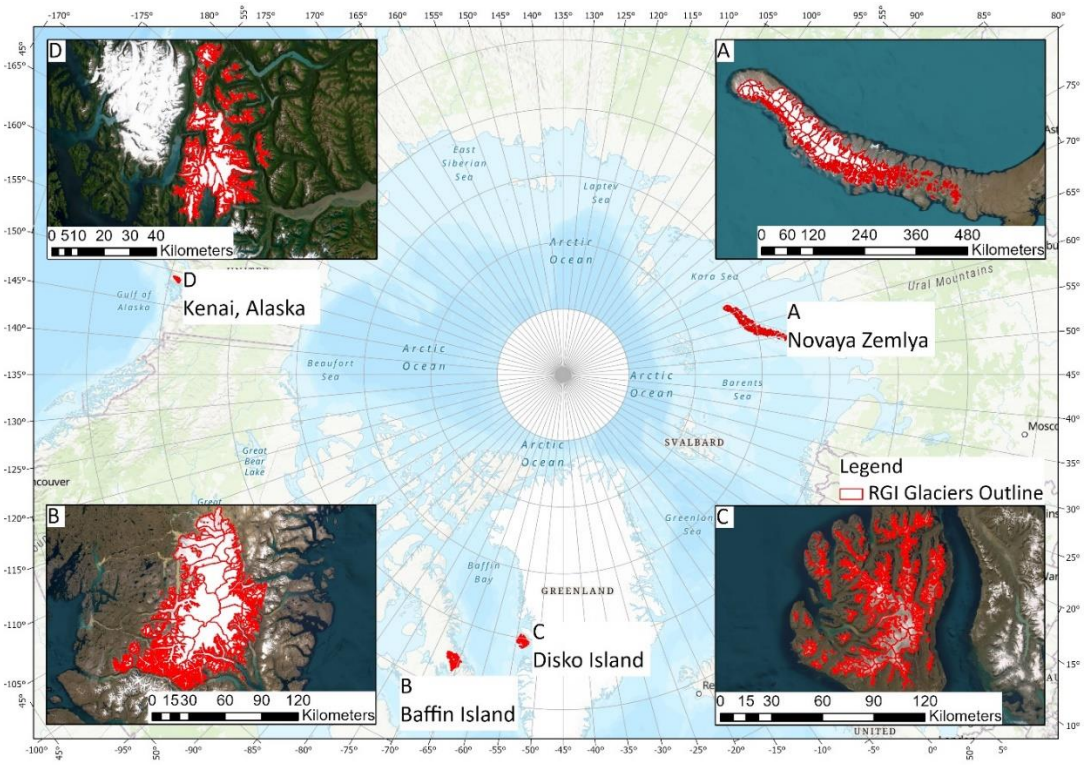

Figure 24:The four study areas are, A) Novaya Zemlya; B) Baffin Island; C) Disko Island; and D) Kenai, Alaska. The red polygons in the insert images are the selected glaciers from RGI.

5.4. Method

5.4.1. Data sources

NASA's Landsat satellite programme has been collecting imagery of the Earth since 1972 and is the longest-running earth observation satellite programme (Masek et al. 2020). Landsat satellites collect data in the visible to infrared part of the electromagnetic spectrum to monitor different features of the Earth such as land cover, vegetation, surface temperature, and more. The main sensors of Landsat satellites are Multi-Spectral Scanner (MSS), Thematic Mapper (TM), Enhanced Thematic Mapper Plus (ETM+), Operational Land Imager (OLI), and Thermal Infrared Sensor (TIRS) (Hemati et al. 2021). This study uses Landsat 5 (TM), Landsat 7 (ETM+), and Landsat 8 (OLI/TIRS) for glacier mapping.

Because of the large swath width, the multispectral capabilities, and the long time span of data collection, Landsat data have proven to be an effective asset for glacier mapping and for creating multi-temporal outlines of glaciers (e.g., Mölg et al. 2018; Nuth et al. 2013). The images for this study were carefully selected in GEE during the summer-time period (July-September) with the least amount of cloud cover. To map glaciers, we use Collection 1 Level-2 Tier 1 surface reflectance products (Table 11). These images are orthorectified and atmospherically corrected. In particular, Tier 1 images have the best quality, and are considered suitable for time-series analysis (Masek et al. 2020). The United States Geological Survey (USGS) also provides images in Tier 2; however, Tier 2 images have issues with geometric correction but may still be usable (Hemati et al. 2021).

Table 11: Details of images that are used in this study for each location.

Serial Number	Satellite	Date image acquired	WRS-2 Path/Row	GEE Image IDs
Novaya Zemlya, Russian Arctic				
01	Landsat 5	26/07/1986	174/6	LANDSAT/LT05/C01/T1_SR/LT05_174006_19860726
02	Landsat 5	03/08/1987	177/6	LANDSAT/LT05/C01/T1_SR/LT05_177006_19870803
03	Landsat 5	06/08/1989	179/6	LANDSAT/LT05/C01/T1_SR/LT05_179006_19890806
04	Landsat 5	06/08/1989	179/7	LANDSAT/LT05/C01/T1_SR/LT05_179007_19890806
05	Landsat 5	06/08/1989	179/8	LANDSAT/LT05/C01/T1_SR/LT05_179008_19890806
06	Landsat 7	25/08/2000	174/6	LANDSAT/LE07/C01/T1_SR/LE07_174006_20000825
07	Landsat 7	31/07/2000	175/6	LANDSAT/LE07/C01/T1_SR/LE07_175006_20000731
08	Landsat 7	12/08/2000	179/6	LANDSAT/LE07/C01/T1_SR/LE07_179006_20000812
09	Landsat 7	12/08/2000	179/7	LANDSAT/LE07/C01/T1_SR/LE07_179007_20000812
10	Landsat 7	08/08/2001	178/8	LANDSAT/LE07/C01/T1_SR/LE07_178008_20010808
11	Landsat 8	20/08/2019	176/5	LANDSAT/LC08/C01/T1_SR/LC08_176005_20190820
12	Landsat 8	20/08/2019	176/6	LANDSAT/LC08/C01/T1_SR/LC08_176006_20190820
13	Landsat 8	23/08/2021	178/7	LANDSAT/LC08/C01/T1_SR/LC08_178007_20210823
14	Landsat 8	18/08/2020	180/6	LANDSAT/LC08/C01/T1_SR/LC08_180006_20200818
15	Landsat 8	19/09/2020	180/7	LANDSAT/LC08/C01/T1_SR/LC08_180007_20200919
16	Landsat 8	19/09/2020	180/8	LANDSAT/LC08/C01/T1_SR/LC08_180008_20200919
Baffin Island, Canadian Arctic				
17	Landsat 5	19/08/1985	18/13	LANDSAT/LT05/C01/T1_SR/LT05_018013_19850819
18	Landsat 7	13/08/2000	17/13	LANDSAT/LE07/C01/T1_SR/LE07_017013_20000813
19	Landsat 7	01/08/2002	19/13	LANDSAT/LE07/C01/T1_SR/LE07_019013_20020801

20	Landsat 8	25/07/2020	19/13	LANDSAT/LC08/C01/T1_SR/LC08_019013_20200725
21	Landsat 8	30/07/2021	17/13	LANDSAT/LC08/C01/T1_SR/LC08_017013_20210730
Disko Island, Greenland				
22	Landsat 5	03/09/1985	11/11	LANDSAT/LT05/C01/T1_SR/LT05_011011_19850903
23	Landsat 7	29/08/2001	12/11	LANDSAT/LE07/C01/T1_SR/LE07_012011_20010829
24	Landsat 8	01/09/2019	11/11	LANDSAT/LC08/C01/T1_SR/LC08_011011_20190901
Kenai, Alaska				
25	Landsat 5	28/07/1986	67/18	LANDSAT/LT05/C01/T1_SR/LT05_067018_19860728
26	Landsat 7	01/08/2002	67/18	LANDSAT/LE07/C01/T1_SR/LE07_067018_20020801
27	Landsat 8	18/08/2019	67/18	LANDSAT/LC08/C01/T1_SR/LC08_067018_20190808

5.4.2. Glacier mapping: Object-based image analysis

Object-based classification uses both spectral and spatial information such as size, shape, texture, and context from the surrounding pixels for image classification (Blaschke 2010). As pixel-based classification relies entirely on the spectral information contained within each pixel, it can result in “salt and pepper” noise in the final classification (Ma et al. 2019). In this study, we used Object-based Image Analysis (OBIA) approach in Google Earth Engine to map glacier changes. Google Earth Engine is a cloud-based platform for Earth Observation data processing and scientific research that allows users to access, analyse, and visualise multi-petabyte catalogue of data, making GEE one of the most powerful tools available for remote sensing analysis (Gorelick et al. 2017). Below, we provide a brief summary of the approach used as the full details of the methodology are provided in Ali et al. (Accepted 2023).

In the OBIA approach, segmentation is an important step that groups similar pixels into a cluster or image objects. In this study, we use Simple Non-Iterative Clustering (SNIC), an improved version of simple linear clustering, to segment the Landsat image (Achanta and Süsstrunk 2017). Based on the segmented image, a Random

Forest algorithm with ten trees was trained on manually selected samples of "glacier" and "non-glacier" classes throughout the scene (e.g., Nery et al. 2016; Praticò et al. 2021). To train the classifier, we used approximately 100 "glacier" and 100 "non-glacier" samples per image. To create glacier outlines, the classified image was converted from raster to vector, and outlines were exported from GEE to ArcMap 10.5.1. Each glacier outline was carefully examined and corrected where required for the area change analysis. The RGI 6.0 internal boundaries were used to divide the connected glaciers to enable the computation of area change for each glacier.

5.4.3. Map description

The main map contains more than two thousand glacier outlines that were produced using our approach. This breaks down to 480 glacier outlines in Novaya Zemlya, 523 in Baffin Island, 748 in Disko Island and 452 in Kenai. The main map was produced using ESRI ArcGIS Pro in A1 size (594mm x 841mm). Because each area was located in a different part of the Arctic, a specific Universal Transverse Mercator (UTM) projection was set for each study region (Table 12). To provide better visualisation and topographic context of the mapped glacier outlines, we used the built-in base maps of ArcGIS Pro, a World Ocean base map for the main layouts, and for the inset map a hill shaded World Topographic map was used.

Table 12 Shows the UTM projection information used for each study area.

Region	Projection	Base Map
Novaya Zemlya, Russia	WGS1984 UTM 41N	World ocean
Baffin Island, Canada	WGS1984 UTM 21N	World ocean
Disko Island, Greenland	WGS1984 UTM 22N	World ocean
Kenai, Alaska	WGS1984 UTM 6N	World ocean

The main map shows the area change of each glacier in percentages from 1985-89 to 2019-21, A) shows Novaya Zemlya, B) Baffin Island, C) Disko Island, and D) Kenai. The light-yellow colours show glaciers that have lost the least amount of area in percentage (0 to 0.9%) while dark red represents the glaciers that have lost more than 30% of their area. The colours of this map were carefully selected to be colour blind safe using the COLORBREWER 2.0 website "https://colorbrewer2.org/".

5.5. Results

In this study, we created a new dataset of glacier outlines at three time periods: 1985-89, 2000-02, and 2019-21 (Figure 25), that shows the area change of each glacier in both percentage and km^2 in two time periods (1985-89 to 2000-02 and 2000-02 to 2019-21), which is essential for understanding the impact of climate change on glaciers over time. This dataset also provides the specific date of when the image was captured by the satellite, as well as the area change analysis which was carried out on the manually corrected outlines.

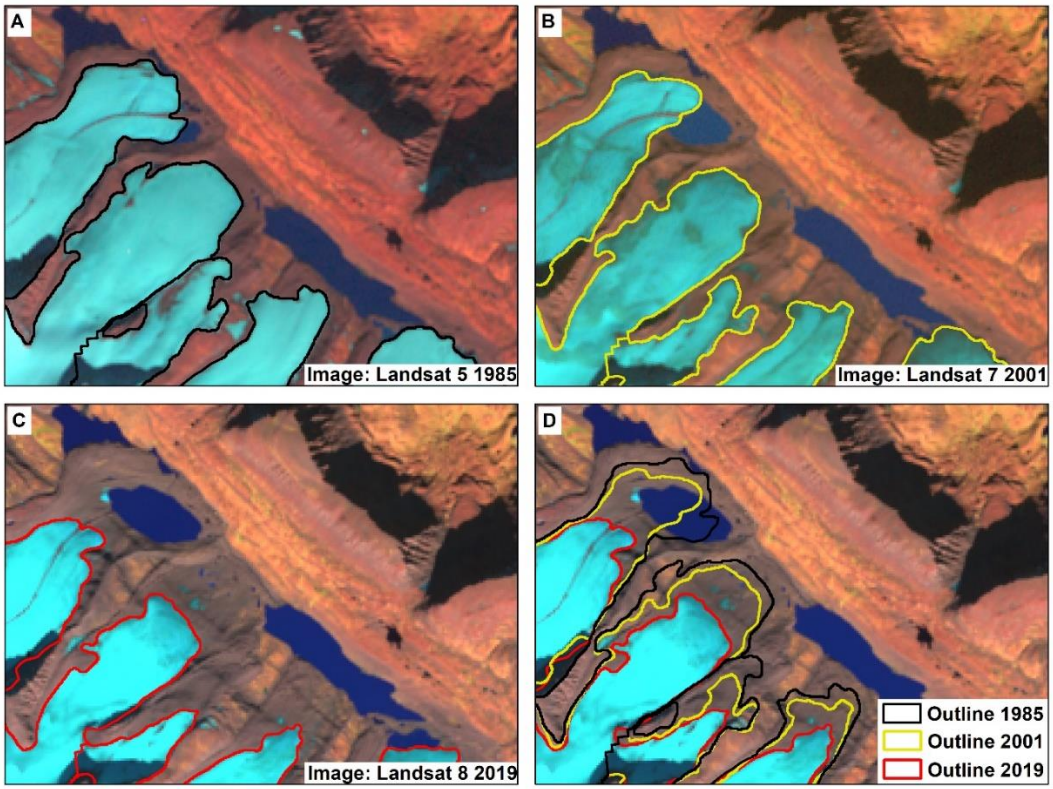

Figure 25. A close-up example of the area changes of glaciers mapped in Disko Island in 1985, 2001, and 2019. The Landsat images used for mapping are labelled in A-C. Black polygons were derived from Landsat 5 in 1985, Yellow from Landsat 7 in 2001 and Red from Landsat 8 in 2019. D shows a composite of the mapping done in three time periods, each colour represents a separate year and clearly illustrates the level of glacial change at this location.

Using these multi-temporal glacier outlines, Novaya Zemlya showed a total reduction in glacier area of 1319±419 km^2 (5.7%) from 1985-89 to 2019-21, area of selected glaciers at Baffin's declined by 452±227 km^2 (6.6%), Disko Island glacier area decreased by 457±168 km^2 (23.6%), while the selected glaciers at Kenai decreased by 196±84 km^2 (25.7%). Between 1986-89 to 2019-21, seventy-three glaciers have completely disappeared, including sixty-nine on Disko Island, three in Novaya Zemlya and one in Kenai.

Figure 26 shows the total area loss of glaciers from 1985-89 to 2000-02 and 2000-02 to 2019-21 in Novaya Zemlya, Baffin Island, Disko Island, and Kenai, revealing

that the area loss was higher from 2000-02 to 2019-21, compared to 1985-89 to 2000-02. Between 1985-89 and 2000-02, glaciers in Novaya Zemlya lost 2% of their area, Baffin Island lost 4.1% of its glacierized area, Disko lost 16.7%, and the Kenai glacier area declined by 19.5%. The glacial area loss of Novaya Zemlya increased by 1.7% from 2000-01 to 2019-21, while Baffin Island's loss increased by 1.9%, Disko Island's loss increased by 8.4%, and Kenai's loss increased by 11.7%.

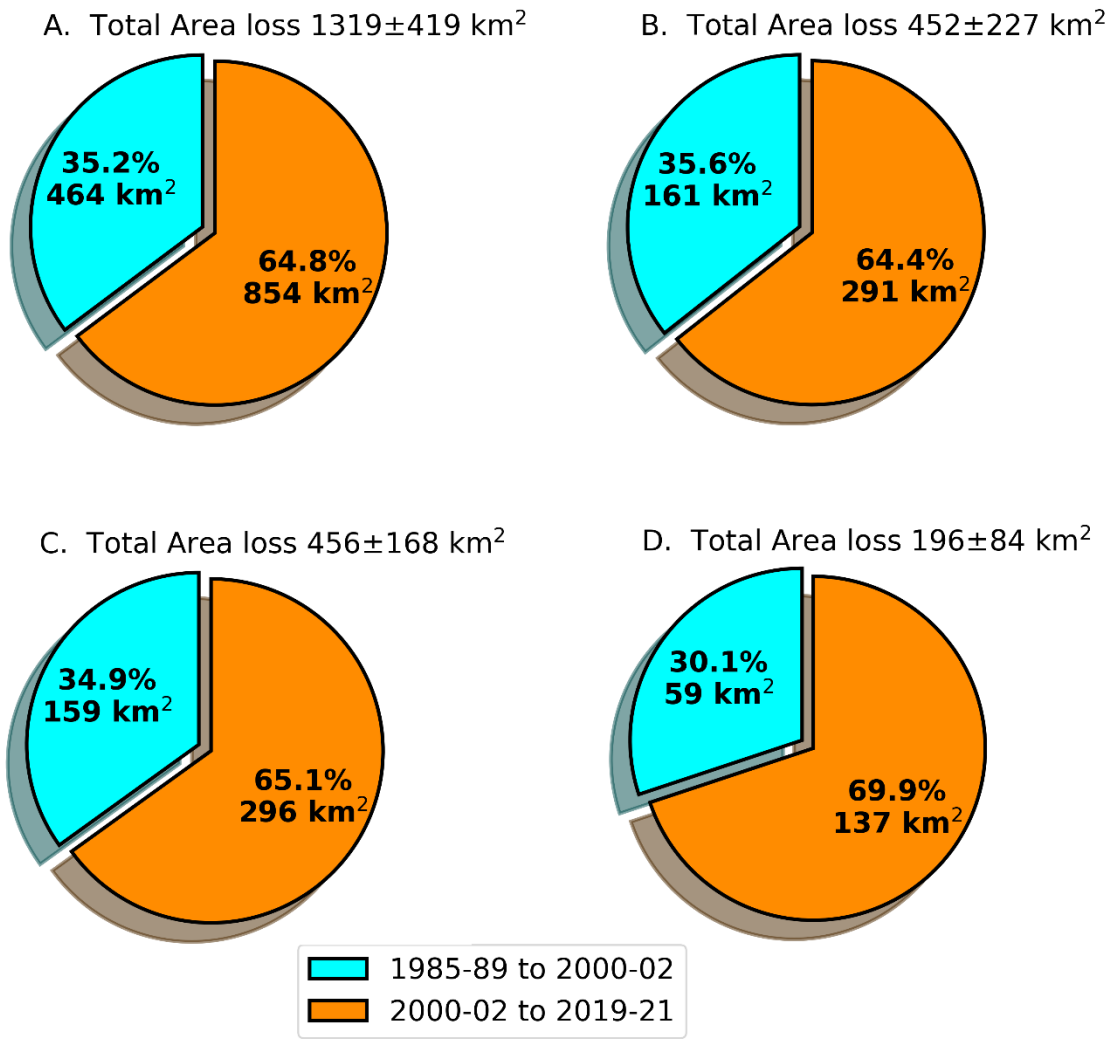

Figure 26. A) the area loss of glacier in Novaya Zemlya, B) Baffin Island, C) Disko Island, and D) Kenai from 1985-89 to 2000-02 and between 2000-02 to 2019-21.

5.6. Conclusion

Based on Landsat data and utilizing an OBIA approach in GEE, we created outlines of more than two-thousand glaciers from four different regions of the Arctic: Novaya Zemlya, Baffin Island, Disko Island, and Kenai for three different time periods: 1985-89, 2000-02, and 2019-21. These multi-temporal outlines enable the computation of the total area change of each glacier within the study area in km^2 and percentage for three time periods, which is an important data set for rapidly quantifying the impacts of climate change on glacier loss in the Arctic and high latitudes.

The final map enables the glacier outlines to be viewed in greater detail, providing valuable visual insights about the state of glaciers in each of four study regions. The data allowed the glacier changes in each location to be quantified and show that in the timeframes of this study outlined in Table 11.

Novaya Zemlya glaciers cover an area of 22,990±301 km^2 in 1986-89 and experienced a 5.7% decline in total area, Baffin Island covers 7,211±158 km^2 in 1985 and lost a total of 6.6% of its glacier area, Disko Island covers 1,929±127 km^2 in 1985 and lost 23.6% of its glacier area and the Kenai glaciers cover 764±60 km^2 in 1986 having lost 25.7% of its glacier area. Seventy-three glaciers have completely retreated, including sixty-nine on Disko Island, three on Novaya Zemlya, and one in Kenai.

Between 1985-89 and 2019-21, the results show a clear reduction in the total glacier area in all four regions and demonstrated that all glaciers in the four areas are responding to climate change. However, the impact of climate change on glaciers

was greater in 2000-02 to 2019-21, compared to 1985-89 to 2000-02, resulting in higher area loss of glacier in 2000-02 to 2019-21 than 1985-89 to 2000-02.

It is important to conduct comprehensive regional analysis on glacier behaviour in the Arctic and high latitudes in order to comprehend the decadal changes and the likely direction of glaciers in these regions as the world continues to warm. Because the melting of these glaciers may have a significant impact on global sea levels rise, accurate measurements and mapping large extend changes, as well as the precise tools that can facilitate rapid mapping of glacier are necessary at the regional scale. Platforms such as Google Earth Engine, combined with the extensive Landsat archive and approaches such as Object-Based Image Analysis, help provide these valuable tools.

5.7. Software

The initial outlines of glaciers were created using Google Earth Engine, and the main map was created using ArcGIS Pro desktop software.

At the following link, an example Google Earth Engine script is available demonstrating the object-based image analysis process to create initial glacier outlines:

https://code.earthengine.google.com/?accept_repo=users/buner_shapfile/OBIA_Example_code.

5.8. References

Achanta, Radhakrishna, and Sabine Süsstrunk, eds. 2017. 'Superpixels and Polygons Using Simple Non-Iterative Clustering'. *30Th Ieee Conference On Computer Vision And Pattern Recognition (Cvpr 2017)*. doi: 10.1109/Cvpr.2017.520.

Ali, Asim, Paul Dunlop, Sonya Coleman, Dermot Kerr, Robert W. McNabb, and Riko Noormets. 2023. 'Glacier Area Changes in Novaya Zemlya from 1986-89 to 2019-21 Using Object-Based Image Analysis in Google Earth Engine'. *Journal of Glaciology 1–12*. doi: 10.1017/jog.2023.18.

AMAP. 2017. *Snow, Water, Ice and Permafrost in the Arctic (SWIPA) 2017. Arctic Monitoring and Assessment Programme (AMAP), Oslo, Norway. Xiv + 269 Pp. ISBN 978-82-7971-101-8*.

Blaschke, T. 2010. 'Object Based Image Analysis for Remote Sensing'. *ISPRS Journal of Photogrammetry and Remote Sensing* 65(1):2–16. doi: 10.1016/j.isprsjprs.2009.06.004.

Consortium, R. G. I. 2017. 'Randolph Glacier Inventory 6.0 - A Dataset of Global Glacier Outlines: Version 6.0. Technical Report, Global Land Ice Measurments from Space, Boulder, Colorado, USA. Digital Media'. doi: 10.7265/n5-rgi-60.

Dai, Aiguo, Dehai Luo, Mirong Song, and Jiping Liu. 2019. 'Arctic Amplification Is Caused by Sea-Ice Loss under Increasing CO 2'. *Nature Communications* 10(1):1–13. doi: 10.1038/s41467-018-07954-9.

Ding, Yongjian, Cuicui Mu, Tonghua Wu, Guojie Hu, Defu Zou, Dong Wang, Wangping Li, and Xiaodong Wu. 2021. 'Increasing Cryospheric Hazards in a Warming Climate'. *Earth-Science Reviews* 213:103500. doi: 10.1016/j.earscirev.2020.103500.

Gorelick, Noel, Matt Hancher, Mike Dixon, Simon Ilyushchenko, David Thau, and Rebecca Moore. 2017. 'Google Earth Engine: Planetary-Scale Geospatial Analysis for Everyone'. *Remote Sensing of Environment* 202(2016):18–27. doi: 10.1016/j.rse.2017.06.031.

Hemati, MohammadAli, Mahdi Hasanlou, Masoud Mahdianpari, and Fariba Mohammadimanesh. 2021. 'A Systematic Review of Landsat Data for Change Detection Applications: 50 Years of Monitoring the Earth'. *Remote Sensing* 13(15):2869. doi: 10.3390/rs13152869.

Hock, Regine, Andrew Bliss, Ben Marzeion, Rianne H. Giesen, Yukiko Hirabayashi, Matthias Huss, Valentina Radić, and Aimée B. A. Slangen. 2019. 'GlacierMIP – A Model Intercomparison of Global-Scale Glacier Mass-Balance Models and Projections'. *Journal of Glaciology* 65(251):453–67. doi: 10.1017/jog.2019.22.

IPCC, 2019. n.d. 'Climate Change and Land: An IPCC Special Report on Climate Change, Desertification, Land Degradation, Sustainable Land Management, Food Security, and Greenhouse Gas Fluxes in Terrestrial Ecosystems [P.R. Shukla, J. Skea, E. Calvo Buendia, V. Masson-Delmotte, H.-O. Pörtner, D. C. Roberts, P. Zhai, R. Slade, S. Connors, R. van Diemen, M. Ferrat, E. Haughey, S. Luz, S. Neogi, M. Pathak, J.

Petzold, J. Portugal Pereira, P. Vyas, E. Huntley, K. Kissick, M. Belkacemi, J. Malley, (Eds.)].' Retrieved 9 November 2021 (https://www.ipcc.ch/srccl/cite-report/).

IPCC, 2021. 2021. *IPCC, 2021: Climate Change 2021: The Physical Science Basis. Contribution of Working Group I to the Sixth Assessment Report of the Intergovernmental Panel on Climate Change. [Masson-Delmotte, V., P. Zhai, A. Pirani, S.L. Connors, C. Péan, S. Berger, N. Caud, Y. Chen, L. Goldfarb, M.I. Gomis, M. Huang, K. Leitzell, E. Lonnoy, J.B.R. Matthews, T.K. Maycock, T. Waterfield, O. Yelekçi, R. Yu, and B. Zhou (Eds.)]. Cambridge University Press, Cambridge, United Kingdom and New York, NY, USA, In Press, Doi:10.1017/9781009157896.*

Ma, Lei, Yu Liu, Xueliang Zhang, Yuanxin Ye, Gaofei Yin, and Brian Alan Johnson. 2019. 'Deep Learning in Remote Sensing Applications: A Meta-Analysis and Review'. *ISPRS Journal of Photogrammetry and Remote Sensing* 152(March):166–77. doi: 10.1016/j.isprsjprs.2019.04.015.

Masek, Jeffrey G., Michael A. Wulder, Brian Markham, Joel McCorkel, Christopher J. Crawford, James Storey, and Del T. Jenstrom. 2020. 'Landsat 9: Empowering Open Science and Applications through Continuity'. *Remote Sensing of Environment* 248:111968. doi: 10.1016/j.rse.2020.111968.

Mölg, Nico, Tobias Bolch, Philipp Rastner, Tazio Strozzi, and Frank Paul. 2018. 'A Consistent Glacier Inventory for Karakoram and Pamir Derived from Landsat Data: Distribution of Debris Cover and Mapping Challenges'. *Earth System Science Data* 10(4):1807–27. doi: 10.5194/essd-10-1807-2018.

Nery, Thayse, Rohan Sadler, Maria Solis-Aulestia, Ben White, Maksym Polyakov, and Morteza Chalak. 2016. 'Comparing Supervised Algorithms in Land Use and Land Cover Classification of a Landsat Time-Series'. Pp. 5165–68 in *2016 IEEE International Geoscience and Remote Sensing Symposium (IGARSS)*.

Nuth, C., J. Kohler, M. König, A. Von Deschwanden, J. O. Hagen, A. Kääb, G. Moholdt, and R. Pettersson. 2013. 'Decadal Changes from a Multi-Temporal Glacier Inventory of Svalbard'. *Cryosphere* 7(5):1603–21. doi: 10.5194/tc-7-1603-2013.

Praticò, Salvatore, Francesco Solano, Salvatore Di Fazio, and Giuseppe Modica. 2021. 'Machine Learning Classification of Mediterranean Forest Habitats in Google Earth Engine Based on Seasonal Sentinel-2 Time-Series and Input Image Composition Optimisation'. *Remote Sensing* 13(4):586. doi: 10.3390/rs13040586.

Previdi, Michael, Karen L. Smith, and Lorenzo M. Polvani. 2021. 'Arctic Amplification of Climate Change: A Review of Underlying Mechanisms'. *Environmental Research Letters* 16(9):093003. doi: 10.1088/1748-9326/ac1c29.

Rantanen, Mika, Alexey Yu Karpechko, Antti Lipponen, Kalle Nordling, Otto Hyvärinen, Kimmo Ruosteenoja, Timo Vihma, and Ari Laaksonen. 2022. 'The Arctic Has Warmed Nearly Four Times Faster than the Globe since 1979'. *Communications Earth & Environment* 3(1):1–10. doi: 10.1038/s43247-022-00498-3.

Raup, Bruce, Adina Racoviteanu, Siri Jodha Singh Khalsa, Christopher Helm, Richard Armstrong, and Yves Arnaud. 2007. 'The GLIMS Geospatial Glacier Database: A New

Tool for Studying Glacier Change'. *Global and Planetary Change* 56(1–2):101–10. doi: 10.1016/j.gloplacha.2006.07.018.

Schädel, Christina, Charles D. Koven, David M. Lawrence, Gerardo Celis, Anthony J. Garnello, Jack Hutchings, Marguerite Mauritz, Susan M. Natali, Elaine Pegoraro, Heidi Rodenhizer, Verity G. Salmon, Meghan A. Taylor, Elizabeth E. Webb, William R. Wieder, and Edward AG Schuur. 2018. 'Divergent Patterns of Experimental and Model-Derived Permafrost Ecosystem Carbon Dynamics in Response to Arctic Warming'. 13(10):105002. doi: 10.1088/1748-9326/aae0ff.

Screen, James A., and Ian Simmonds. 2010. 'The Central Role of Diminishing Sea Ice in Recent Arctic Temperature Amplification'. *Nature* 464(7293):1334–37. doi: 10.1038/nature09051.

You, Qinglong, Ziyi Cai, Nick Pepin, Deliang Chen, Bodo Ahrens, Zhihong Jiang, Fangying Wu, Shichang Kang, Ruonan Zhang, Tonghua Wu, Pengling Wang, Mingcai Li, Zhiyan Zuo, Yanhong Gao, Panmao Zhai, and Yuqing Zhang. 2021. 'Warming Amplification over the Arctic Pole and Third Pole: Trends, Mechanisms and Consequences'. *Earth-Science Reviews* 217:103625. doi: 10.1016/j.earscirev.2021.103625.

Zemp, M., M. Huss, E. Thibert, N. Eckert, R. McNabb, J. Huber, M. Barandun, H. Machguth, S. U. Nussbaumer, I. Gärtner-Roer, L. Thomson, F. Paul, F. Maussion, S. Kutuzov, and J. G. Cogley. 2019. 'Global Glacier Mass Changes and Their Contributions to Sea-Level Rise from 1961 to 2016'. *Nature* 568(7752):382–86. doi: 10.1038/s41586-019-1071-0.

Chapter 6

Discussion

6. Discussion and summary

6.1. Discussion

Google Earth Engine (GEE) provides access to a vast amount of geospatial data, including satellite imagery from a variety of sensors which allows users to perform analysis at a large scale and over a long time period (Gorelick et al., 2017). GEE also provides a range of machine learning algorithms for analysing geospatial data, which enables users to develop automated workflows for processing large amounts of data, and for more efficient and accurate analysis (e.g., Mahdianpari et al., 2020; Zhang et al., 2019).

Rastner et al., (2014) used the Red/SWIR band ratio technique to compare OBIA to pixel-based classification, demonstrating that OBIA performed better than pixel-based classification and reduced the time required for manual corrections, despite the longer processing time. In this study, the OBIA approach showed an accuracy between 93% and 98% when compared with reference datasets. This automated approach removes the time required for downloading, extracting, and storing the images, as demonstrated in this study is easily applicable to other regions and reduces the amount of manual correction required, compared with pixel-based methods.

To address the effects of climate change on glaciers, and its potential impacts on coastal communities and beyond, precise mapping methods to monitor glaciers at the regional scale needs to be developed and utilised. As in this study, the OBIA method can help researchers to accurately map glacier changes. This can provide

insights into the impact of climate change on glaciers as well as help in predicting future changes, which can improve climate change mitigation and adaptation policy. The OBIA method for glacier mapping in GEE has the potential to make useful contributions to both glaciology community and policymaking.

As reported in different studies (Gardner et al., 2011; Melkonian et al., 2016; Yang et al., 2020; Yde & Knudsen, 2007), glaciers are retreating in Novaya Zemlya, Baffin Island, Disko Island, and Kenai. This study also showed that glaciers have all retreated between 1985-89 and 2019-21 at various rates in the same regions. According to the Arctic Monitoring and Assessment Programme (AMAP, 2017), glaciers, ice caps, and the Greenland ice sheet have all started to retreat faster since 2000. The same trend has been observed in this study, with glacier area loss and temperature both increase in all four regions.

When both the area loss and temperature between 1985-89 and 2000-02 were compared to the area loss and temperature during 2000-02 and 2019-21, it was found that Novaya Zemlya had the highest temperature increase (2 °C) followed by Disko Island (1.7 °C), However, Disko Island (6.9 km^2/year) showed a higher retreat rate in glacier area than Novaya Zemlya (5.9 km^2/year). Baffin glacier retreat rates increased by 3.2 km^2/year with the increase in temperature of 1.1°C and temperature in Kenai increased by 1 °C with the increased in retreat rates of 4.3 km^2/year.

Glaciers are melting worldwide as a result of rising temperatures, and the rate of melting is increasing rapidly. According to the IPCC (2019) report, the rate of mass loss has accelerated in the last few decades and glaciers have been losing mass since

the 1950s as a result of rising temperatures. This study compared mass loss from Hugonnet et al., (2021) with area loss from 2000 to 2020, and found that all four regions; Novaya Zemlya, Baffin Island, Disko Island, and Kenai have lost glacier area as well as mass, as reported in other studies as well (Zemp et al., 2019; Ciracì et al., 2018; Gardner et al., 2011; Zwally et al., 2011). The Kenai glaciers lost the most area (19.4%) and mass (0.89 m a-1) followed by Disko Island, while Novaya Zemlya glaciers lost the least amount of area (3.7%).

The effects of climate change on glaciers in the Arctic and high latitude regions are becoming increasingly evident by a higher rate of glacier area loss and an overall rise in temperature during the second time period of the study. These findings highlight the accelerating effects of climate change on glaciers over time.

The decadal area changes of glaciers are an important dataset for the glaciologists and policy makers. This data can provide insights on glaciers behaviour and response to climate change as well can assist decisions related to climate change mitigation and adaptation. Glaciologists can use this glacier area change data to improve their understanding of glacier behaviour in the Arctic and high altitudes, as well as to validate and improve glacier models, which are important for predicting future glacier behaviour and assessing the potential impacts of climate change.

6.2. Summary

This study successfully developed an automated method using Google Earth Engine (GEE) and accurately mapped larger glacierized area of approximately 32,894 km^2 across four regions: Novaya Zemlya, Baffin Island, Disko Island, and Kenai. Based on

random sampling approach, the method accuracy was evaluated by comparing manually corrected outlines, resulting an impressive overall accuracy ranging between 93% and 98%. The implementation of this automated approach in GEE not only significantly reduced the processing time required for analysing large images on desktop computers or laptops but also overcame the challenge of mapping on a large scale. These findings demonstrate the potential of GEE as a powerful tool for efficient and accurate mapping in different regions in the Arctic.

Utilising this automated approach, we produced a dataset that has more than two thousand glacier outlines across four distinct regions for three different time periods (1985-89, 2000-02, and 2019-21). The results obtained from this dataset show that all glaciers in Novaya Zemlya, Baffin Island, Disko Island, and Kenai have been affected by climate change, and have experienced substantial loss in glacierized area between 1985-89 and 2019-21.

A comprehensive analysis of this dataset reveals a consistent trend of increasing impact of climate change on glaciers across all four regions. The period from 2000-02 to 2019-21 shows a greater impact compared to the previous period of 1985-89 to 2000-02. The results also show that between 1985-89 and 2019-21, a total of seventy-three glaciers have completely retreated, with the highest number of retreats occurring on Disko Island (sixty-nine), followed by Novaya Zemlya (three), and Kenai (one).

As a result of climate change, glaciers in the Arctic and high latitude are melting, and start retreat faster after 2000-02 that may have a significant impact on global sea-level rise, which can have far-reaching effects on coastal communities and

across the world. These retreats of glaciers show the clear evidence of the changing climate that require the urgent need for action to mitigate and adapt to the consequences of climate change. Therefore, it is necessary to have accurate tools that can enable rapid mapping of glaciers at a regional scale.

6.3. Recommendations for future work

This study established a method that maps glaciers automatically based on OBIA in GEE using a single image at a time, which is a step forward in glacier mapping. Yet, there is still room for more research, one potential direction for future research is to improve this method that can map glaciers at multiple points in time (e.g., 1985, 2001, 2021) in a single run of script, which will save more time.

Another potential direction to improve this method is to connect GEE to external platforms such as Google Colab in order to use strong computational resources to build and implement deep learning models (e.g., ANN and CNN) for glacier mapping, which can improve mapping accuracy and efficiency, especially in complex and various glacier environments.

In this study, we investigated the glacier area changes with temperature changes which is an essential aspect of glaciology research. However, other climatic and environmental factors such as precipitation, oceanic currents, humidity, elevation, and location all can influence glacier area changes. Therefore, examining the relationship between glacier area changes with these climatic and environmental factors can provide valuable insights into the response of glaciers to changing

climate and such datasets can help in reforming policies related to climate change adaptation and disaster risk reduction.

Global sea-level rise poses a major threat to coastal communities all over the world and these glaciers in the Arctic and high altitude are particularly vulnerable to climate change. Therefore, predicting the potential sea-level rise from these selected glaciers and quantifying their contribution to total sea-level rise is an important area of future research work. Such research can assist to inform climate change policy and minimize the financial impacts of sea-level rise on coastal populations and infrastructure.

6.3. References

AMAP. (2017). Snow, Water, Ice and Permafrost in the Arctic (SWIPA) 2017. Arctic Monitoring and Assessment Programme (AMAP), Oslo, Norway. Xiv + 269 pp. ISBN 978-82-7971-101-8. In *Arctic Monitoring and Assessment Programme (AMAP)*. https://www.amap.no/documents/doc/snow-water-ice-and-permafrost-in-the-arctic-swipa-2017/1610

Ciracì, E., Velicogna, I., & Sutterley, T. C. (2018). Mass Balance of Novaya Zemlya Archipelago, Russian High Arctic, Using Time-Variable Gravity from GRACE and Altimetry Data from ICESat and CryoSat-2. *Remote Sensing*, *10*(11), Article 11. https://doi.org/10.3390/rs10111817

Gardner, A. S., Moholdt, G., Wouters, B., Wolken, G. J., Burgess, D. O., Sharp, M. J., Cogley, J. G., Braun, C., & Labine, C. (2011). Sharply increased mass loss from glaciers and ice caps in the Canadian Arctic Archipelago. *Nature*, *473*(7347), 357–360. https://doi.org/10.1038/nature10089

Gorelick, N., Hancher, M., Dixon, M., Ilyushchenko, S., Thau, D., & Moore, R. (2017). Google Earth Engine: Planetary-scale geospatial analysis for everyone. *Remote Sensing of Environment*, *202*(2016), 18–27. https://doi.org/10.1016/j.rse.2017.06.031

Hugonnet, R., McNabb, R., Berthier, E., Menounos, B., Nuth, C., Girod, L., Farinotti, D., Huss, M., Dussaillant, I., Brun, F., & Kääb, A. (2021). Accelerated global glacier mass loss in the early twenty-first century. *Nature*, *592*(7856), Article 7856. https://doi.org/10.1038/s41586-021-03436-z

IPCC. (2019). Climate Change and Land: An IPCC special report on climate change, desertification, land degradation, sustainable land management, food security, and greenhouse gas fluxes in terrestrial ecosystems [P.R. Shukla, J. Skea, E. Calvo Buendia, V. Masson-Delmotte, H.-O. Pörtner, D. C. Roberts, P. Zhai, R. Slade, S. Connors, R. van Diemen, M. Ferrat, E. Haughey, S. Luz, S. Neogi, M. Pathak, J. Petzold, J. Portugal Pereira, P. Vyas, E. Huntley, K. Kissick, M. Belkacemi, J. Malley, (eds.)]. September, 43.

Mahdianpari, M., Salehi, B., Mohammadimanesh, F., Brisco, B., Homayouni, S., Gill, E., DeLancey, E. R., & Bourgeau-Chavez, L. (2020). Big Data for a Big Country: The First Generation of Canadian Wetland Inventory Map at a Spatial Resolution of 10-m Using Sentinel-1 and Sentinel-2 Data on the Google Earth Engine Cloud Computing Platform. *Canadian Journal of Remote Sensing*, *46*(1), 15–33. https://doi.org/10.1080/07038992.2019.1711366

Melkonian, A. K., Willis, M. J., Pritchard, M. E., & Stewart, A. J. (2016). Recent changes in glacier velocities and thinning at Novaya Zemlya. *Remote Sensing of Environment*, *174*, 244–257. https://doi.org/10.1016/j.rse.2015.11.001

Rastner, P., Bolch, T., Notarnicola, C., & Paul, F. (2014). A comparison of pixel- and object-based glacier classification with optical satellite images. *IEEE Journal of Selected Topics in Applied Earth Observations and Remote Sensing*, *7*(3), 853–862. https://doi.org/10.1109/JSTARS.2013.2274668

Yang, R., Hock, R., Kang, S., Shangguan, D., & Guo, W. (2020). Glacier mass and area changes on the Kenai Peninsula, Alaska, 1986–2016. *Journal of Glaciology*, *66*(258), 603–617. https://doi.org/10.1017/jog.2020.32

Yde, J. C., & Knudsen, N. T. (2007). 20th-century glacier fluctuations on Disko Island (Qeqertarsuaq), Greenland. *Annals of Glaciology*, *46*, 209–214. https://doi.org/10.3189/172756407782871558

Zemp, M., Huss, M., Thibert, E., Eckert, N., McNabb, R., Huber, J., Barandun, M., Machguth, H., Nussbaumer, S. U., Gärtner-Roer, I., Thomson, L., Paul, F., Maussion, F., Kutuzov, S., & Cogley, J. G. (2019). Global glacier mass changes and their contributions to sea-level rise from 1961 to 2016. *Nature*, *568*(7752), 382–386. https://doi.org/10.1038/s41586-019-1071-0

Zhang, J., Jia, L., Menenti, M., & Hu, G. (2019). *remote sensing Glacier Facies Mapping Using a Machine-Learning Algorithm: The Parlung Zangbo Basin Case Study*. https://doi.org/10.3390/rs11040452

Zwally, H. J., Li, J., Brenner, A. C., Beckley, M., Cornejo, H. G., DiMarzio, J., Giovinetto, M. B., Neumann, T. A., Robbins, J., Saba, J. L., Yi, D., & Wang, W. (2011). Greenland ice sheet mass balance: Distribution of increased mass loss with climate warming; 2003–07 versus 1992–2002. *Journal of Glaciology*, *57*(201), 88–102. https://doi.org/10.3189/002214311795306682

Appendix

This map is the part of chapter 05, representing the area change of each glacier in percentages from 1985-89 to 2019-21, A) shows Novaya Zemlya, B) Baffin Island, C) Disko Island, and D) Kenai.